UNIVERSITAT POLITÈCNICA DE VALÈNCIA

INSTITUTO DE DISEÑO Y FABRICACIÓN

SIMULATION STUDIES OF THIN FILM PHOTOVOLTAIC DEVICES

Hanif Ullah

TESIS DOCTORAL

Febrero 2015

UNIVERSITAT POLITÈCNICA DE VALÈNCIA

INSTITUTO DE DISEÑO Y FABRICACIÓN

SIMULATION STUDIES OF THIN FILM PHOTOVOLTAIC DEVICES

HANIF ULLAH

Director:

Bernabé Marí Soucase

Febrero 2015

Acknowledgments

In the name of Allah, the Merciful, the Compassionate. Praise be to Allah, the Lord of the entire universe, The Merciful, the Compassionate and The Master of the Day of Recompense. First and foremost I will thank Almighty Allah, the Compassionate and the almighty Merciful, who kindly helped me to complete my thesis.

The success of this thesis is attributed to the extensive support and assistance from my supervisor Professor Dr. Bernabé Marí Soucase. I would like to express my grateful gratitude and sincere appreciation to him for his guidance, valuable advice, supervision, encouragement and kindness to me throughout this study. I appreciate the efforts that he put for me to get admitted to the Polytechnic University of Valencia (UPV) and the opportunity to study and perform research under his expert supervision. I would also like to thank Professor Dr. Krishan Chander Singh for incessantly support, generous advice and direction as well as for proofreading and fruitful amendments. Many thanks go to Prof. Dr. Luis Manuel Sánchez Ruiz, Prof. Juan Antonio Monsoriu Serra, Prof. M. Mollar and Carlos Jiménez Rico (international office UPV) for their support, extension of grant and advices. I would also like to thank my friends and colleagues, Laura, Poula, Jesus, Othmane, Thierno Sall and Shafi-Ullah at the 'Laboratory of Optoelectronic and Semiconductor' of ETSID at Universitat Politècnica de València for their assistance and encouragement.

My deepest gratitude goes to my father, thank you for supporting me in whatever I do. I know, in particular, the great distance between us has been hard for you at times. My family and my kids, for always giving their best to stay in touch and who make our breaks from work so enjoyable.

My deepest gratitude goes to committee members (reviewers) for reviewing this manuscript, Prof. Ramos Barrado, José Ramón, Abellan Rubio, Mª Angeles, Prof. Makin, Sanjeev Kumar.

Thanks to many colleagues in the thin-film community that have stimulated a lot of this work with engaged discussions and their good work; Prof. Marc Burgelman for providing SCAPS-1D and continuous support, Pennsylvania State University for providing the software package AMPS-1D. The author gratefully acknowledges the Erasmus Mundus, Innovation and Design for Euro-Asian Scholars (IDEAS) Action-II for providing grant for this work.

Symbols

$\boldsymbol{\alpha}$	absorption coefficient	[cm^{-1}]
$\mathbf{A}$	diode quality factor	
$\Delta\mathbf{E_C}$	conduction-band offset	[eV]
$\Delta\mathbf{E_V}$	valence-band offset	[eV]
$\Delta\mathbf{E_{Ba}}$	band-gap increase toward the back	[eV]
$\Delta\mathbf{E_{Fr}}$	band-gap increase toward the front	[eV]
$\mathbf{d_g}$	distance between two columnar GBs = "grain size"	[cm]
$\boldsymbol{\varepsilon}$	electric field	[V/cm]
$\boldsymbol{\epsilon}$	electric permittivity	[F/m]
$\boldsymbol{\epsilon/\epsilon_0}$	dielectric constant	
$\mathbf{E_{C,}E_V}$	conduction-band minimum and valence-band maximum	[eV]
$\mathbf{E_f}$	equilibrium Fermi level	[eV]
$\mathbf{E_{fn,.}E_{fp}}$	electron and hole quasi-Fermi level	[eV]
$\mathbf{E_g}$	band-gap energy of the semiconductor	[eV]
$\mathbf{FF}$	fill factor	[%]
$\boldsymbol{\Phi}$	photon flux density	[#/cm^2s]
$\boldsymbol{\emptyset_{gb}}$	electrostatic grain-boundary potential	[eV]
$\mathbf{G}$	generation rate	[$cm^{-3}s^{-1}$]
$\boldsymbol{\eta}$	solar-cell efficiency under one-sun illumination	[%]
$\mathbf{J_o}$	diode saturation current density	[mA/cm^2]
$\mathbf{J_{sc}}$	short-circuit current density	[mA/cm^2]
$\mathbf{k}$	Boltzmann constant	[J/K]
$\mathbf{m_e^*, m_h^*}$	electron and hole effective mass	[kg]
$\boldsymbol{\mu_{e,}\mu_h}$	electron and hole mobility	[cm/vs]
$\mathbf{n}$	free electron density	[cm^{-3}]
$\mathbf{N_C, N_V}$	effective density of states in the conduction and valence band	[cm^{-3}]
$\mathbf{n_i}$	intrinsic carrier density	[cm^{-3}]

$\mathbf{N_A}$	uniform acceptor density	$[cm^{-3}]$
$\mathbf{N_D}$	shallow uniform donor density	$[cm^{-3}]$
$\mathbf{N_{gb}}$	density of grain-boundary states	$[cm^{-3}]$
$\mathbf{p}$	free hole density	$[cm^{-3}]$
$\mathbf{q}$	Elementary charge	[C]
$\mathbf{R_{bulk}}$	bulk recombination rate	$[cm^{-3}s^{-1}]$
$\mathbf{R_F}$	front reflection	
$\mathbf{R_{gb}}$	GB recombination rate	$[cm^{-2}s^{-1}]$
$\mathbf{S_{gb}}$	GB recombination velocity	[cm/s]
$\mathbf{T}$	absolute temperature	[K]
$\boldsymbol{\tau_e}$, $\boldsymbol{\tau_h}$	electron and hole lifetime	[s]
$\mathbf{V_{oc}}$	open-circuit voltage	[V]
$\mathbf{W_{SCR}}$	width of the space-charge region	[cm]
$\mathbf{W_{QNR}}$	width of the quasi-neutral region	[cm]

Abbreviations

ADEPT-F	A Drift-diffusion based solar cell simulator
AFORS-HET	Automat FOR Simulation of HETerostructures
AM1. 5	Standard terrestrial solar spectrum 'Air Mass 1.5'
AMPS	Analysis of Microelectronics and Photonics Structures
ASA	Amorphous Semiconductor Analysis
BL	Baseline [model]
BOS	Balance of system
BSF	Base surface field
CSG	Crystalline Silicon on glass
CBD	Chemical bath deposition
CBO	Conduction-band offset
CE	Collection efficiency
CGS	$CuGaSe_2$
CIGS	$Cu(In,Ga)Se_2$
CIS	$CuInSe_2$
CZTSSe	$Cu_2ZnSn(S,Se)_4$ Copper-Zinc-Tin-Sulphide/Selenide
F(E)	Fermi distribution
IB	Intermediate band
GB	Grain boundary
J-V	Current-density vs. voltage [curve]
MJ	Multi-junction
one − sun	Used as a synonym for AM1.5 illumination
PV	Photovoltaic
PX	Polycrystalline
QE	Quantum efficiency
SCAPS	Solar Cell Capacitance Simulator
QNR	Quasi-neutral region
SCR	Space-charge region

Se	Selenium
SEM	Scanning electron microscopy
SRH	Shockley-Read-Hall [recombination]
WKB	Wentzel-Kramers-Brillouin [approximation]
TCO	Transparent conduction oxide
ZnO	Zinc Oxide

List of Figures

List of Tables

Table of Contents

Motivation

Majority of the world population relies on oil, coal and natural gas for its energy requirements. Fossil fuels are non-renewable, that is, they draw on finite resources that will eventually dwindle, becoming too expensive or too environmentally damaging to retrieve. Moreover electricity generation is the leading cause of industrial air pollution in the world. Most of world electricity comes from fossil fuels (oil, coal, natural gas), nuclear, and other non-renewable power plants. Producing energy from these resources takes a severe toll on our environment, polluting our air, land, and water. Renewable energy sources can be used to produce electricity with fewer environmental impacts. It is possible to make electricity from renewable energy sources without producing carbon dioxide (CO_2), the leading cause of global climate change. Renewable energy is energy derived from natural resources that replenish themselves over a period of time without depleting the Earth's resources. These resources also have the benefit of being abundant, available in some capacity nearly everywhere, and they cause little (if any) environmental damage. Energy from the sun, wind, and thermal energy stored in the Earth's crust are examples. For comparison, fossil fuels such as oil, coal, and natural gas are not renewable, since their quantity is finite—once we have extracted them they will cease to be available for use as an economically viable energy source. While they are produced through natural processes, these processes are too slow to replenish these fuels as quickly as humans use them, so these sources will run out sooner or later.

In contrast, the many types of renewable energy resources, such as wind and solar energy are constantly replenished and will never run out. Most renewable energy comes either directly or indirectly from the sun. Sunlight, or solar energy, can be used directly for heating and lighting homes and other buildings, for generating electricity, and for hot water heating, solar cooling, and a variety of commercial and industrial uses. The power of the sun is almost unlimited and it provides nearly as much energy in one hour at earth's surface as the total amount of energy consumed in a year. The total power emitted by the sun is calculated by multiplying the emitted power density by the surface area of the sun which gives 9.5×10^{25} W. But solar power remains relatively untapped, a niche technology even in the most photon drenched areas of the world. Harnessing photons efficiently and converting them economically into energy remains a technological challenge. Today, photovoltaic technologies are dominated by wafer based crystalline silicon (monocrystalline, polycrystalline and ribbon silicon). The

major drive for research and development on PV cells during last three decades has been to reduce the cost of PV generated electricity. Cost of a solar cell or a module is primarily influenced by the interplay between its operational lifetime, its manufacturing cost per unit area and power conversion efficiency. Therefore, ongoing research efforts are focused on further increasing the efficiency of silicon-based solar cells with different grades of silicon, which can be manufactured at lower cost. Despite the constant improvement in bulk crystalline technologies, alternative photovoltaic approaches have been developed simultaneously during the past few decades. In an effort to reduce manufacturing costs, thin film technologies that require lesser materials and can be processed onto thin and lower cost substrates using high throughput fabrication processes have been subject to active research and development.

At present there are various techniques, challenges and directions in modelling photovoltaic systems. Photovoltaics solar cells are very necessary because, (1) solar energy is the world's major renewable energy source and is available everywhere in different quantities. (2) Photovoltaic panels do not have any moving parts, operate silently and generate no emissions. (3) Solar technology is highly modular and can be easily scaled to provide the required power for different loads. It is nearly pollution-free energy source, low maintenance power plants with inexhaustible fuel supplies, the most obvious drawbacks are that the energy supply is irregular (the sun does not shine at night, at cloudy day, in fog etc.) and that at present the cost of solar electricity is several times that of conventional power.

Thin film solar cells (TFSC) are a promising approach; can be deposited on a variety of substrates (metal or insulator, flexible or rigid), by using different manufacturing techniques (ECD, PVD, CVD, plasma-based, hybrid, etc.). This flexibility and diversity of techniques gives superiority over crystalline silicon (c-Si), since they rely on the deposition of highly absorbing materials which allow for photoactive layers of a few micrometre thicknesses. Hence they can be produced by economical, high-volume manufacturing techniques. Thin-film (only a few microns thick, deposited on a substrate) solar cells are typically 100-times thinner than silicon cells. Thinner devices need less raw materials and can easily be deposited on low-cost substrates such as glass or foils. Proper understanding of thin-film deposition processes can help in achieving high-efficiency devices over large areas, as has been demonstrated commercially for different cells. TFSC will provide an important contribution to the global energy demand in the near future.

Currently I-III-VI_2 based thin film solar cells, including Cu(In,Ga)Se_2 (CIGS), which have achieved laboratory efficiencies of over 21%, are highly attractive, because their band gap is near the optimal value. CdTe, low cost SnS, CZTS and high band gap ZnTe based solar cells are also getting their laboratory importance in the research field. Although steady progress has been made for CIS/CGS alloy (CIGS solar cells), this progress has largely been driven by experiential optimization rather than by in-depth understanding of appropriate physical models.

This work have intended to correlate some of the well define forms of solar cells with newly emerged types, and fill some gaps that exist between state-of-the-art experimental solar cells and their device physics by modelling and simulation approach. Modelling and simulation is an important part of any engineering practice. In the current scenario, by using a computer and related software, an extremely complex system can be simulated and their performance can be predicted and monitored. If problem is complicated and not solved in a simple way "Numerical Simulation" in Engineering then means: instead of trying to solve all equations for a problem in the entire problem domain, split the problem into smaller pieces, solve those separately with appropriate methods and finally merge the partial results into the solution for the entire problem. Experimental and proper design and fabrication of novel nanostructured photovoltaic devices requires keen knowledge of the underlying physics governing solar cells performance. Fabrication runs are costly and time consuming, so it is beneficial to have a firm theoretical foundation on which to base future work. For simulation purposes different types of software are available for research community some of them are for commercial use. We plan to test and check the different free available software and choose the best-suited software for this purpose. By modelling PV devices we hope to contribute to achieve better performance of present and future PV solar cells. This work is going to be a decent contribution to the development of green energies.

Objectives

The main objective of this thesis is to explore the possibilities of numerical simulation as a tool for improving the performance of thin film solar cells. A systematic and detailed analysis of thin-film solar cells based on several materials have been done by using a dedicated software such as Solar Cell Capacitance Simulator (SCAPS).

The dominant topics for thin-film solar cells based in different materials such as CdTe, CIGS, SnS and ZnTe solar cells will be covered and discussed. This work establishes a detailed and well-explained baseline model for CdTe, CIGS, ZnTe, SnS solar cells and also give comprehensive simulation analysis for CIGS, CdTe, SnS and ZnTe based solar cells. The analysis focusing on J-V characteristic analysis, quantum efficiency analysis (QE), Fill-Factor (FF) and eta (%) (Efficiency (only under illumination)) analysis.

The conversion efficiency of CIGS solar cells depends on the amount of Ga in the CIGS absorber because the bandgap of the absorber depends on the Ga content. The trend is the higher the Ga content the lower the value of the energy of the bandgap. However, the conversion efficiency reaches a maximum for a certain amount of Ga. Therefore to contribute to the understanding of CIGS solar cells a detailed analysis for CIGS based solar cell as a function of the variation in the Ga/(Ga+In) stoichiometry ("grading") is required. Theoretically the quantum efficiency (QE) increases as a function of Ga concentration up to a 66% y in contrast with experimental values (31%). The reason is due the defects in the layer that causes recombination and hence QE not increases further. The simulated result shows an increase in the open circuit voltage (V_{OC}) as the band gap increases with Ga concentration, Fill-Factor (FF) and eta also increases with an analogous manner, whereas the short circuit current density (J_{SC}) decreases which is good for a solar cell, as for an ideal diode (solar cells) high value of V_{OC} and low value of J_{SC} gives high/improved value of QE and preferably decent results.

As mentioned before the bandgap of CIGS can be fitted by changing the amount of Ga. This is a way to improve the efficiency of PV devices but there is a second approach based in the use of multilayers with different bandgaps to harvest the maximum of solar radiation. In this context the modelling of such multilayer devices can be very useful to build more efficient PV devices. The simulated result for multi-layer ZnO/CdS/$CuInSe_2$/$CuGaSe_2$ gives very encouraging results even with a thinner value of the absorber layer that will further decrease

the material use. A multi-layer CIS/CGS based solar cell will provide cheap and efficient alternate solution.

Some PV devices (II-V based devices) increase their conversion efficiency with they are illuminated with concentrated sun light. In fact at present world record efficiencies of about 44.7% are achieved by using 4-mutijunctions under illumination of 297 SUN. The effect of multi-sun irradiation on the CIGS-based solar cells can also be modelled through SCAPS. Multi-sun analysis for CIS/CGS-based solar cells will further enhance the efficiency.

Modelling solar cells based on II-VI semiconductor materials are among the leading candidates for low-cost photovoltaic conversion of solar energy due to their high absorption coefficient and will overcome the deficiency of rare materials. Rare materials (In, in ICGS) are a bottleneck for Tera Watt (TW) production of solar system. Therefore alternate material solution will might be fulfil the dream of green universe. ZnTe-based solar cells analysis is an effort in this direction. Optimization of layer parameters and volume was briefly simulated for optimum values, the energy band diagram, J-V characteristic curve, FF, eta and efficiency were simulated in detail.

Intermediate band is an interesting concept for improving conversion efficiency and deserves to be studied. Theoretically the maximum conversion efficiency for a PV device based on a single absorber layer is limited by the called 'Queisser-Schotcklsy limit'. However, using Intermediate Band materials as absorbers PV devices can surpass this limit. For such materials efficiencies up to 60% have been proposed. Unfortunately the viability of these IB materials has not been definitively established experimentally. But it is possible to simulate the absorption coefficient of such an IB solar cells and we then use SCAPS for assessing the behaviour and performance of this kind of materials and devices. We have used SCAPS for analyse the main PV parameters of a PV solar cell based on ZnTe:O (IB) as an absorber layer (ZnTe:O/CdS/ZnO) solar cell, should provide high efficiency. The reason for high boosting of QE is the harassment of low energy photons that wasted otherwise.

And last but not least it is always convenient to have a tool for predicting the behaviour of PV devices based on new materials. For example, sulphurs materials are abundant and cheap materials and it is possible to predict the behaviour and performance of PV devices based on these cheap absorbers if the main optoelectronic characteristics of these materials are known. Numerical analysis of SnS based polycrystalline solar cells were described, effect of N_A, N_C and N_D on the overall performance on the cell.

SUMMARY

The modelling of solar cells enables us to understand the physical phenomena underlying the device behaviour. The use of computer-assisted numerical modelling is convenient for exploring novel solar cell design concepts as well as perform the simulation and analysis of such devices. Numerical modelling is well suited to look deep insight in the details of the physical operation of thin-film solar cells. Till date several modelling tools specific to thin-film PV devices have been developed. Such an approach is beneficial for two primary reasons. First, it is important to know the theoretical parameters towards which we proceed. This helps to support motivation for the experimental work to be undertaken and gives an accurate gauge of how the work is progressing. Second, realistic, physical device simulations enable for the analysis and possible optimization of experimental devices without the need for physically making the supposed devices. This allows for the crucial saving of resources by performing only the experiments and fabrications that are truly necessary. It is hopeful that this work may serve as a guide to the next series of modelling and simulation efforts that will aid in the development of novel photovoltaic devices and that the analysis performed herein will aid in their experimental realization. A numerical simulation programme, known as Solar Cell Capacitance Simulator (SCAPS) has been used for this purpose.

We have used SCAPS to model and study the behaviour of thin-film solar cells based in different materials such as CdTe, CIGS, SnS and ZnTe. Besides new concepts in photovoltaics such as multilayers solar cells, concentration and intermediate bands have also been covered in this work.

Study of the baseline parameters for the thin-film solar cells discussed in this work was carried out in detail, the comparative analysis for CIGS vs CdTe reveals that CdTe has high open circuit voltage (V_{OC}) and short circuit current (J_{SC}) as compare to CIGS, due to it high band-gap. Conversely, CIGS has better quantum efficiency (QE) then CdTe. ZnTe has high band gap, have high V_{OC} and J_{SC} but its QE is low, but suitable for the concept of intermediate band gap, if inserted, its QE will increase dramatically.

Modern, chalcogenide-based, thin film solar cells based on $CuIn_{(1-x)}Ga_xSe_2$ p-type absorbers are promising candidates for generating pollution-free electricity. CIGS-based devices have bandgaps, which are well suited for absorption of sunlight. Thin-film based on pure Indium,

$CuInSe_2$ (CIS) has a band gap of 1.0eV and that made of pure Ga, $CuGaSe_2$ (CGS) has 1.76eV, and anyhow substituting Gallium (Ga) for Indium (In) in $CuIn_xGa_{(1-x)}Se_2$, changes the band gap from 1.0 to 1.76eV.

The main photovoltaic parameters of a solar cell made of ZnO/CdS/CIGS has been obtained by numerical simulation with SCAPS. For this device we have performed a detailed study of the effect of Ga content on the overall parameters of solar cells. The obtained results have revealed that the increase of Ga concentration in the absorber layer results in higher efficiency up-to an extent, reaching the maximum efficiency for Ga content about 66%. After optimization of device parameters a maximum efficiency of 30.95% was reached for 66% Gallium content. The effect of other layers, ZnO and CdS was also considered, and layers' thicknesses were optimized for better performance. Decreasing of thickness is in favour of good result, but its handling and manufacturing are the issues. The effect of the concentration of donors and acceptors (N_A and N_D) in the CIGS absorber on the overall performance on the cell has been analysed.

The behaviour of ZnO/CdS/CIGS (Ga, 45 %) as a function of the concentrated irradiation has also been studied. The conversion efficiency reaches a maximum for about 20 SUN illumination and ranges from 27 % for 1 SUN and 3 % for 20 SUN.

SnS is a promising nontoxic and earth-abundant material suitable for photovoltaic applications. The photovoltaic cell consists of SnS absorber layer, CdS as buffer and ZnO as optical window layer, following the sequence p-SnS/CdS/ZnO. Photovoltaic solar cells based on Tin Sulphide (SnS) absorbers have been analysed by using SCAPS. After optimization of different parameters and layer thicknesses a maximum efficiency of 10.6%, V_{OC} of 0.92 Volts, J_{SC} of 13.4 mA/cm^2 and Fill Factor of 86.3% were reached. Simulation studies by varying several solar cell parameters such as thickness of various layers reveal that increasing the thickness of absorber layer results in higher efficiency. The concentration of shallow acceptors in the SnS has a crucial effect in the conversion efficiency, which rises up to about 15% for acceptor concentrations of 10^{19} cm^{-3}. The effect of the compensation ratio between donors and acceptors was also analysed but its effect on conversion efficiency is insignificant.

Solar cells based on II-VI semiconductors are also among the leading candidates for low-cost photovoltaic conversion of solar energy due to their high absorption coefficients and therefore the low material consumption for their production. The analysis of zinc telluride based (ZnTe) thin films solar cells was carried out by using SCAPS. The I-V characteristics, based

on dark and under illumination were simulated for the different configuration of input parameters. It has been revealed that increasing the ZnTe thickness (0.5–2.0 μm) results in higher efficiency of PV devices. Parameters such as thickness of various layers reveal that increasing the thickness of absorber layer results in higher efficiency. ZnTe is a p-type semiconductor with a bandgap of about 2.2-2.6 eV, which is too high for an efficient harvesting of solar photons but is suitable for hosting an intermediate band and spread the range of photons absorption.

Intermediate band (IB) is an interesting concept for improving the conversion efficiency of photovoltaic devices and deserves to be studied. Theoretically the maximum conversion efficiency for a PV device based on a single absorber layer is limited by the so called 'Queisser-Schotckly limit'. However, using Intermediate Band materials as absorbers PV devices can surpass this limit. For such materials efficiencies up to 60% have been proposed. It is possible to simulate the absorption coefficient of such an IB solar cells and we then use SCAPS for assessing the behaviour and performance of this kind of materials and devices. We have analysed the main PV parameters of a PV solar cell based on ZnTe:O as an absorber layer. The simulation of the structure ZnO/CdS/ZnTe:O solar cell gives an efficiency of 60%, while the structure ZnO/CdS/ZnTe without IB reaches efficiency below 10%. The reason for high boosting of QE is the harassment of low energy photons that wasted otherwise. $CuGaS_2$ has been proposed as a suitable material for hosting an IB by doping with V and Cr ($CuGaS_2$:V and $CuGaS_2$:Cr). Theoretical calculations for solar cells based on this IB material predict conversion efficiencies as high as 46.7%. However, this work attempts for modelling such a device did not produce results because SCAPS simulation always failed.

Multi-layer concept opens a new door for researcher, if they boost the performance further. Replacing the existing CIGS by multilayer, and simulated, ZnO/CdS/$CuInSe_2$/$CuGaSe_2$ gives very encouraging results of efficiency 30-40%, with a thinner value of the absorber layer that will further decrease the material use by 35-40%.

RESUMEN

La modelización numérica de las células solares resulta muy útil para comprender los fenómenos físicos que gobiernan el comportamiento de los dispositivos fotovoltaicos y permite explorar nuevos conceptos de diseño de células solares, así como simular y analizar el comportamiento de tales dispositivos. Actualmente existen varias herramientas de modelización específicas para dispositivos fotovoltaicos de capa fina. Estas herramientas son útiles por dos razones fundamentales. En primer lugar, es importante conocer los fundamentos teóricos sobre los que se basan los dispositivos. Esto ayuda a mantener la motivación para entender trabajo experimental y puede ayudar mejorar el rendimiento de los dispositivos. En segundo lugar, las simulaciones de los dispositivos físicos permiten analizar y optimizar diversos parámetros de los dispositivos experimentales sin necesidad de construir físicamente tales dispositivos. Esto permite un ahorro importante de los recursos y dejar la experimentación y fabricación de los dispositivos para cuando se tiene optimizado el dispositivo. Sin duda los avances realizados en el modelado y simulación de dispositivos ayudan al desarrollo de nuevos dispositivos fotovoltaicos y a su realización experimental. Un programa de simulación adaptado a células solares de capa fina y conocido como Solar Cell Capacitance Simulator (SCAPS) se ha utilizado para este propósito.

Hemos utilizado el SCAPS para modelar y estudiar el comportamiento de las células solares de película delgada basadas en materiales diversos como CdTe, CIGS, SnS y ZnTe. Además hemos usado la simulación para explorar nuevos conceptos en fotovoltaica como las células solares multicapas, el efecto de la concentración solar y los materiales de banda intermedia..

Se han estudiado y discutido en detalle los parámetros básicos que gobiernan el comportamiento de las células solares de película delgada. El análisis comparativo de dispositivos basados en CIGS y CdTe revela que el CdTe tiene una mayor tensión en circuito abierto (V_{OC}) que el CIGS mientras que la corriente de cortocircuito (J_{SC}) son similares. a CIGS. Esto es consecuencia de la mayor anchura de la banda prohibida del CdTe. Por el contrario, CIGS tiene mejor eficiencia cuántica (QE) que el CdTe.

Por otra parte el ZnTe tiene una banda prohibida de mayor energía, lo que significa un elevado V_{OC} pero tanto la corriente en corto circuito como (J_{SC}) pero su la eficiencia cuántica (QE) son bajas. Sin embargo el elevado valor de la banda prohibida del ZnTe hacen de este material un candidato interesante para alojar una banda de absorción intermedia que permite incrementar drásticamente la QE.

Las modernas células solares de capa fina basada en calcógenuros tipo p como el $CuIn_{(1-x)}Ga_xSe_2$ son candidatos prometedores para la generación de electricidad limpia. Las capas finas de CIGS tienen energías de las bandas prohibidas bien adaptadas a la absorción de la luz solar. Las capas finas basadas en indio, $CuInSe_2$ (CIS), tienen una banda prohibida de 1.0eV

mientras que las de galio, $CuGaSe_2$ (CGS) tienen 1.76 eV. Por tanto, jugando con la concentración relativa de Ga e In es posible ajustar la energía de la banda prohibida entre 1.0 y 1.76 eV.

Los principales parámetros fotovoltaicos de una célula solar de ZnO/CdS/CIGS han sido obtenidos por simulación numérica con SCAPS. Para este dispositivo hemos realizado un estudio detallado del efecto del contenido de Ga en los parámetros fotovoltaicos de las células solares. Los resultados obtenidos han puesto de manifiesto que el aumento de la concentración de Ga en los resultados capa absorbente produce una mayor eficiencia en el dispositivo alcanzando la máxima eficiencia para el contenido de Ga alrededor del 66%. Después de la optimización de diversos parámetros del dispositivo simulado se alcanzó una eficiencia máxima del 30.95% para un absorbente CIGS con un contenido del 66% de galio. También se consideró el efecto de las otras capas del dispositivo, la capa ventana de ZnO y la capa buffer de CdS, y se optimizaron los espesores de dichas capas para conseguir el mejor rendimiento. La disminución del grosor de algunas de las capas puede producir mejores resultados pero puede resultar un reto en el proceso de fabricación de los dispositivos. El efecto de la concentración de dadores y aceptores (N_A y N_D) en la capa absorbente de CIGS sobre el rendimiento global de la célula también ha sido analizado.

Se ha estudiado el comportamiento de la célula de ZnO/CdS/CIGS (Ga=45%) para una iluminación con concentración. La eficiencia de conversión alcanza un máximo para una iluminación de 20 soles y oscila entre 27% para 1 sol (Condición AM1.5) y 30% para 20 soles. La mejora de la eficiencia es más acusada en múltiples capas ejemplo de película delgada, donde la eficiencia es un 50% por 10 soles y 55% para 30 soles.

El sulfuro de estaño (SnS) es un material no tóxico y abundante en la tierra y que resulta prometedor para aplicaciones fotovoltaicas. La célula fotovoltaica consiste en una capa absorbente de SnS, CdS como buffer y ZnO como capa de ventana óptica, siguiendo el secuencia ZnO/CdS/p-SnS. Células solares fotovoltaicas basadas en capas absorbentes de SnS han sido modelizadas mediante SCAPS. Después de optimizar diferentes parámetros y espesores de las capas se consigue una eficiencia máxima del 10.6%, V_{OC} de 0.92 voltios, J_{SC} de 13.4 mA/cm^2 y factor de llenado del 86.3%. Estudios de simulación mediante la variación de varios parámetros de las células solares tales como el grosor de las diversas capas revelan que el aumento del espesor de los resultados capa absorbente en una mayor eficiencia. La concentración de aceptores poco profundos en el SnS tiene un efecto decisivo en la eficiencia de conversión, y esta se eleva hasta aproximadamente 15% para las concentraciones de aceptores entorno a 10^{19} cm^{-3}. También se analizó el efecto de la compensación entre los dadores y aceptores pero su efecto sobre la eficiencia de conversión es insignificante.

Las células solares basadas en semiconductores II-VI también se encuentran entre los principales candidatos a bajo costo la conversión fotovoltaica de la energía solar debido a sus

altos coeficientes de absorción y por lo tanto el bajo consumo de material para su producción. El análisis de las células solares basadas en capas finas de teluro de zinc (ZnTe) se ha realizado mediante el software SCAPS. Se han simulado las características IV, en oscuridad e iluminación en función de diferentes parámetros de entrada. Se ha puesto de manifiesto que el aumento del espesor ZnTe (0.5-2.0 micras) resulta en una mayor eficiencia de los dispositivos fotovoltaicos. Parámetros tales como el grosor de las diversas capas revelan que el aumento del espesor de los resultados capa absorbente en una mayor eficiencia. ZnTe es un semiconductor tipo p con una banda prohibida de aproximadamente 2.2-2.6eV, que es demasiado alta para un aprovechamiento eficiente de fotones solares, pero resulta adecuada para albergar una banda intermedia y extender el rango de absorción de fotones solares.

La materiales con banda intermedia representan un concepto interesante de nuevos materiales para mejorar de la eficiencia de conversión y por tanto merece ser estudiado. Teóricamente la eficiencia de conversión máxima para un dispositivo fotovoltaico basado en una sola capa absorbente está limitado por el llamado 'límite Queisser-Schotckly'. Sin embargo, el uso de materiales de banda intermedia en la capa absorbente de los dispositivos fotovoltaicos permite superar este límite. Para tales materiales se han propuesto eficiencias de hasta 60%. Es posible simular el coeficiente de absorción de un material con banda intermedia y luego analizar el comportamiento y el rendimiento de este tipo de materiales y dispositivos de banda intermedia con el SCAPS. En esta tesis hemos analizado los principales parámetros fotovoltaicos de una célula solar fotovoltaica basada en ZnTe:O como una capa absorbente. La simulación de la estructura ZnO/CdS/ZnTe:O alcanza una eficiencia del 60% mientras que estructura ZnO/CdS/ZnTe sin banda intermedia da una eficiencia por debajo del 10%. La razón de esta elevado valor de QE es la absorción de fotones de baja energía que de otro modo se desperdician porque no contribuyen a la generación de pare electrón-hueco. El $CuGaS_2$ ha sido propuesto teóricamente como un material adecuado par albergar una banda intermedia si se dopa con vanadio o cromo ($CuGaS_2$:V y $CuGaS_2$:Cr). Los cálculos teóricos para células solares basadas en este material con banda intermedia predicen eficiencias de conversión del 46.7%. Sin embargo nuestros intentos de modelizar tal dispositivo con SCAPS no han dado resultados debido a que la simulación no convergía y el software no era capaz de ofrecer resultados razonables.

El concepto de capas múltiples también ha sido investigado mediante SCAPS como una alternativa interesante para aumentar el rendimiento de las células de CIGS. Sustituyendo las capas de CIGS actuales por varias capas de CGS y CIS con distintas energías de las respectivas bandas prohibidas se consigue abarcar un espectro mas amplio y mejorar la eficiencia de conversión. La simulación de un dispositivo fotovoltaico basado en la secuencia ZnO/CdS/$CuInSe_2$/$CuGaSe_2$ ofrece resultados muy alentadores con una eficiencia del 30-40% que es superior a los dispositivos de una sola capa de CIGS. Además se consigue disminuir el espesor de la capa absorbente en un 35-40% lo que repercute en un ahorro de material

SUMARI

El modelatge de les cèl·lules solars ens permet comprendre els fenòmens físics subjacents al comportament del dispositiu. L'ús de la modelització numèrica assistida per ordinador és molt útil per explorar nous conceptes de disseny de cèl·lules solars, així com realitzar la simulació i l'anàlisi d'aquests dispositius. La modelització numèrica és molt adequada per obtenir una visió profunda dels detalls de l'operació física de les cèl·lules solars de pel·lícula fina. Fins hui s'han desenvolupat diverses eines de modelatge específiques per a dispositius fotovoltaics de capa fina. Tal enfocament és beneficiós per dues raons principals. En primer lloc, és important conèixer els paràmetres teòrics cap als quals, es procedeix. Això ajuda a mantenir la motivació per al treball experimental a realitzar i que dóna una mesura precisa de com el treball està progressant. En segon lloc, les simulacions de dispositius físics permeten analitzar i optimitzar els dispositius sense la necessitat de fer-los físicament. Això permet un important estalvi dels recursos mitjançant la realització dels experiments només i fabricacions que són veritablement necessàries. Aquest treball pot servir de guia per al desenvolupament de nous dispositius fotovoltaics i l'anàlisi realitzat en aquest document ajudarà en la seva realització experimental. Un programa de simulació numèrica conegut com Solar Cell Capacitance Simulator (SCAPS) s'ha utilitzat per a aquest propòsit.

Hem utilitzat el SCAPS per modelar i estudiar el comportament de les cèl·lules solars de pel·lícula prima basades en materials diversos com CdTe, CIGS, SnS i ZnTe. A més hem fet servir la simulació per explorar nous conceptes en fotovoltaica com són les cèl·lules solars multicapes, l'efecte de la concentració solar i els materials de banda intermèdia.

S'han estudiat i discutit en detall els paràmetres bàsics que governen el comportament de les cèl·lules solars de pel·lícula prima. L'anàlisi comparativa de dispositius basats en CIGS i CdTe revela que el CdTe té una major tensió en circuit obert (V_{OC}) que el CIGS mentre que el corrent de curtcircuit (J_{SC}) són similars per ambdós materials. Això és conseqüència de la major amplada de la banda prohibida del CdTe. Per contra, CIGS té millor eficiència quàntica (QE) que el CdTe.

D'altra banda el ZnTe té una banda prohibida de major energia, el que significa un elevat V_{OC} però tant el corrent en curt circuit com (J_{SC}) però la seva l'eficiència quàntica (QE) són baixes. No obstant això l'elevat valor de la banda prohibida del ZnTe fan d'aquest material un candidat interessant per allotjar una banda d'absorció intermèdia que permet incrementar dràsticament la QE.

Les modernes cèl·lules solars de capa fina basada en calcogenurs tipus p com el $CuIn_{(1-x)}Ga_xSe_2$ són candidats prometedors per a la generació d'electricitat neta. Les capes fines de CIGS tenen energies de les bandes prohibides ben adaptades a l'absorció de la llum solar. Les capes fines basades en indi, $CuInSe_2$ (CIS), tenen una banda prohibida de 1.0 eV mentre que

les de gal·li, $CuGaSe_2$ (CGS) tenen 1.76 eV. Per tant, jugant amb la concentració relativa de Ga i In és possible ajustar l'energia de la banda prohibida entre 1.0 i 1.76 eV.

Els principals paràmetres fotovoltaics d'una cèl·lula solar de ZnO/CdS/CIGS han estat obtinguts per simulació numèrica amb SCAPS. Per a aquest dispositiu hem realitzat un estudi detallat de l'efecte del contingut de Ga en els paràmetres fotovoltaics de les cèl·lules solars. Els resultats obtinguts han posat de manifest que l'augment de la concentració de Ga en els resultats capa absorbent produeix una major eficiència en el dispositiu aconseguint la màxima eficiència per al contingut de Ga voltant del 66%. Després de l'optimització de diversos paràmetres del dispositiu simulat es va assolir una eficiència màxima del 30.95% per a un absorbent CIGS amb un contingut del 66% de gal·li. També es va considerar l'efecte de les altres capes del dispositiu, la capa finestra de ZnO i la capa buffer de CdS, i es van optimitzar els gruixos d'aquestes capes per aconseguir el millor rendiment. La disminució del gruix d'algunes de les capes pot produir millors resultats però pot resultar un repte en el procés de fabricació dels dispositius. L'efecte de la concentració de donadors i acceptors (N_A i N_D) a la capa absorbent de CIGS sobre el rendiment global de la cèl·lula també ha estat analitzat.

S'ha estudiat el comportament de la cèl·lula de ZnO/CdS/CIGS (Ga=45%) per a una il·luminació amb concentració. L'eficiència de conversió arriba a un màxim per una il·luminació de 20 sols i oscil·la entre el 27% per a 1 sol (Condició AM1.5) i 30% per 20 sols. La millora de l'eficiència és més acusada en múltiples capes exemple de pel·lícula prima, on l'eficiència és un 50% per 10 sols i 55% per 30 sols.

El sulfur d'estany (SnS) és un material no tòxic i abundant a la terra i que resulta prometedor per aplicacions fotovoltaiques. La cèl·lula fotovoltaica consisteix en una capa absorbent de SnS, CdS com buffer i ZnO com a finestra òptica, seguint la seqüència ZnO/CdS/p-SnS. Cèl·lules solars fotovoltaiques basades en capes absorbents de SnS han estat modelitzades mitjançant SCAPS. Després d'optimitzar diferents paràmetres i gruixos de les capes s'aconsegueix una eficiència màxima del 10.6%, V_{OC} de 0.92 volts, J_{SC} de 13.4 mA / cm^2 i factor d'ompliment del 86.3%. Els estudis de simulació variant paràmetres diversos de les cèl·lules solars com ara el gruix de les diverses capes revelen que l'augment del gruix dels resultats capa absorbent en una major eficiència. La concentració de acceptors poc profunds en el SnS té un efecte decisiu en l'eficiència de conversió, i aquesta s'eleva fins a aproximadament 15% per a les concentracions de acceptors entorn a 10^{19} cm^{-3}. També es va analitzar l'efecte de la compensació entre els donadors i acceptors però el seu efecte sobre l'eficiència de conversió és insignificant.

Les cèl·lules solars basades en semiconductors II-VI també es troben entre els principals candidats a baix cost la conversió fotovoltaica de l'energia solar a causa dels seus alts coeficients d'absorció i per tant el baix consum de material per a la seva producció. L'anàlisi de les cèl·lules solars basades en capes fines de telur de zinc (ZnTe) s'ha realitzat mitjançant

el programari SCAPS. S'han simulat les característiques IV, en foscor i il·luminació en funció de diferents paràmetres d'entrada. S'ha posat de manifest que l'augment del gruix ZnTe (0.5-2.0 micres) resulta en una major eficiència dels dispositius fotovoltaics. Paràmetres com ara el gruix de les diverses capes revelen que l'augment del gruix dels resultats capa absorbent en una major eficiència. ZnTe és un semiconductor tipus p amb una banda prohibida d'aproximadament 2.2-2.6 eV, que és massa alta per a un aprofitament eficient de fotons solars, però resulta adequada per albergar una banda intermèdia i estendre el rang d'absorció de fotons solars.

La materials amb banda intermèdia representen un concepte interessant de nous materials per a millorar de l'eficiència de conversió i per tant mereix ser estudiat. Teòricament l'eficiència de conversió màxima per a un dispositiu fotovoltaic basat en una sola capa absorbent està limitat per l'anomenat 'límit Queisser-Schotckly'. No obstant això, l'ús de materials de banda intermèdia en la capa absorbent dels dispositius fotovoltaics permet superar aquest límit. Per aquests materials s'han proposat eficiències de fins a 60%. És possible simular el coeficient d'absorció d'un material amb banda intermèdia i després analitzar el comportament i el rendiment d'aquest tipus de materials i dispositius de banda intermèdia amb el SCAPS. En aquesta tesi hem analitzat els principals paràmetres fotovoltaics d'una cèl·lula solar fotovoltaica basada en ZnTe: O com una capa absorbent. La simulació de l'estructura ZnO/CdS/ZnTe:O arriba a una eficiència del 60% mentre que estructura ZnO/CdS/ZnTe sense banda intermèdia dóna una eficiència del 10%. La raó d'aquesta elevat valor de QE és l'absorció de fotons de baixa energia que d'altra manera no contribueixen a la generació de parells electró-buit. El $CuGaS_2$ ha estat proposat teòricament com un material adequat parell albergar una banda intermèdia si es dopa amb vanadi o crom ($CuGaS_2$:V i $CuGaS_2$:Cr). Els càlculs teòrics per a cèl·lules solars basades en aquest material amb banda intermèdia prediuen eficiències de conversió 46.7%. No obstant això els nostres intents de modelitzar tal dispositiu amb SCAPS no han donat resultats a causa de que la simulació no convergia i el programari no va ser capaç d'oferir resultats raonables.

El concepte de capes múltiples també ha estat investigat mitjançant SCAPS com una alternativa interessant per augmentar el rendiment de les cèl·lules de CIGS. Substituint les capes de CIGS actuals per diverses capes de CGS i CIS amb diferents energies de les respectives bandes prohibides s'aconsegueix abastar un espectre més ampli i millorar l'eficiència de conversió. La simulació d'un dispositiu fotovoltaic basat en la seqüència ZnO/CdS/$CuInSe_2$/$CuGaSe_2$ ofereix resultats molt encoratjadors amb una eficiència del 30-40% que és superior als dispositius d'una sola capa de CIGS. A més s'aconsegueix disminuir l'espessor de la capa absorbent en un 35-40% el que repercuteix en un estalvi de material.

CHAPTER 1

An Introduction to Photovoltaics

1 An Introduction to Photovoltaics

Satisfying world´s growing energy demand is one of the most significant challenges. As world population grows and living standard improves, the total energy demand also increases. Today major share of the energy produced by mankind comes from fossil fuels, but unfortunately there are limited reserves of fossil fuels, the primary sources of energy. The use of fossil fuel causes environmental hazards and contributes to global warming as well as these resources are on the decline. There is an urgent need to rely on technologies that are economically feasible and environmentally friendly. The energy from sources based on newer technologies such as the solid state semiconductor photovoltaic devices have emerged as a relatively sustainable energy source, environmentally clean and cost competitive if produced on a large scale. Solar energy in one form or another is the source of nearly all energy on the earth. All animals and plants (living things) rely on the sun for warmth and food. People harness the sun energy in different ways. An average of 125000TW solar power strikes our planet at any time. Therefore solar energy is ideal for power generation as it is abundant, clean and renewable.

1.1 Introduction

To harness solar energy directly and convert solar power into electrical power, newer technologies as the solid state semiconductor photovoltaic cells (PV) are used. PVs have emerged as a relatively sustainable energy source, environmentally clean and cost competitive if produced on a large scale.

On the other hand, the later evolution in industry is resulting in a continuous drop in cell and modules prices, which along with the steady increase in energy price, is bringing closer than ever the long awaited parity grid. However, there is still a long way to go both in efficiency increase and cost reduction in order to benefit from the full potential of solar energy. A PV system is consisting of PV cells assembled into modules, connected in arrays and a balance of system (BOS) component. The set of components in the BOS consist of batteries, wiring, fuses, inverters etc. In some systems sun tracking system is used, although it may cause an increase in the efficiency but boost the overall module cost. As at night time (dark) or in cloudy weather it does not work therefore the efficiency and performance are affected a lot.

1.2 Solar cells – some historical facts

Energy plays a pivotal role in technological and socio-economic development of humanity. Majority of the population count on oil, coal and natural gas to supply most of their energy needs, all these fossil fuels have finite resource. The world will run out of fossil fuels as well as it will become too expensive. The use of fossil fuels also produce greenhouse gases that contribute to global warming, and causes soil, air and water pollution. With increase of population, the global demand for energy continuously increases, as energy is the lifeline and status symbol of civilized societies. As a well-known major energy resource, petroleum reserves are utilizing intensively with increase in human population and high industrial development. It seems humankind is heading towards an energy crisis. Action must be taken to develop new sources of energy to explore and effectively utilize renewable bases and to cope with this crisis. Renewable energy resources that mainly consist of wind, solar, hydropower, biomass, geothermal, hydrogen and ocean sources, offer clean alternatives to fossil fuels. They will never run out, and they produce no pollution or greenhouse gases.

Solar energy is abundant, clean, cheap, renewable, with no harmful waste product, available everywhere and a very attractive alternative source. Photovoltaic effect is the direct conversion of solar energy to electricity via electronic devices called solar cells (SC). SC are mainly made from silicon (Si), the most common element on earth, being mechanically simple and with no moving part to wear out, can operate for many years with no (little) maintenance, also work in cloudy weather [1].

In 1839, French scientist Edmond Becquerel discovered the photovoltaic effect, for the first time. He observed that a voltage was developed, when he directed sun light on to the electrode in an electrolyte while experimenting with an electrolytic cell made up of two metal electrodes placed in an electricity–conducting solution. He observed that electricity generation increased when exposed to light [2]. In 1860, French mathematician August Mouchet introduced the idea of solar steam engine, and then he and Abel Pifre constructed the first solar powered engine. Modern parabolic dish collectors are the prototypes of that engine. William Grylls Adams and Richard Evans Day observe the PV effect in selenium [3]. In 1880, Samuel P. Langly invented the measuring device for light and named it as “bolometer” [4]. The first solar cell (1% efficient) from selenium wafers came into being in 1838, the inventor was an American scientist Charles Fritts, who coated the semiconductor Selenium with an extremely thin layer of gold to form the junctions [5]. The progress

continue and in 1891, Clarence Kemp patented a device related to solar water heater [6]. A number of other researchers and scientists proceeded further in this development, Wilhelm Hallwachs in 1904 discovered that a combination of Copper and Cuprous Oxide is photosensitive [7]. Polish scientist Jan Czochralski developed a way to grow single crystal silicon in 1918, the backbone of modern Si technology [8]. The milestone led by a group of scientist in Bell Labs of United States (US), where they made the first solar cell with 4% conversion efficiency in 1953 [9]. Reynolds developed Cadmium-Sulphide with the similar efficiency in the same decade [10]. This development and enhancement is still in booming and in the current era, different generation and types of the PV cells have been developed.

Recently the use of Photovoltaic solar cells has dramatically increased and a number of research centers and PV industries are contributing to the exploitation and harassment of solar energy. The highest confirm one sun as well as concentrated modules efficiencies and other related parameters (basic and necessary) are listed in a latest literature [11]. In this paper it is briefly described the different generation and current trends for achieving highest efficiency for the development of PV solar technologies.

In the year 1767 a Swiss scientist named Horace-Benedict de Saussure created the first solar collector, an insulated box covered with three layers of glass to absorb heat energy. Saussure's box became widely known as the first solar oven, reaching temperatures of 230 degrees Fahrenheit.

In 1873, Willoughby Smith discovered photoconductivity of a material known as selenium. The discovery was to be further extended in 1876 when the same man discovered that selenium produces solar energy. Attempts were made to construct solar cells using selenium. The cell did not work out well but an important lesson was learned – that solid could convert light into electricity without heat or moving parts. The discovery laid a strong base for future developments in the history of solar power.

1883-1891 Light Discoveries and Solar Cells During this time several inventions were made that contributed to the evolution of solar energy use. In 1883 the first solar cell was introduced. The cell was to be wrapped with Selenium wafers. Later in 1887 there was the discovery of the ultraviolet ray capacity to cause a spark jump between two electrodes. This was done by Heinrich Hertz. Later, in 1891 the first solar heater was created.

In 1908, William J. Baileys invented a Copper collector which was constructed using Copper coils and boxes. The Copper collector was an improvement of the earlier one collector but the

only difference was the use of Copper insulation. The improvements of the invention are being used to manufacture today's equipment.

In 1905, Photoelectric Effect was explained by Albert Einstein in a research paper on photoelectric effect still there was no experimental evidence about it. In 1916 a scientist known as Robert Millikan experimentally verified the photoelectric effect. In 1947, solar power popularity in the US following the Second World War, increased and solar power equipment started being popular among many people in the USA. There was a huge demand of solar energy equipment.

In 1958, Solar Energy in Space Solar power was used to power space exploration equipment such as satellites and space stations. This was the first commercial use of solar energy. There was major discussion about the efficiency of solar cells and reduction of its production costs between 1959 to 1970. Up to that time, the efficiency of the solar cells was only 14% and was not compatible to the high cost of their production. However in the 1970′s, Exxon Corporation designed an efficient solar panel which was less costly to manufacture. This was a major milestone in the history of solar energy.

In 1977 the US government embraced the use of solar energy by launching the Solar Energy Research Institute. Other governments across the world soon followed. In 1981, Paul Macready produced the first solar powered aircraft. The aircraft used more than 1600 cells, placed on its wings. The aircraft flew from France to England. In the year 1982 there was the development of the first solar powered cars in Australia. Between1986-1999 large scale solar energy plants with advancement were made and installed successfully. By the year 1999 the largest plant was developed producing more than 20 kilowatts. The most efficient solar cell was developed, with a photovoltaic efficiency of 36%. Due to the global financial crisis in the year 2008, the Spanish government reduced subsidies on ongoing solar power production in the country. This had a negative effect on the industry across the world. In 2010, Evergreen Solar and Solyndra solar two leading solar companies failed. This was due to lack of market for their high technology produced products.

The past few years have seen enormous investment in utility-scale solar plants, with records for the largest frequently being broken. As of 2012, the history's largest solar energy plant is the Golmud Solar Park in China, with an installed capacity of 200 megawatts. This is arguably surpassed by India's Gujarat Solar Park, a collection of solar farms scattered around the Gujarat region, boasting a combined installed capacity of 605 megawatts.

1.3 Solar cell – basic principles

Most photovoltaic (PV) technologies work under the same general principle. PV cell work almost analogous as a pn-junction diode. When PV cell is struck by a photon with appropriate energy, electrons are knocked free and their movement from one layer to the other generate electricity. In summary photovoltaic process is a 4-steps process [12].

1. A light absorption process which causes a transition in a material (the absorber) from a ground state to an excited state,
2. The conversion of the excited state into (at least) a free negative – charge and a free positive- charge carrier pair,
3. A discriminating transport mechanism, which causes the resulting free negative-charge carriers to move in one direction (cathode) and the resulting free positive-charge carriers to move in another direction (anode)
4. Closing the circle, the absorber goes to ground state

Existing technologies exploit this phenomenon with varying degrees of success. However, despite many years of research and development, these technologies are still far from being counted among the main energy sources. Some of the reasons for this stagnation are the relatively low conversion efficiency of standard industrial cells fabricated nowadays, while production and installation costs remained high until not long ago.

1.4 Different types of solar cells

1.4.1 Silicon based Solar cells

Crystalline silicon (c-Si) solar cell first developed in the Bell Lab in 1953 with an efficiency of 6%, yet have dominated the Photovoltaic market from their first birth and due to the prominence of silicon in the integrated circuit market. Si solar cell have been used in the space program from that time. Silicon is abundantly available hence cheap and used abundantly in many electronic devices. The highest efficiency reported yet is 25% for c-Si solar cell [13]. Basic schematic of crystalline silicon on glass (CSG) shown in Figure 1.1. The top layer is the emitter and the bulk material is consider as base. Si has a low absorption coefficient and its indirect band gap is low from that of the ideal 1.5eV. The market share for c-Si solar cell is above 80%. The subdivision of Si solar cells are monocrystalline, multi-crystalline and ribbon silicon solar cell [14].

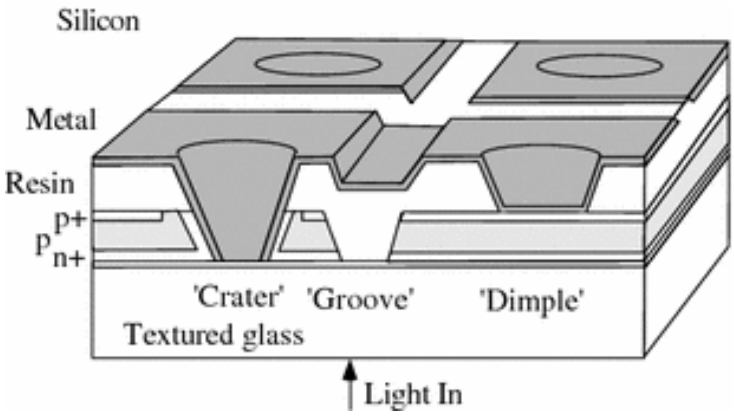

Figure 1. 1 Crystalline silicon on glass (CSG) unit cell structure

Crystalline Silicon on Glass (CGS) is the new era in silicon-based technology [15]. To overcome the difficulties for silicon wafer-based technology at the lowest possible prices for large-scale photovoltaic application, the CGS might be the best alternative.

1.4.2 Thin-film chalcogenide Solar cells

The I-III-VI chalcopyrite materials have some very desirable properties for PV application. The bandgap for $CuInSe_2$ is 1.53eV, an Ideal material for PV purposes. Further, the bandgap can be controlled by alloying with Ga, Al or S [16]. Moreover $Cu(In,Ga)Se_2$ has gained worthy reputation with high efficiency. The experimental results reported yet give the efficiency above 20%. A higher value of 20.1% and 20.3% efficient CIGS solar cell for 1 sun is reported [17]. The basic schematic of a thin-film CIGS solar cell is given in Figure 1.2.

The efficiency for concentrated (multi sun) is 22.8% reported in the latest literature. The basic schematic for CIGS in Figure 1.2, consist of a p-CIGS absorber layer with combination of n-CdS layer and ZnO window layer. The bandgap here is a function of Gallium and can be varied from 1.0 – 1.72 eV, its change causes the effect in the variation of other solar cell parameters [18].

Simulation results giving efficiency above 25% are also published. Though its efficiency is high but still it difficult to commercialize due to the availability of resources and particularly the rare metals Indium (In) and Gallium (Ga), that add to the cost of CIGS based technology [19].

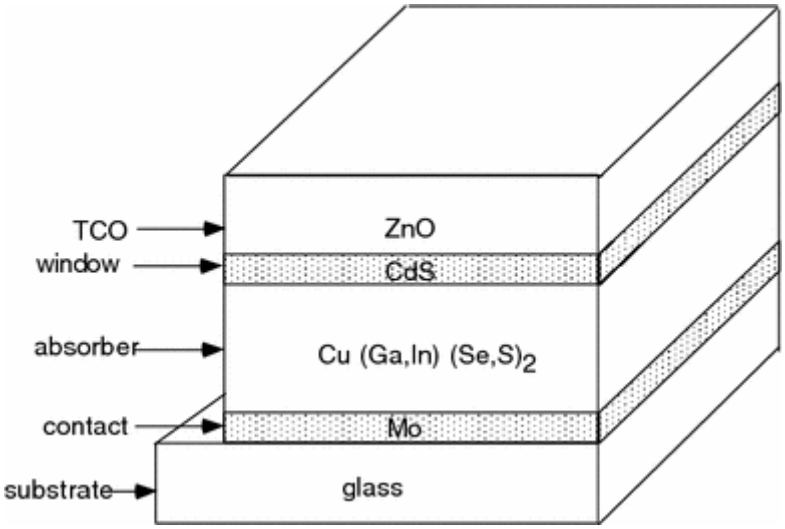

Figure 1. 2 Schematic of a thin film CIGS solar cell

1.4.3 Cadmium Telluride (CdTe) solar cells

CdTe has a direct bandgap with 1.5eV an ideal absorber material for high efficiency with low cost. It absorption coefficient (~10^5 /cm) is very good, a layer thickness of a few micrometre is sufficient to absorb ~ 90% of the incident photon. With a very good and high- efficiency of 19.6% is reported [11].

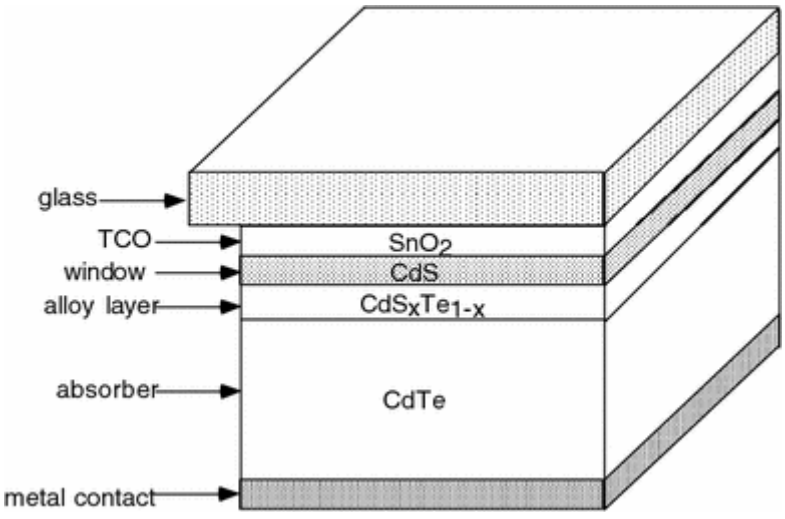

Figure 1. 3 Device schematic for a cadmium telluride cell

1.4.4 Tandem (multi-junction) solar cells

The aim of multi-junction solar cells is to exploit and convert all the incident photon from the sun into electricity. Because the major factor of energy loss is due to the gap between the photon energy and the bandgap energy Eg of absorber material.

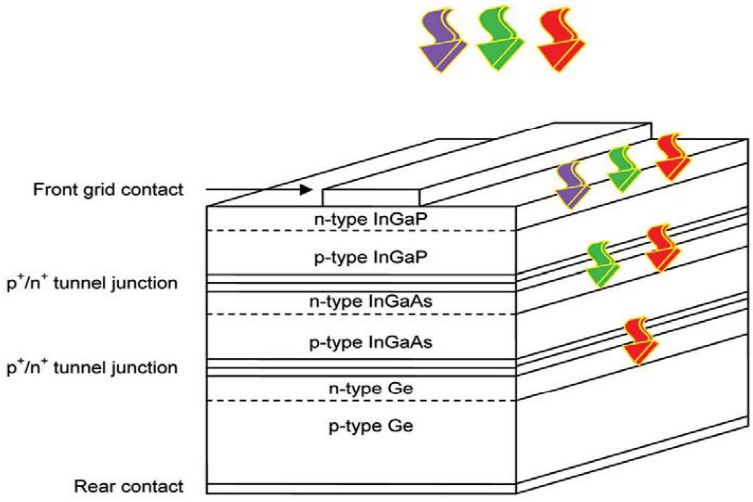

Figure 1. 4 A simplified schematic of a three-bandgap tandem solar cell. The bandgap of each cell decreases from the front to the back, giving both spectrum splitting and photon selectivity

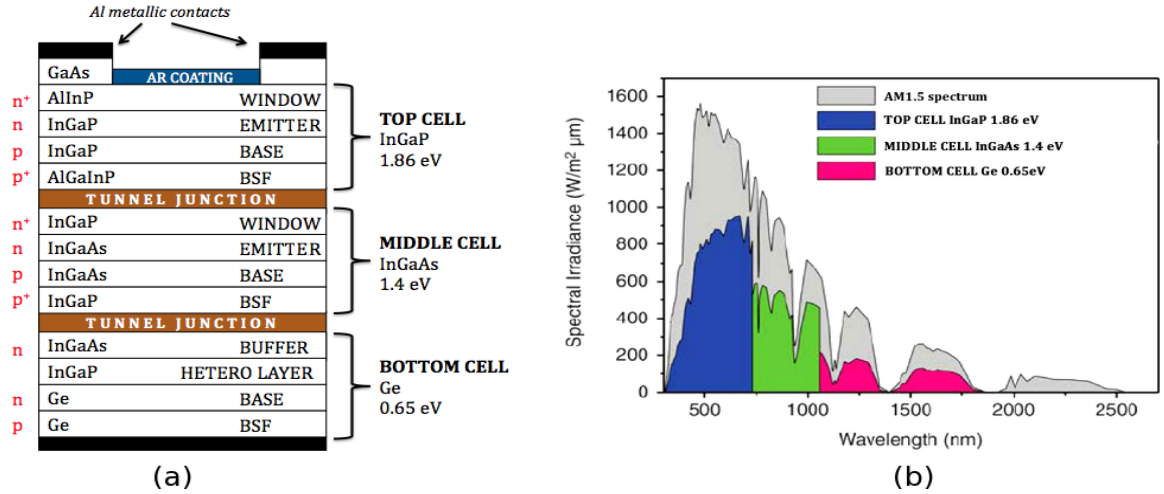

Figure 1. 5 The structure of a MJ solar cell. There are six important types of layers: pn junctions, back surface field (BSF) layers, window layers, tunnel junctions' anti-reflexive coating and metallic contacts

(b) Graph of spectral irradiance vs. wavelength λ over the AM1.5 solar spectrum.

A tandem (multi-junction) solar cell is the combination of two or more solar cell and an intervening buffer layer between two cells. Each cell absorbs the corresponding wavelength and the resultant efficiency increases. The highest efficiency with 44.7% is reported recently for a concentration of 297 suns [20].

1.5 Other Solar cell Technologies

Apart from the activities outlined above, a number of other kind of organic, non-organic and mixed solar cell have also been manufactured. The efficiency of organics solar cells is moderately lower than other type of solar cells, but they are catching up at a fast pace, due to cheap material availability and processing. Many centres like Mitsubishi chemical, Konarka, Heliatek and Solarmer Energy Inc. work on organic solar cell and have claimed efficiencies above 8.13%, Organic thin-film with efficiency of 10.7% is reported in [21]. Dye sensitised solar cell with efficiency of 11.9% [22] and with a mini-module, 9.9% is reported [23]. A low cost thin film-solar cell $Cu_2ZnSn(S,Se)_4$ abbreviated as CZTSSe solar cells have gained a high research attention. 12% efficiency is reported for a small area Copper-Zinc-Tin-Sulphide/Selenide (CZTSSe) cell that is fabricated by IBM and measured at the Newport Technology and Application Centre [24]. The research and development in the field is booming, the challenges to improve the energy conversion efficiency, as well as to improve the durability and stability of the devices.

References

[1] Treble, F. C., "Solar cells," IEE Proceedings (A Physical Science, Measurement and Instrumentation, Management and Education, Reviews) 127(8), 505-527, 1980.

[2] Becquerel, E., "On electric effects under the influence of solar radiation," *CR Acad. Sci, 9*, 711-4, 1839.

[3] Adams, W. G., "The Action of Light on Selenium," *Proceedings of the Royal Society of London, 25(171-178)*, 113-117, 1876.

[4] Langley, S. P., "The bolometer and radiant energy," *In Proceedings of the American Academy of Arts and Sciences . John Wilson and Son.*, 342-358, 1880.

[5] Sun, S. F., "Organic solar cell optimizations," *Journal of materials science, 40(6)*, 1429-1443, 2005.

[6] Raisul Islam, M. S., "Solar water heating systems and their market trends," *Renewable and Sustainable Energy Reviews, 17,* 1-25, 2013.

[7] Grondahl, L. O., "The copper-cuprous-oxide rectifier and photoelectric cell, "*Reviews of Modern Physics, 5(2)*, 141, 1933.

[8] Tomaszewski, P. E., "Jan Czochralski—father of the Czochralski method," *Journal of crystal growth, 236(1)*, 1-4, 2002.

[9] Chapin, D. M., "A New Silicon p-n Junction Photocell for Converting Solar Radiation into Electrical Power," *Journal of Applied Physics, 25(5)*, 676-677, 1954.

[10] Reynolds, D. C., "Photovoltaic effect in Cadmium Sulfide," *Physical Review, 96*, 533-534,1954.

[11] Green, M. A., "Solar cell efficiency tables (version 43)," *Prog. Photovolt: Res.* Appl., 22, 1-9, 2014.

[12] Fonash, S. J., "Solar cell device physics," Elsevier Inc., Amsterdam, 2nd Edn., 2010.

[13] Zhao, J. W., "19.8% efficient "honeycomb" textured multicrystalline and 24.4% monocrystalline silicon solar cells," *Applied Physics Letters, 73(14)*, 1991-1993, 1998.

[14] Glunz, S. W., R. Preu, and D. Biro, "Crystalline silicon solar cells: state-of-the-art and future developments," *Comprehensive Renewable Energy, Vol, 1: Photovoltaic Solar Energy, Elsevier, New York, NY, USA*, 353, 2012.

[15] Green, M. A., "Crystalline silicon on glass (CSG) thin-film solar cell modules," *Solar energy, 77(6)*, 857-863, 2004.

[16] Chopra, K. L., "Thin-film solar cells: an overview," *Progress in Photovoltaics. Research and Applications, 12(2-3)*, 69-92, 2004.

[17] Jackson, P. H., "New world record efficiency for Cu(In,Ga)Se_2 thin-film solar cells beyond 20%," *Progress in Photovoltaics: Research and Applications, 19(7)*, 894-897, 2011.

[18] Ullah, H., Marí, B., & Cui, H. N., "Investigation on the Effect of Gallium on the Efficiency of CIGS Solar Cells through Dedicated Software," Applied Mechanics and Materials, 448, 1497-1501, 2014.

[19] Andersson, B. A., "Materials availability for large-scale thin-film photovoltaics," *Progress in photovoltaics: research and applications, 8(1),* 61-76, 2000.

[20] Dimroth, F., Grave, M., Beutel, P., Fiedeler, U., Karcher, C., Tibbits, T. N., and Schwarzburg, K., "Wafer bonded four-junction GaInP/GaAs//GaInAsP/GaInAs

concentrator solar cells with 44.7% efficiency," Progress in Photovoltaics: Research and Applications, 22(3), 277-282, 2014.

[21] Robert, F., "Outlook Brightens for Plastic Solar Cells," *Science, 332(6027)*, 293, 2011.

[22] Komiya, R. F., "Improvement of the conversion efficiency of a monolithic type dye-sensitized solar cell module," *Technical Digest, 21st International Photovoltaic Science and Engineering Conference*, (pp. 2C-5O-08), Fukuoka, 2011.

[23] Morooka, M. O., "Development of dye-sensitized solar cells for practical applications," *Electrochemistry, 77*, 960–965, 2009.

[24] Winkler, M. W., "Optical designs that improve the efficiency of $Cu_2ZnSn(S,Se)_4$ solar cells," *Energy and Environmental Science*. doi:10.1039/c3ee42541j, 2013.

[25] Retrieved from pveducation: http://www.pveducation.org/pvcdrom/design/ solar-cell-parameters, 2014.

CHAPTER 2

Background

2 Background

The current chapter aims to give a brief introduction on the important principles and properties of semiconductors and photovoltaic solar cells. This includes a brief description of state-of-the-art CIGS thin film solar cells. The dissertation mainly focused on numerical simulations of solar cells; therefore, it is essential to review basic measurement, theory principle and governing mathematical and physical processes. As there are many processes inside the solar cells, hence our discussion is limited to the basic current density vs. voltage (J-V), Quantum Efficiency (QE), Eta (efficiency (only under illumination, **η**)) and Fill Factor (FF) measurements.

2.1 Solar-cell Basics

Semiconductor materials have electrical properties somewhere in the middle, between those of conductors and in an insulator. They are neither good conductors nor good insulators, therefore they are termed as semi-conductors. In other words, it is a family of solids in which there exists a moderate gap of a few electron volts in the distribution of allowed energy states. According to the energy band theory, at $T = 0^0$ K, in a pure material, this gap separates one entirely filled band called valence band from one that is entirely empty band called conduction band [1]. When temperature rises i.e. for $T > 0^0$ K, a finite number of electrons get energy and moves to conduction band (free electrons) leaving behind states for the electrons in the valence-band (free holes). These free states (electron and holes) can gain kinetic energy since a quasi-continuum of higher or lower states are available to them respectively, hence they are able to respond to electric fields and concentration gradients that allow for macroscopic current flow. Figure 2.1 illustrates the comparison of band diagram for the three states of materials [2, 3].

2.1.1 Important semiconductor concepts

The ability of a semiconductor to conduct electricity can be greatly improved by adding certain impurities called dopant (donors or acceptors) to this crystalline structure, that can produce more free electrons than holes or vice versa. The so called process is doping.

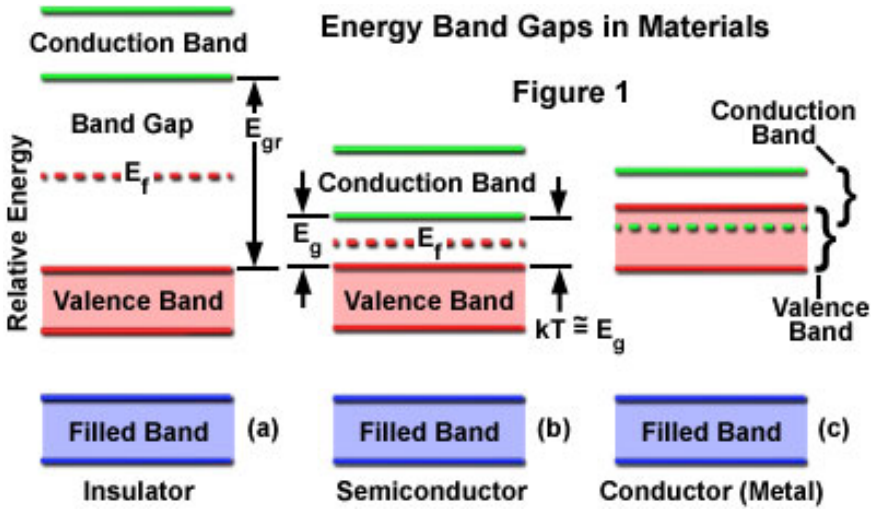

Figure 2. 1 Description of the electronic bands in solids

The equilibrium concentration of electrons and holes can be modified by extrinsic dopants as well as by defect level (additional states with in the band gap) that are intrinsic to the semiconductor.

The occupation of conduction and valence band states is governed by Fermi-Dirac statistics,

$$f(E) = \frac{1}{1+\exp\left(\frac{E-E_F}{kT}\right)} \qquad 2.1$$

where K is the Boltzmann constant and T the absolute temperature. Equation 2.1 describes the probability of electron occupation in the conduction band and, similarly, $1 - f(E)$ describes the probability for holes in the valence band. There is a unique relation in the difference from Fermi-level $f(E)$ with either edge, if $E(C) - f(E) \gg kT$ and $f(E) - EV \gg kT$, then $f(E)$ and $1 - f(E)$ can be replaced by the Boltzmann factors for many practical purposes. The simplified form is as below,

$$\exp\left(-\frac{E-E_f}{kT}\right) \text{ and } \exp\left(-\frac{E_F-E}{kT}\right) \qquad 2.2$$

The equations are for electrons in the conduction band and holes in the valence band, respectively. A semiconductor may be either n-type or p-type depending on whether electrons or holes are the majority carriers. Further information related to semiconductors is available in the literature and textbooks [4-6].

To calculate the Fermi level, the following relation is used, termed as carrier concentration.

2.1.2 Carrier Concentration in Equilibrium

The carrier concentration in equilibrium is given in equation 2.3 for n-type materials and in equation 2.4 for p-type materials.

$$\boldsymbol{n} = N_c \exp\left(\frac{E_F - E_c}{kT}\right) = n_i \exp\left(\frac{E_F - E_i}{kT}\right) cm^{-3} \quad 2.3$$

$$\boldsymbol{p} = N_V \exp\left(\frac{E_V - E_F}{kT}\right) = n_i \exp\left(\frac{E_i - E_F}{kT}\right) cm^{-3} \quad 2.4$$

Law of mass action is: $np = n_i^2$ 2.5

Carrier concentration for n-type material is:

$$n \approx N_D, \qquad p = \frac{n_i^2}{N_D} cm^{-3} \quad 2.6a$$

and for p-type material, the carrier concentration is:

$$p \approx N_A, \quad n = \frac{n_i^2}{N_A} cm^{-3} \quad 2.6b$$

2.1.3 Carrier Concentration under Bias

$$\boldsymbol{n} = n_i \exp\left(\frac{E_{FN} - E_i}{kT}\right), \qquad p = n_i \exp\left(\frac{E_i - E_{FP}}{kT}\right) cm^{-3}$$

a) Generation

Number of photons:

$$N_{ph} = N_s \exp(-\alpha\chi)\, cm^{-2} sec^{-1} \quad 2.7$$

Generation rate:

$$G = \alpha N_s \exp(-\alpha\chi)\ carriers\ sec^{-1} cm^{-3} \quad 2.8$$

Generation, homogeneous semiconductor: G = constant

P-type:$\Delta n = G\tau_n$

N-type:$\Delta p = G\tau_p$

b) Recombination

There are several different recombination mechanisms that prevents carriers from being extracted and that thus determines the carrier lifetime. A photo-generated exciton can

recombine geminately (recombination between the electron and hole originating from the same excitation), mono-molecularly through recombination centres, or bi-molecularly with another carrier generated elsewhere, or recombination through defects. General SRH recombination rate is given by the equation:

$$U = \frac{np - n_i^2}{\tau_p(n + n_1) + \tau_n(p + p_1)}\ carriers\ sec^{-1}cm^{-3} \quad 2.9$$

And under low injection conditions:

For electrons: $U_n = \frac{\Delta n}{\tau_n}$

For holes: $U_p = \frac{\Delta p}{\tau_p}$

$$\frac{1}{\tau_{TOT}} = \frac{1}{\tau_{AUG}} + \frac{1}{\tau_{RAD}} + \frac{1}{\tau_{SRH}} \quad 2.10$$

The fundamental operation of a pn-junction can be explain by the following set of equations:

1. Poisson's equation, it is a partial differential equation of elliptic type with broad utility in electrostatics and theoretical physics. It is used, for instance, to describe the potential energy field caused by a given charge or mass density distribution.

$$\frac{\partial \hat{E}}{\partial x} = \frac{\rho}{\varepsilon} = p + N_D^+ - n - N_A^- \quad 2.11$$

2. Transport equations:

$$J_n = q\mu_n n\hat{E} + qD_n \frac{dn}{dx}, \quad 2.12a$$

$$J_p = q\mu_p n\hat{E} + qD_p \frac{dp}{dx} \quad 2.12b$$

3. Continuity equations:

$$\frac{\partial n}{\partial t} = \frac{1}{q}\frac{\partial J_n}{\partial x} + G_n - U_n,\ \frac{\partial p}{\partial t} = \frac{1}{q}\frac{\partial J_p}{\partial x} + G_p - U_p \quad 2.13$$

General solution for no electric field, constant generation

$$\Delta n(x) = Aexp\left(-\frac{x}{L_n}\right) + Bexp\left(\frac{x}{L_n}\right) + G\tau_n \quad 2.14$$

2.2 Equations for PN Junction

The equation for built-in voltage pn-homojunction is given by,

$$V_0 = \frac{kT}{q}\ln\left(\frac{N_A N_D}{n_i^2}\right) \qquad 2.15$$

general ideal diode equation:

$$I = I_0\left(\exp\left(\frac{qV}{kT}\right) - 1\right) \qquad 2.16$$

I_0 for wide base diode:

$$I_0 = qA\left(\frac{D_n}{L_n}\frac{n_i^2}{N_A} + \frac{D_p}{L_p}\frac{n_i^2}{N_D}\right)$$

I_0 for narrow base diode:

$$I_0 = qA\left(\frac{D_n}{W_{p-type}}\frac{n_i^2}{N_A} + \frac{D_p}{W_{n-type}}\frac{n_i^2}{N_D}\right) \qquad 2.16a$$

Full diode saturation current equation:

$$I_0 = qA\left(\frac{D_n}{L_n}\frac{n_i^2}{N_A}\theta_n + \frac{D_p}{L_p}\frac{n_i^2}{N_D}\theta_p\right) \qquad 2.16b$$

$$\theta_n = \frac{\frac{S_n L_n}{D_n}\cosh\left(\frac{W_{p-type}}{L_n}\right) + sinh\left(\frac{W_{p-type}}{L_n}\right)}{cosh\left(\frac{W_{p-type}}{L_n}\right) + \frac{S_n L_n}{D_n}sinh\left(\frac{W_{p-type}}{L_n}\right)} \qquad 2.17a$$

$$\theta_p = \frac{\frac{S_p L_p}{D_p}\cosh\left(\frac{W_{n-type}}{L_p}\right) + sinh\left(\frac{W_{n-type}}{L_p}\right)}{cosh\left(\frac{W_{n-type}}{L_p}\right) + \frac{S_p L_p}{D_p}sinh\left(\frac{W_{n-type}}{L_p}\right)} \qquad 2.17b$$

Depletion region recombination:

$$I = I_{rec}\ exp\left(\frac{qV}{2kT}\right) \qquad 2.18$$

$$I = I_0\left[exp\left(\frac{q(V - IR_{series})}{kT}\right) - 1\right] \qquad 2.18a$$

2.2.1 Solar Cell Equations

$$J = J_0\left(\exp\left(\frac{qV}{nkT}\right) - 1\right) - J_{sc},\ J_{sc} \approx J_L \qquad 2.19a$$

$$V_{OC} = \frac{nkT}{q}\ln\left(\frac{I_{SC}}{I_0} + 1\right) \qquad 2.19b$$

$$J_L = qG(L_n + L_p + W) \quad 2.19c$$

for constant G, wide base

$$J_L = q\int_0^W G(x)CP(x)dx = q\int_0^W [\propto(\lambda)H_0 \exp(-\propto(\lambda)x)d\lambda]CP(x)dx \quad 2.20$$

2.2.2 Material Constants and Common Units

Intrinsic carrier concentration:

$$n_i = \sqrt{N_C N_V}\exp\left(\frac{-E_C}{2kT}\right) cm^{-3} \quad 2.21$$

Effective density of states:

$$N_C = 2[\frac{m_n^* kT}{2\pi h^2}]^{\frac{3}{2}},\ N_V = 2[\frac{m_p^* kT}{2\pi h^2}]^{\frac{3}{2}} cm^{-3} \quad 2.22$$

Intrinsic energy level:

$$E_i = \frac{E_G}{2} + \frac{kT}{2}\ln\left(\frac{N_V}{N_C}\right) \approx \frac{E_G}{2}\ eV \quad 2.23$$

Diffusivity

$$D_n = (\frac{kT}{q})\mu_n,\ D_p = (\frac{kT}{q})\mu_p\ cm^2/\text{s} \quad 2.23$$

Minority carrier diffusion length

$$L_n = \sqrt{D_n\tau_n},\ L_p = \sqrt{D_p\tau_p}\ (length\ units) \quad 2.24$$

Resistivity and conductivity:

$$\rho = \frac{1}{\sigma} = \frac{1}{q(\mu_n n + \mu_p p)}\Omega cm \quad 2.25$$

Resistance, homogeneous:

$$R = \rho\frac{l}{A}\Omega \quad 2.25a$$

Permittivity:

$$\varepsilon = \varepsilon_S\varepsilon_O = \mathrm{K}_S\varepsilon_O\ Farad/cm \quad 2.26$$

2.2.3 Radiant Energy

Wavelength and energy of a photon:

$$E = \frac{hc}{\lambda} \quad 2.27$$

If E is in eV and λ is in μm

$$E(eV) = \frac{1.24}{\lambda(\mu m)} \quad 2.27a$$

Spectral irradiance for black body:

$$F(\lambda) = \frac{2\pi hc^2}{\lambda^5\left(\exp\left(\frac{hc}{\lambda}\frac{1}{kT}\right)-1\right)} \quad 2.27b$$

Power density of a non-ideal black body:

$$H\left(\frac{W}{m^2}\right) = \varepsilon\sigma T^4 \quad 2.28$$

Photon flux and power density:

$$H\left(\frac{W}{m^2}\right) = \Phi\times\frac{E(J)}{photon} = q\Phi E(eV) = q\Phi\frac{1.24}{\lambda} \quad 2.29$$

$$I_{D1} = I_{SD1}[\exp\left(\frac{q(V_L + I_L R_s)}{n_1 kT}\right) - 1] \quad 2.30a$$

$$I_{D2} = I_{SD2}\left[\exp\left(\frac{q(V_L + I_L R_s)}{n_2 kT}\right) - 1\right] \quad 2.30b$$

$$I_{sh} = \frac{V_L + I_L R_s}{R_{sh}} \quad 2.30c$$

2.3 Basic parameters and electrical characterization methods

2.3.1 Overall Current (I)

The mathematically expression for the current is given in (equation 2.19a), that is also elaborate with a little extension,

$$Over\ all\ current\ (I) = Diode\ dark\ current(I_D) - light - induced\ current\ (I_L)$$

$$I = I_0\left[\exp\left(\frac{eV}{kT}\right) - 1\right] - I_L \quad 2.31$$

Here I_0 is the saturation current also known as the leakage current or diffusion current, e is electron charge and k is Boltzmann's constant. Both I_L *and* I_0depends on the solar cell structure.

2.3.2 Short circuit current (I_{sc})

Short-circuit current is the largest current which may be drawn from the solar cell and will define as the current through the solar cell when the load is zero (when the solar cell is short circuited). $\boldsymbol{I_{sc}}$ is due to the generation and collection of light-generated carriers. The $\boldsymbol{I_{sc}}$ depends mainly on the area of the solar cell, the number of incident photons as well as its spectrum, the collection probability and the optical properties. The diffusion length and surface passivation are critical material parameters. The graphical value for short-circuit current is $\boldsymbol{(I_{SC})}$ is exposed in Figure 2.2.

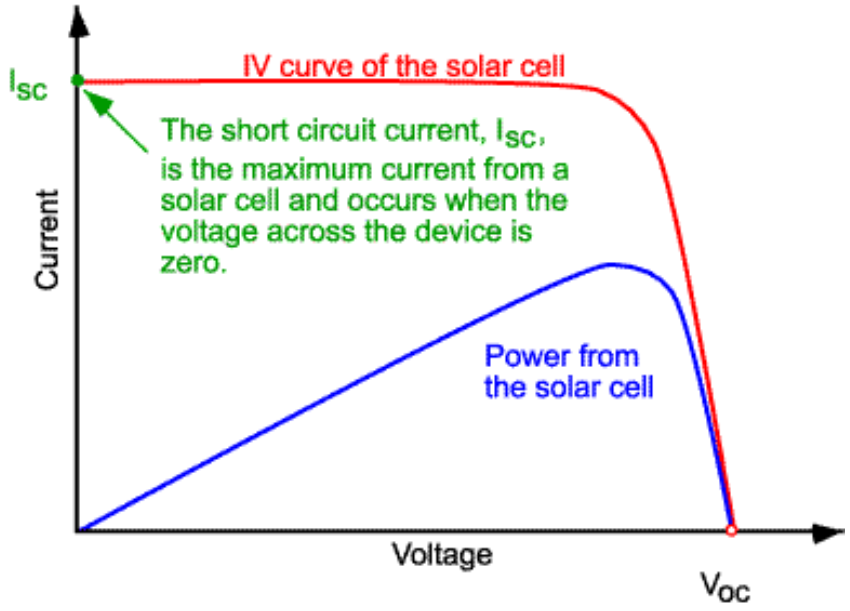

Figure 2. 2 The short-circuit current and open-circuit voltage in a V-I curve

2.3.3 Open circuit voltage (V_{0C})

The open circuit voltage $\boldsymbol{(V_{0C})}$ occurs, when there is no current passing through the cell. It is a maximum voltage available from a solar cell at zero current, the equation is given

$$V(at\ I = 0) = V_{0C} = \frac{nkT}{q} \ln\left(\frac{I_L}{I_0} + 1\right) \qquad 2.32$$

It is the Voltage for maximum load in the circuit for forward-bias power quadrant. The open-circuit voltage $\boldsymbol{(V_{0C})}$ is shown in Figure 2.2.

2.3.4 Fill-Factor *(FF)*

It is a parameter which, in conjunction with V_{oc} and I_{sc}, determines the maximum power from a solar cell. The FF is defined as the ratio of the maximum power from the solar cell to

the product of V_{oc} and I_{sc}. Graphically the FF also known as the curve factor is a measure of the "squareness" of the solar cell and is also the area of the largest rectangle which will fit in the I-V curve. It's ideal value is one, which is not possible, for silicon solar cells it's maximum value is 0.88. It's mathematical expression is

$$FF = \frac{P_{max}}{V_{OC} \times I_{SC}} = \frac{V_{max} \times I_{max}}{V_{OC} \times I_{SC}} \quad 2.33$$

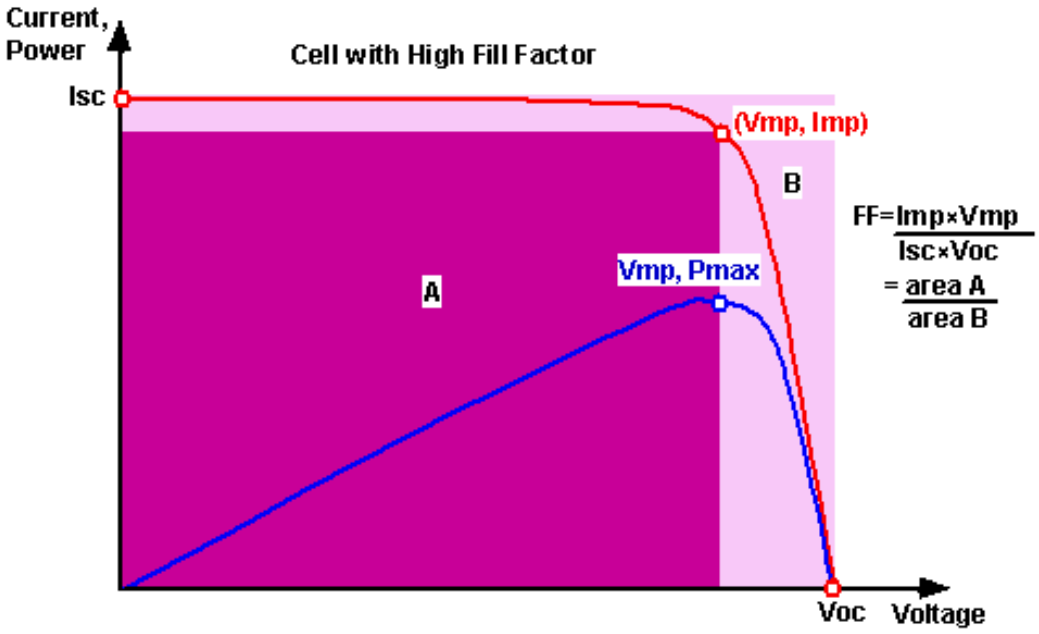

Figure 2. 3 Graph of cell output current (red line) and power (blue line) as function of voltage

Also shown are the cell short-circuit current (I_{sc}) and open-circuit voltage (V_{oc}) points, as well as the maximum power point (V_{mp}, I_{mp}) [7]

2.3.5 Maximum Power (P_{max})

The power output is defined as

$$P_{out} = V_{out} \times I_{out} \quad 2.34a$$

No power is generated under short-circuited or open circuited condition, when any or both of these are zero out- put power (P) will be zero. The device will provide maximum power (P_{max}) for maximum values of V and I.

$$P_{max} = V_{max} \times I_{max} \quad 2.34b$$

In term of Fill-Factor the maximum power is

$$P_{max} = V_{oc} \times I_{SC} \times FF \quad 2.34c$$

2.3.6 Quantum efficiency (QE)

Quantum efficiency (QE): when light (packets) shining on the solar cell, a number of charge carriers produces, "The ratio of the number of charge carriers collected by a photovoltaic cell to the number of photons (packet of light) of a given energy shining on the solar cell". In other words, QE relates to the response of a solar cell to different wavelengths. QE therefore, is a function of energy or wavelength. The power conversion efficiency of a solar cell is given as

$$\eta = \frac{P_{max}}{P_{in}} = \frac{I_{max} \times V_{max}}{Incident\ \ solar\ radiation \times Area\ of\ solar\ cell} \qquad 2.35$$

where $I_{max}\ and\ V_{max}$ are the current and voltage for maximum power. Another term that is conversion efficiency of a PV cell and define as the percentage of the solar energy shining on a PV device that converted into electrical energy. Improving conversion efficiency is a key goal of research that will cause effect the cost and other solar market. There are many factors that affecting the conversion efficiency including temperature, reflection, and wavelength of light, recombination and natural resistance of the material.

2.3.7 J-V characteristic of a PV device

Solar cell is working as a large diode if there is illumination on it, and the curve is the same as for a forward biased diode. On illuminating, the IV cure shifts due to power generation. The shift increase as the illumination increases. Basically the I-V curve is the superposition of curves in these two different conditions. According to diode law, illuminating a cell adds to the normal dark current in the diode, and mathematically expressed as, also in (Eqn, 2.18).

$$I = I_0 \left(\exp\left(\frac{qV}{kT}\right) - 1 \right)$$

The current-voltage curve is given in Figure 2.4, for dark and illumination. For dark it give a minimum value of current that is due to the minority carriers. By illuminating the cell by 1-Sun, Air Mass 1.5 global spectrum, on a horizontal plane the PV process starts and due to the charge carriers produced by incident photons is produced current [8, 9].

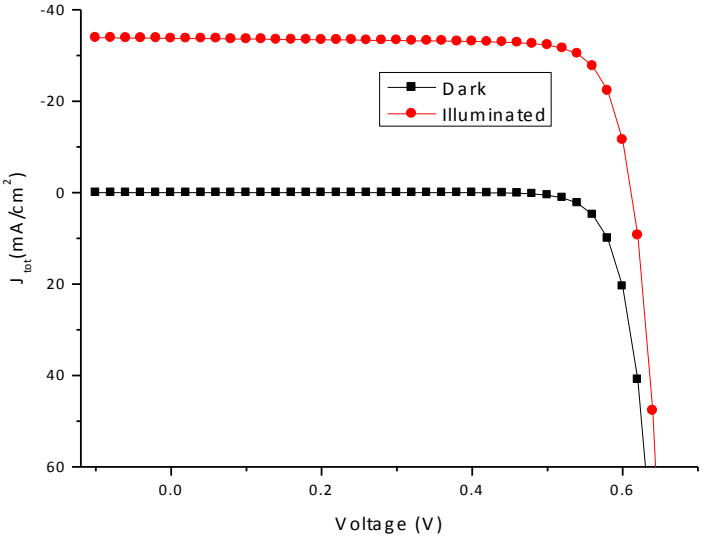

Figure 2. 4 J-V characteristic of a PV device for dark and illumination

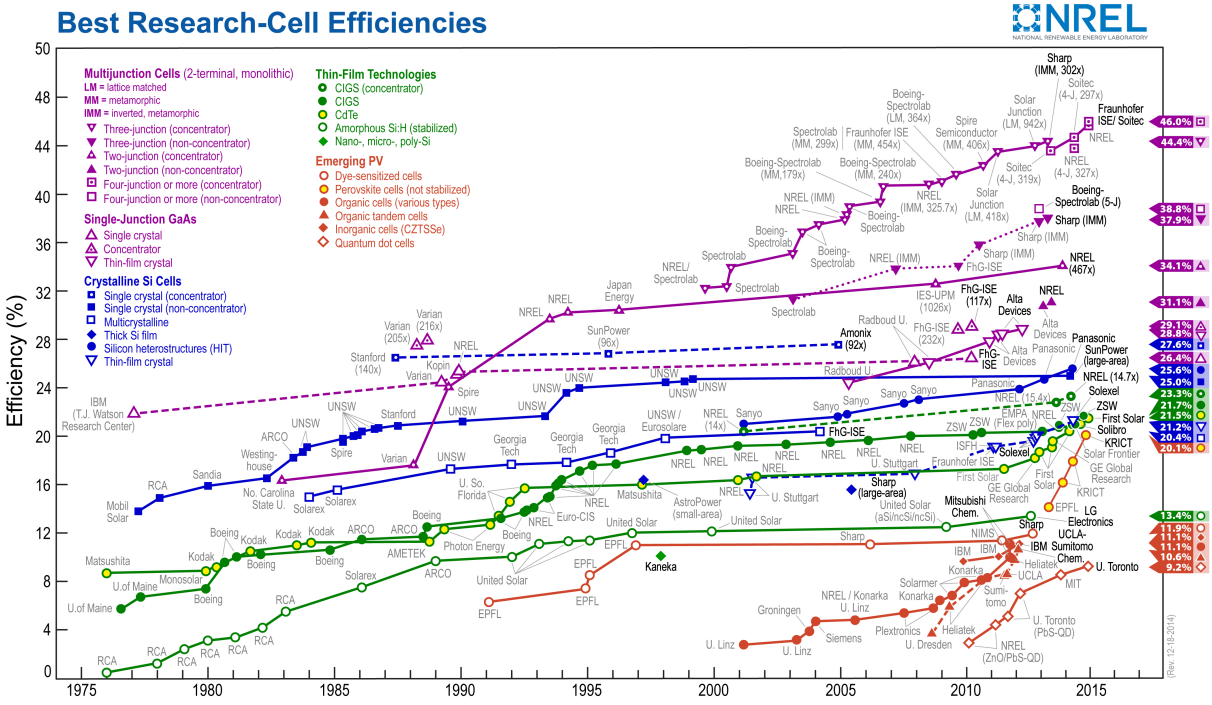

Figure 2. 5 New World Record with Two-Junction Solar Cell (NREL Sets), Best research-cell Efficiencies [10, 11]

The efficiency chart is given in Figure 2.5, the details of each curve, group and types is given in details in references [10, 11].

References

[1] S. Fonash., "*Solar cell device physics*," Elsevier, 2012.

[2] J. Singleton., "*Band Theory and Electronic Properties of Solids,"* Oxford Master Series in Condensed Matter Physics, 2001.

[3] http://www-opto.e-technik.uni-ulm.de/lehre/cs/

[4] S. M. Sze, "Physics of Semiconductor Devices," John Wiley & Sons, 2nd ed. 1981.

[5] M. A. Green., "Solar Cells," Prentice Hall, Englewood Cliff, NJ, 1982.

[6] A. L. Fahrenbruch and R. H. Bube, "Fundamentals of Solar Cells," Academic Press, Inc., New York, 1983.

[7] Fill Factor http://pveducation.org/pvcdrom/solar-cell-operation/fill-factor/07/05/2014

[8] Bird and Riordan, "Solar Cells," vol 15, p.365-391 1985.

[9] Partain, "Solar Cells and their applications," Wiley, p. 532, 1995.

[10] Special Coating Improves Performance of Solar Cells (17 Feb 2015) http://energyinformative.org/author/mathias/

[11] NREL Sets New World Record with Two-Junction Solar Cell, (17 Feb 2015) http://energyinformative.org/nrel-efficiency-record-two-junction-solar-cell

CHAPTER 3

Basics of numerical simulations

3 Basics of numerical simulations

Numerical modelling of photovoltaic solar cells is an important strategy to test the viability of proposed physical structure and its performance. This chapter introduces the concept of numerical simulation and explains the relevant physical models for the inside physical phenomenon like generation, recombination and transport of charge carriers (holes and electrons) in photovoltaic materials. This will be done with essential input parameters, to have consistent and acceptable results. It is extremely useful to have a common baseline or starting point [1]. This numerical analysis will produce results for, fitting of modelling out-put to experimental results, predicting the effect of changes in material properties and geometry of cell performance and testing the viability of proposed physical explanation. Subsequently baseline parameter sets are presented that describe various (CdTe, CIGS, etc.) thin-film solar cells. These models can be used as a baseline for more complicated models.

3.1 Governing equation

The mathematical and physical formulation for the solar cells are briefly described. The problem is presented in the form of the Poisson and continuity equations [2].

$$\nabla . \varepsilon \nabla \emptyset = -q\,(p - n + N_{D+} - N_{A-}) , \tag{3.1}$$

and

$$\nabla . \vec{J}_n = q\,(R - G) + q\frac{\partial n}{\partial p} , \tag{3.2}$$

$$-\nabla . \vec{J}_p = q(R - G) + q\frac{\partial p}{\partial t} , \tag{3.3}$$

where ε is the dielectric constant, $\emptyset$ is the electrostatic potential, n and p are the free carriers concentrations, N_{D+} and N_{A-} are the density of ionized donor and acceptor levels, Jn and Jp are the electron and hole current density, R is the recombination rate, and G is the generation rate . Here if we only investigate the steady state solution, then,

$$\frac{\partial n}{\partial t} = 0 \text{ and } \frac{\partial p}{\partial t} = 0 . \tag{3.4}$$

In Eqn. 3.2 and 3.3 the recombination term, have non-linear dependence on the carrier concentrations n and p. Hence equation, (3.1)-(3.3) represent a set of coupled nonlinear differential equations, which will be solved by numerical method with a typical approach: (1) discretization/meshing of the device, (2) discretization of equation 3.1-3.3, (3) application of boundary conditions (contacts), and solution of the resulting matrix equation by iteration. The solution consist of the three state variables, $\emptyset$, E_{fn}, and E_{fp}, which are sufficient to

deduce all other characteristics in steady state condition. All simulations utilize Fermi-Dirac Statistics.

3.1.1 Transport equation

The set of equations composed of the drift-diffusion equation, the Poisson equation, and the continuity equations is called the "transport equations" the equation allow one to derive most of the properties of semiconductor devices [3].

In the absence of magnetic fields and temperature gradients, carrier transport in semiconductors occurs by drift and diffusion only and can be expressed by the equations:

$$J_n = qu_n\, n\varepsilon + qD_n\, \nabla n \tag{3.5}$$

and

$$J_p = qu_p\, p\varepsilon - qD_p\, \nabla p, \tag{3.6}$$

the variables listed here are, μs are the carriers mobility, Ds are the carriers diffusion constant and $\widehat{E}$ is the electrostatic field [2] . After the definition of quasi-Fermi levels, Ef_n and Ef_p (Eq. 2.7) and quasi-Fermi potential, $\emptyset f_n = -(Ef_n/q)$ and $\emptyset f_p = (Ef_p/q)$ from the previous equation, these equation can be simplified as:

$$J_n = -qu_n\, n\, \nabla\, \emptyset_{fn} \tag{3.7}$$

And

$$J_p = -qu_p p \nabla\, \emptyset_{fp} \tag{3.8}$$

Equations (3.7) and (3.8) are applied to find the solution of Eqn. (3.1)–(3.3), which describe transport due to electric fields, diffusion, and effective fields (e.g., band-gap grading or variations in N_C and N_V).

3.1.2 Generation equation

If we assume that, optical generation is wavelength-independent, then reflection at front (RF) and back surfaces (RB). Then photon flux density, Φ, decays exponentially vs. depth, $\emptyset(z) = \emptyset(z_0).\exp(-\alpha_x(z - z_o))$, here Φ is the flux density in units of (photons/cm2s), and α_x

is the absorption constant, and the subscript *x* stands for ZnO, CdS, or CIGS.

The equation for generation rate G(z) is given by the following equation:

$$G(z) = -\frac{d\emptyset}{dz} = \alpha_x\,.\,\emptyset(z_0)\,.\exp(-\alpha_x\,(z - z_0)) \tag{3.9}$$

This equation applies in all layers under consideration of the appropriate $\emptyset(z_0)$ and z_o, given in Table 3.1. The situation becomes more complex if the band-gap energy, and therefore the absorption spectra, is spatially non-uniform and this will be discussed later. Back reflection implies that a fraction of the light that reaches the back contact, $R_B < 1$, reverses its propagation direction at the back contact and is then incident on the device "from the back" If W_{CIGS} is the CIGS absorber thickness, the intensity of the reflected light is

$$\Phi_{\text{reflection}} = R_B \,.\, \Phi(W_{CIGS}) \qquad 3.10$$

Equation 3.9 describes generation due to a monochromatic light source. In practice, a spectrum of light is incident and the simulation assumes a standard "one-sun" illumination, also referred to by "AM1.5" [4]. The total generation profile is the sum of the signal wavelength generation.

3.1.3 Recombination equation

Recombination is the process when the excited electron stabilizes back down into the valence band, which remove a hole and hence one electron-hole pairs lost without any useful process. In the conduction band, the electron is in meta-stable state and tend to a stable state. The recombination processes have three basic types that are radiative, Auger and Shockley-Read-Hall (SRH) recombination.

3.2 Graphical demonstration

Defect (defect levels - additional states within the band gap) related recombination is typically described by the model developed and verified by Shockley, Read, and Hall (SRH) [5, 6]. This model is resulted from the statistical considerations of transition rates and required only one assumption, namely that a defect level has only two states of existence, i.e., an acceptor level is either neutral or negatively charged. With this restriction, four transitions are possible for each defect, shown for the case of acceptor traps in Figure. 3.1. (Similar diagrams apply to donor traps). Electron capture followed by hole capture leads to a recombination process, whereas, hole emission followed by electron emission leads to generation of an electron-hole pair. In equilibrium, both these processes occur at equal rates. Under optical or electrical injection, however, the capture rates increase linearly with the free

carrier concentrations and, therefore, additional recombination occurs. Carrier emission rates are unaffected by the free carrier concentrations unless the material is degenerate [5, 7]. All the recombination types in solar cells is elaborated in Figure 3.1. The two most important power-loss mechanisms are (1) and (2).

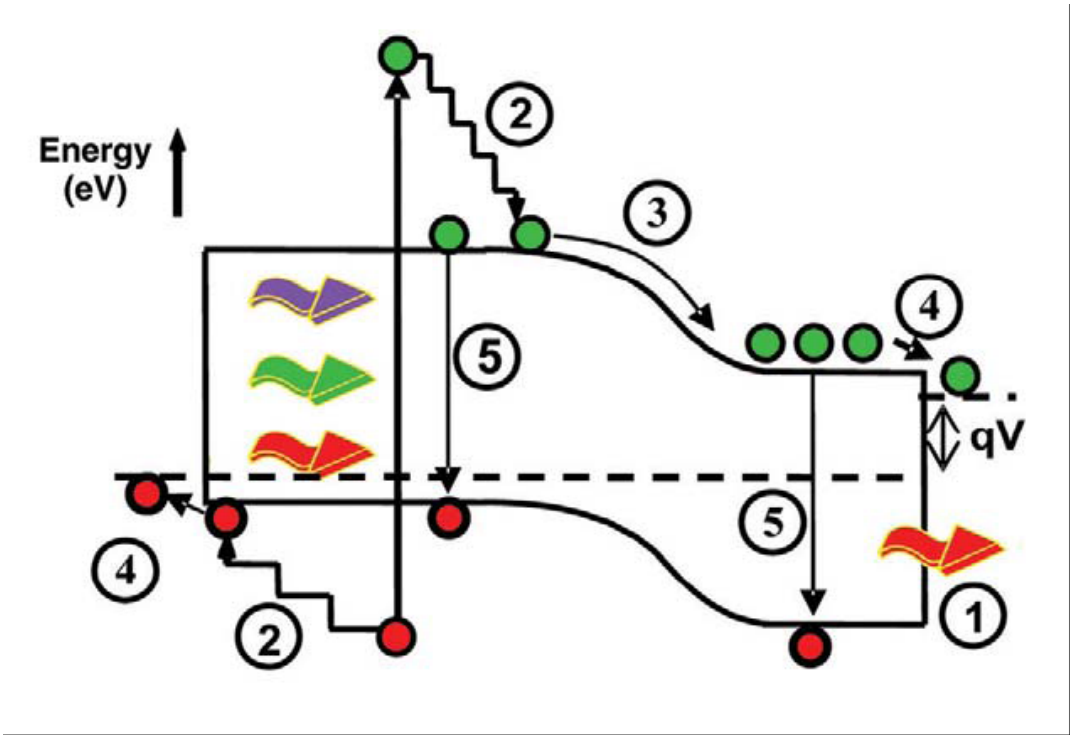

Figure 3. 1 Loss processes in a standard solar cell [8]

Details of numbering in the figure 3.1, (1) non absorption of below bandgap photons; (2) lattice thermalization loss; (3) and (4) junction and contact voltage losses; (5) recombination loss (radiative recombination is unavoidable). The two most important power-loss mechanisms are (1) and (2).

3.3 Software

Numerical modelling is increasingly used to obtained insight in to the details of physical operation of PV solar cells. Several modelling tools have been developed to measure the different parameters of solar cells. Different research groups and universities uses different type of PV software [9]. Some of the most commonly used software are discussed in this section along their properties and shortcomings.

3.3.1 SCAPS–1D

A Solar Cell Capacitance Simulator (SCAPS) is a one dimensional solar cell simulation programme developed at the Department of Electronics and Information Systems (ELIS) of the University of Gent, Belgium. Many researchers have contributed to its development.

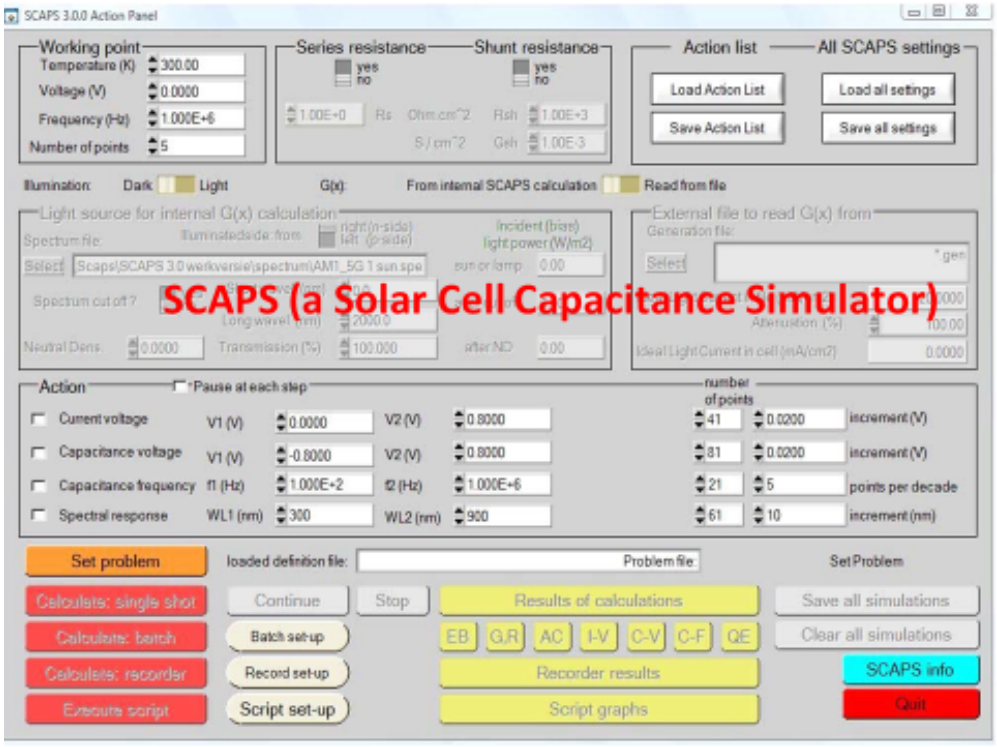

Figure 3. 2 A Solar Cell Capacitance Simulator (SCAPS)

It is designed as a general polycrystalline thin-film device simulator. SCAPS is used for modelling CIS, CGS, CIGS and CdTe based solar cells. The current version available is 3.3, but our discussion is based on 3.2 [10].

It is easy to enter a new problem for new users. Up to seven (7) semiconductor layers can be added to the device and all the required physical parameters can be graded in a new window if required. Some parameters are temperature dependant like effective density of states and the thermal velocity and other parameters such as the band gape and mobility are independent of temperature. Shockley-Read-Hall (SRH) formalism is used for recombination at the interface states and in deep bulk level and their occupation.

SCAPS can be used for measuring spectral response, J-V, C-V, C-f and Q-V. Each measurement can be calculated for light or dark condition and as a function of temperature. All the simulation and measurements are shown on screen for each intermediate voltage or wavelength. These intermediate solution can then be saved to a file. After completing the

measurements it can be saved and can be compare with other measurements and simulations [10].

3.3.2 AMPS–1D

Analysis of Microelectronics and Photonics Structures (AMPS-1D) is the one dimension (1D) program written by S. Fonash and co-workers at Pennsylvania State University [11]. It was engineered to be a very general and versatile computer simulation tool for the analysis of device physics and device design. It is a one-dimensional (1-D) Device Physics code which is applicable to any two terminal device. It can be used for diode, sensor, photo-diode, and photovoltaic device analysis.

Figure 3. 3 Analysis of Microelectronics and Photonics Structures (AMPS-1D)

It is possible to work on several problem simulations simultaneously in a separate window. To enter or define a new problem is an easy task. It has a clear and intuitive user interface and also help function. It support up to 30-layers in which each layer having its own sets of parameter. Some parameters are temperature dependent and other are temperature independent like (effective density of states, band-gap, mobilities). For each layer, up to 50 deep donor and acceptor level can be assigned. Exponential band tails states is also possible

to define in AMPS. It is possible to simulate uniform and graded junctions for several layers. Absorption coefficient, spectrum intensity and wavelength have to be entered manually which is an issue, if it was possible to read directly from the data files, then it would be more user friendly. When all the requirements and definitions for the layers are completed and the simulation requirements are fulfilled, the user can calculate J-V, spectral response measurements for both light and dark, and the case is submitted to the queue (to process) and they will calculate all the parameters and will save it. Once the results are calculated, they can be analysed with any plotting program and the results will be compared and analysed.

3.3.3 AFORS-HET

It is a numerical simulation of solar cells and measurements. AFORS-HET stands for Automat FOR Simulation of HETerostructures. The discussion is based on version 2.4.1 [12].

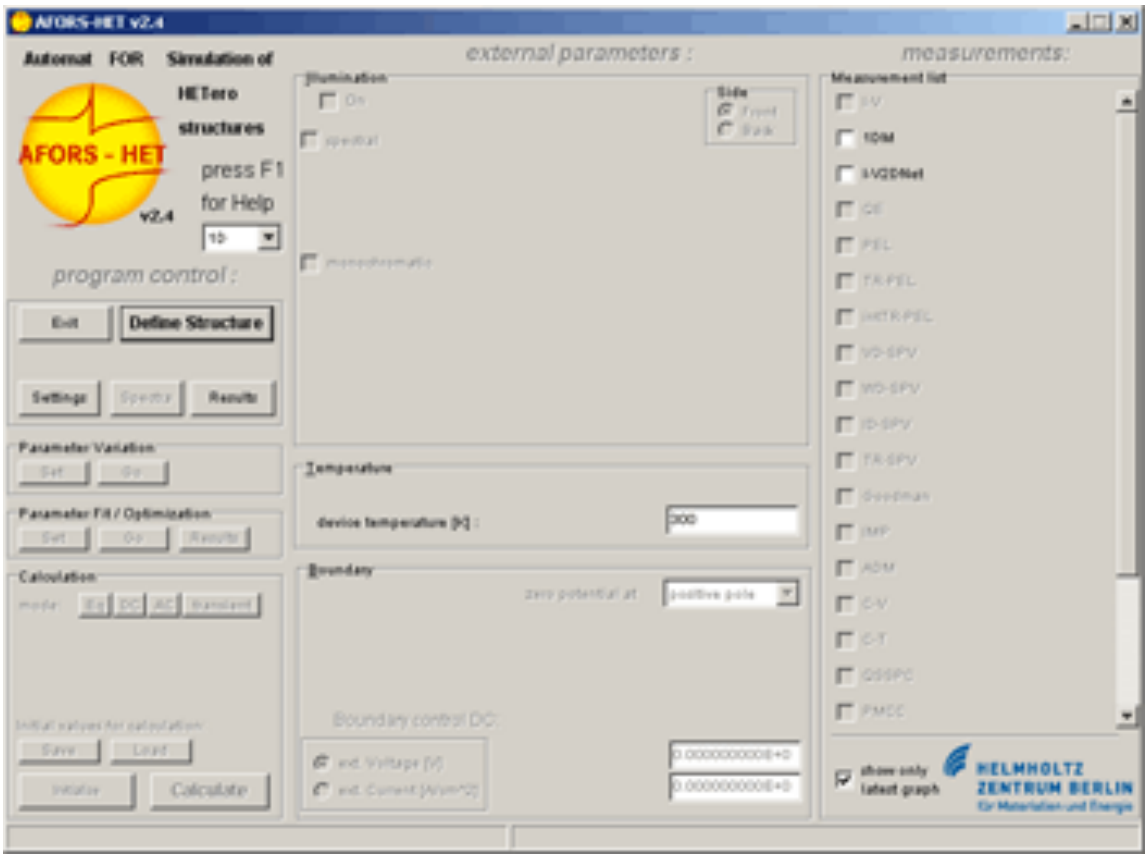

Figure 3. 4 AFORS – HET

It can be used for modelling of an arbitrary 1D sequence of semiconducting layers and interfaces, EQ equilibrium, steady-state DC, small sinusoidal perturbation, AC and general transient (TR) calculation mode. It can be used for arbitrary parameter variation and parameter fitting, band diagram, local cell currents, recombination, phase shift. In DC

measurements I-V, QE etc. can be easily measure. In AC measurements impedance (IMP), capacitance-Voltage C-V, Capacitance-Temperature (C-T) can be measured [13].

3.3.4 PC1D

PC1D was developed in Sandia National Labs by Basore and co-worker. It was further developed by UNSW Australia. It is widely used for Si cells as a standard and widely spread in PV research community. It also used for thin-film cells.

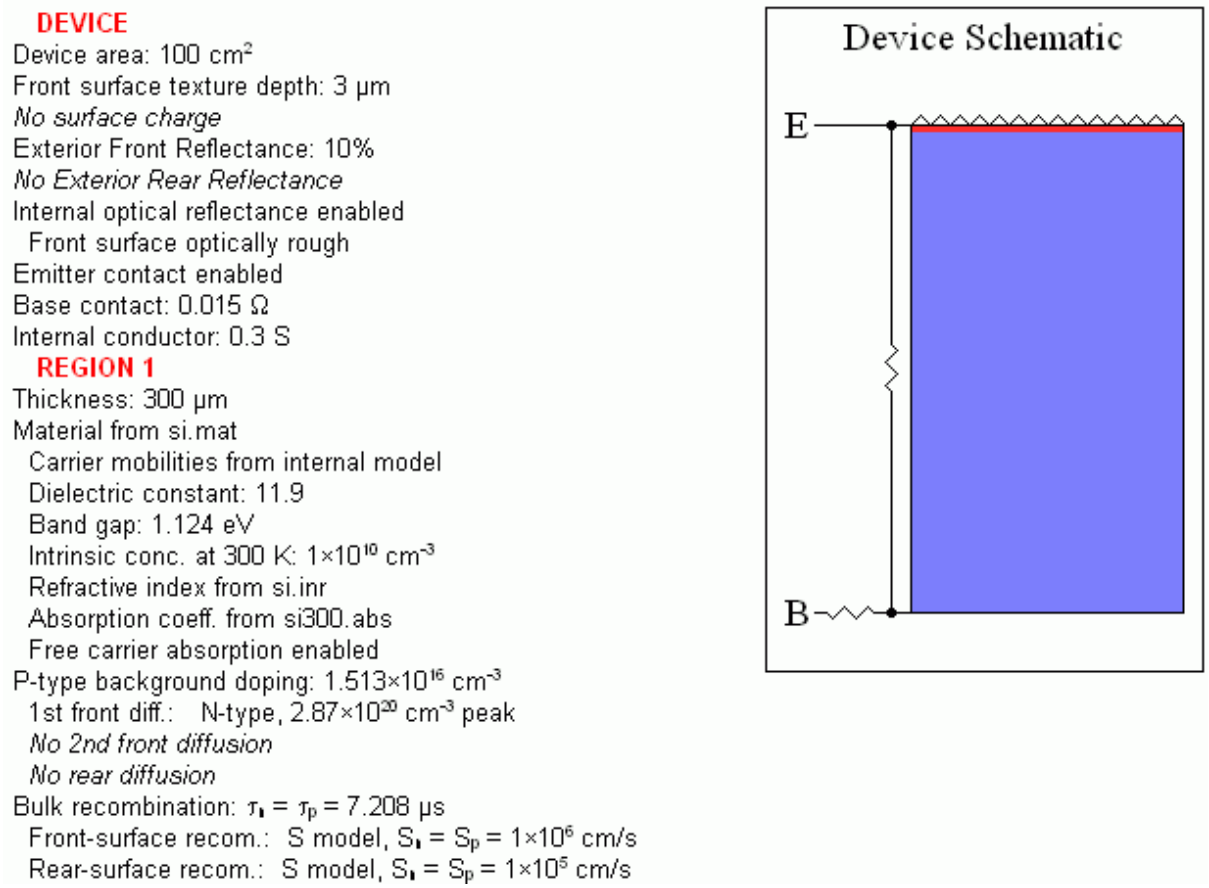

Figure 3. 5 PC1D was developed in Sandia National Labs by Basore and co-worker

To define a new problem in PC1D is quite simple. It has a very clean user interface. The cell and layer structure is shown on the screen, and by clicking on a parameter its values can be altered. It support up to five semiconductor layers which are really less in the case of CIGS/CIS thin-film solar cells. The common recombination mechanisms Auger, band-to-band and trap-assisted tunnelling (Hurkx model) are implemented. In case to introduce a deep level, only one deep level can be introduced. Space charge connection with deep level are not defined. The parameters that can be simulated are J-V characteristic curve, spectral response measurements and transients. The result can be viewed in a separate window and the data can be copied and saved [14].

3.3.5 ASA

Amorphous Semiconductor Analysis (ASA) is especially designed for amorphous silicon devices and was written by M. Zeman, M. Kroon, J.Van den Heuval and other co-worker at the Delft University of Technology. ASA does not use a graphical user interface, but all the previously discussed programs has this facility.

To define a problem and fed into the ASA is not an easy job. This is always done manually. To define a problem, commands are written in an ASCII input file, each command starts with a keyword and is followed by the parameter value.

On the other hand ASA is a very flexible program too, the number of layers as well as the number of discretization nodes are large [8, 15].

3.4 Conclusion

Numerical simulation can lead to better insight into the details of the physical operation of a thin-film cell structure. The Numerical modelling has been developed and applied with several purposes: educational illustration of many complicated physical mechanisms govern the operation of thin-film PV devices, a quantitative understanding of these cells is definitely beyond intuition and simple analytical models, performing specific physical mechanisms, a tool to interpret advanced measurement on complicated cell structures, design and optimization of advanced cell structures, etc.

Here some of the simulators we discussed topic wise but there are other programs that can also be listed briefly. SimWindows is a freely available one-dimensional drift/diffusion simulator for semiconductor devices, ADEPT-F from the group of Jeff Gray, Purdue University has been widely used. The program ASPIN of the University of Ljubljana has been used for CIGS cells and for a-Si cells. Some of these are expensive commercial programs used in silicon microelectronic industry, however in principle also usable for solar cells. Polycrystalline thin-film solar cells appropriately require the use of two- or even three-dimensional programs because of grain boundaries and non-planar interfaces. Though one-dimensional problems effectively average the effect of grain boundary states over the bulk, they have been surprisingly successful. Also, transition to two or three dimensions programs will increase substantially the number of input parameters. Hence to get confidence in a proposed model, the analysis of as many different characteristics, in as many different

conditions as possible should ideally be simulated and compared with measurements will lead to a better understanding.

References

[1] M. Gloeckler, A. L. Fahrenbruch, and J. R. Sites., "Numerical modeling of CIGS and CdTe solar cells: setting the baseline," In Photovoltaic Energy Conversion. Proceedings of IEEE 3rd World Conference, vol. 1, pp. 491-494, 2003.

[2] Sze, Simon M., and Kwok K. Ng, "Physics of semiconductor devices," John Wiley & Sons, 2006.

[3] Colinge, J-P., and Cynthia A. Colinge. Physics of semiconductor devices. Springer, 2005.

[4] A. Luque, and H. Steven, eds. "Handbook of photovoltaic science and engineering," John Wiley & Sons, 2011.

[5] Shockley, We, and W. T. Read Jr. "Statistics of the recombinations of holes and electrons," Physical Review 87(5) 835, 1952.

[6] Neville, Richard C. Solar energy conversion: the solar cell. Elsevier, 1995.

[7] Conibeer, G.,"3rd-generation photovoltaics," Materials today, 10(11), 42-50, 2007.

[8] Burgelman, M., Verschraegen, J., Degrave, S., and Nollet, P.,"Modeling thin-film PV devices," Progress in Photovoltaics: Research and Applications, 12(3), 143-153, 2004.

[9] Burgelman, M., Nollet, P., & Degrave, S., "Modelling polycrystalline semiconductor solar cells," Thin Solid Films, 361, 527-532, 2000.

[10] Fonash, S., Arch, J., Cuiffi, J., Hou, J., Howland, W., McElheny, P., and Rubinelli, F., "A manual for AMPS-1D for Windows 95/NT a one-dimensional device simulation program for the analysis of microelectronic and photonic structures," *The Pen*nsylvania State University, 1997

[11] Stangl, R., Froitzheim, A., Kriegel, M., Brammer, T., Kirste, S., Elstner, L., and Fuhs, W. AFORS-HET, a numerical PC-program for simulation of heterojunction solar cells, Version 1.1 (open-source on demand), to be distributed for public use. *Proc. 19th PVSEC, Paris, France*, 2004.

[12] Stangl, R., M. Kriegel, and M. Schmidt. "AFORS-HET, Version 2.2, a numerical computer program for simulation of heterojunction solar cells and measurements." *Photovoltaic Energy Conversion, Conference Record of the 2006 IEEE 4th World Conference on*. Vol. 2, 2006.

[13] Corkish, R., “Undergraduate and Postgraduate Education in Renewable Energy. Using Technology Tools to Innovate Assessment, Reporting, and Teaching Practices in Engineering Education,” 2014.

[14] Wagner, Sigurd, David E. Carlson, and Howard M. Branz., "Amorphous and microcrystalline silicon solar cells," Photovoltaics for the 21st Century: Proceedings of the International Symposium. Vol. 99. No. 11. The Electrochemical Society, 1999.

[15] R. Schropp and M. Zeman, “Amorphous and Microcrystalline Silicon Solar Cells,” Modeling, Materials, and Device Technology, Kluwer Academic Publishers, Boston-Dordrecht-London, 1998.

CHAPTER 4

Baseline parameters and main simulation work

4 Baseline parameters

Theoretical investigation of a photovoltaic (PV) device based on simulations is used to obtain an optimum solution of the parameters for a proposed model. Hence, numerical modelling of polycrystalline thin-film solar cells is an important strategy to test the viability of proposed physical explanations and to predict the effects of physical changes on cell performance [1]. For this work, a sound knowledge of the related field is very important to module new problems as well as to optimise and improve the existence models. Strategies that should be considered when assigning input parameters for numerical models are briefly discussed here, and subsequently, specific baseline parameters for PV devices (CIGS, ZnTe, SnS and CdTe) are proposed. All efforts reported in the proceeding related to CIGS and other baseline cases have almost a common starting point, although the calculations in different scenario were performed on different platforms and with different aspects in mind [2]. Several universities and other research and development (R&Ds) organizations like Colorado State University, University of New South Wales and Gent University are working to develop models based on numerical modelling on polycrystalline materials for describing thin-film solar cells. Since 1980s, numerous models have been created and used for design purposes. The absence of a precise model implies further attempts to explain the complicated structure of polycrystalline materials. Efforts have been made to find an exact analytic expression for the J-V characteristic [3]. The simulations can, if correctly used and accurately interpreted, be a high-quality compliment to experiments and give a better knowledge of the behaviours in thin-film devices [4].

4.1 Basics for baseline parameters

For each model (simulation) an input parameter sets is used to fit experimental data for J-V and other important quantities. Fitting of experimental data is only conclusive, if a wider set of data like J-V at different temperatures or Quantum efficiency (QE) at different biases is used. Input parameters can be categorized into two types, having minor and negligible effect and the second type having a notable effect on the output performance, the former will be checked once and then kept unchanged and the later will be analysed in detail. After excluding these parameters, the remaining parameters are available for fitting purposes. Only results reported in CIGS, CdTe and SnS cases were utilized to match experimental data, and improved analysis for better performance as well, whereas all other results reported here were

used to identify general principles and to evaluate their effects on device performance, independent of particular experimental results.

4.1.1 Front and back contacts

In general, contacts can be assumed Ohmic or, depending on the focus of the modeling, assigned a Schottky barrier height consistent with experimental observations. Transparent conducting oxide (TCO) and specific metal layers are used for front and back electrical contacts. Efficiencies of solar cells depend on various deposition methods as they control the optoelectronic properties of the layers and interfaces. Certain treatments, such as addition of Na in $Cu(In,Ga)Se_2$ and $CdCl_2$ treatment of CdTe have a direct influence on the electronic properties of the absorber layers and efficiency of solar cells. Processes for the development of superstrate and substrate solar cells are reviewed in a development work for PV thin-film solar cells [5]. Glass is the most commonly used substrate, but recently some effort has been made to develop flexible solar cells on polyimide and metal foils. Highest efficiencies of 12.8% and 17.6% have been reported for CIGS cells on polyimide and metal foils, respectively [6, 7].

The reflection at the back surface has only minor influence on the achievable short-circuit current density (Jsc) and this influence only becomes noticeable if the absorber is chosen to be thin. Typical simulation tools support a constant multiplicative reflection factor for the front surface (i.e., R_F = 0.1, 10% reflection), which reduces the quantum efficiency by this fraction. Neglecting interference effects, QE curves show a fairly flat response of $\sim (1- R_F)$ at intermediate wavelengths. Surface recombination velocities at the front and back contact are chosen to be equal to the thermal velocity. This effectively recombines every minority carrier that reaches the contacts and establishes either a perfect ohmic or a Schottky contact depending on the barrier height parameter [8, 9].

4.1.2 Material parameters

An important parameter for solar cell is energy conversion efficiency (the fraction of incident power, which is converted to electricity). There are many parameters that impact the energy conversion efficiency of the cell. For a simple model structure there are already five important parameters (t, w, P, s, a) [10]. Carrier mobilities for polycrystalline material are chosen lower than the values reported for crystalline material. Effective masses of $m_e^* = 0.2\, m_0$ for electrons and $m_h^* = 0.8\, m_0$ for holes, which are numbers typical for direct-band-gap material, are used unless more specific data is available. The ratio of the carrier mobility, μ_e/μ_h,

should be approximately inversely proportional to the ratio of the effective masses, m_e^*/m_h^*. The effective densities of states, N_C and N_V, can be calculated using (Eq. 2.5). The direct temperature dependence in N_C and N_V is taken into account for temperature-dependent modelling. Carrier concentrations can be experimentally determined from capacitance-voltage analysis; recent work, however, suggests that such measurements may overestimate the free carrier concentrations [11]. Typical concentrations are of the order of 10^{16} cm^{-3} for CIGS and 10^{14} cm^{-3} for CdTe. The band-gap energies of the semiconductors are known to be determined from quantum-efficiency (QE) or absorption measurements. The choice of band creates offsets at interfaces which is further discussed in the specific material sections.

4.1.3 Defects

A large variety of defects can arise during any of the processing steps such as Schottky-type shunts, ohmic shunts, Avalanche and Zener breakdown regions, linear and nonlinear edge shunts, cracks and dislocations and areas of high resistance [12]. Further damage from the environment can also occur, such as oxidation, delamination, or light-induced degradation (e.g. Staebler- Wronski effect). These defects can provide localized parasitic pathways for photo-generated current, thus limiting the power provided to the load. The local high current density at these defects produces heating and sometimes light which can be detected by LIT or infrared camera. Shunt defects are low resistance paths in parallel with the photovoltaic cell that bypass current from the load. Two general categories of shunt defects are linear and nonlinear (weak diode). These categories can be further divided into specific failure mechanisms (e.g. Zener, avalanche, weak-diode etc.). Linear shunts are visible in the forward and reverse bias thermal image, and nonlinear shunts typically appear in forward bias [13].

Unless details can be generally assumed for an entire class of materials or device specific simulations are intended, it is recommended that recombination defect states be assigned to a narrow distribution close to the middle of the band gap (generic mid-gap states). In the SRH formalism, a defect state can change its state of charge only by one elementary charge. Therefore, one can always make the following distinction: An acceptor-like defect state is able to accept one electron, and a donor-like defect state is able to donate one electron. The two possible charge states for donors are positive and neutral and for acceptors it is negative and neutral. It follows that free electrons will be coulomb-attracted to ionized donor-like defect states and, free holes will be coulomb-attracted to ionized acceptor-like defect states, whereas holes (electrons) will have no strong interaction with the donor-like (acceptor-like) defects, giving very small hole (electron) cross-sections. Attractive cross-sections are

assigned corresponding to a radius at which the coulomb potential energy of the carrier in the field of the charged trap equals $\boldsymbol{kT}$ [14].

4.2 Thin-film solar cells-some examples

Major thin film solar cells belong to one of the groups given, Amorphous Si. Nano-crystalline thin film Si, Polycrystalline thin film Si, the $CuIn_xGa_{(1-x)}Se_2$ or "CIGS" family, the CdTe solar cell, the TiO_2 - dye based family and Multi-layer based tandem cells or multi-junction cells. A few examples are given here.

4.2.1 CIGS based thin-film solar cells

In 1974 Wagner et al. produced a $CuInSe_2$/CdS solar cell with an efficiency of 12%, an outstanding achievement at the time [15]. The device was produced by depositing a thin film of CdS onto a wafer of single crystal $CuInSe_2$. The promising result stimulated research into developing cells in which all the layers were deposited using thin film methods [16]. It was also realised that incorporating Ga into the $CuInSe_2$ to produce Cu $In_xGa_{(1-x)}Se_2$ (CIGS) resulted in a widening of the energy bandgap towards the optimum for photovoltaic solar energy conversion, an improvement in crystallinity of the layers, and opened up the possibility for grading the energy bandgap. CIGS has in fact proved to be the most successful chalcopyrite absorber layer investigated to date [17, 18].

Copper Indium Gallium Selenide (CIGS) is a direct bandgap semiconductor useful for the manufacture of thin-film solar cells. It has a polycrystalline nature and has achieved a high conversion efficiency of 20.3% for 1-SUN and 21.5% under mildly concentrated (14.05-SUNs) sun light respectively [19, 20]. All the results stated here are experimental; anyhow, our simulation results are higher (more boosting).

The state of the arts combination of layer structure is given in Figure 4.1. The CIGS solar cell consist of three layers: n-ZnO transparent conduction oxide (TCO) contact, n-CdS window, and p-CIGS absorber. This configuration bear a resemblance to the most common CIGS device. Although a detailed investigation reveals that it has defects and grain boundaries (GBs) that will need additional fields for simulation and finally affect the performance. CIGS thin-films have the capability to gain high efficiency substantially differ from single crystal like Si, non-uniformity of Gallium concentration (Ga/(Ga+In)) composition in the film thickness, that ultimately cause defects complexes and hence affect the performance. The structure that is shown in the figure 4.1 is a typical CIGS solar cell, mostly designed in a substrate configuration, the sequence is glass substrate (soda-lime), stainless steel (or

Polyimide material Mo), the back contact is typically sputtered Mo and forms a non-blocking contact with CIGS.

The deposition of CIGS absorber layer (1.5 – 3 μm) over a substrate can be done by different processes. Its short tabulation is vacuum co-evaporation and two-step salinization processes [21, 22]. A detailed overview of the materials and methods used for fabricating photovoltaic solar cell devices is listed in a work [23]. The technologies discussed include those based on the use of Silicon (in the crystalline, multi-crystalline, amorphous and micro-crystalline forms), the III-V compounds (e.g. Gallium Arsenide, Indium Phosphide and Gallium Antimonide), the polycrystalline compounds (e.g. Cadmium Telluride, Copper Gallium Indium Diselenide and Copper Indium Disulphide), and organic materials (e.g. dyes, polymers and fullerenes). In the same paper the author also addresses the important environmental and energy issues with regard to the manufacture, use and disposal of the solar cells and modules [23].

Co-evaporation deposits all elements simultaneously on a heated substrate, further selenization process deposits all metals onto a film and react them in Selenium (Se) atmosphere to form the intended compound. The three-stage process by which one can make the best CIGS solar cell is a variation on the standard co-evaporation [24].

The metal elemental fluxes are varied during deposition in a Se-rich atmosphere such that a favourable crystal growth under Cu-rich conditions can be combined with an overall Cu-poor composition of the finished film [25].

CdS buffer and ZnO window layers are typically deposited on top of the CIGS absorber by chemical bath deposition (CBD) and RF-sputtering, respectively. A buffer layer, such as CdS, although not necessary in the concept of a heterojunction solar cell, has proven beneficial to device performance. ZnO layers are often realized in a bi-layer configuration of intrinsic and Al-doped material. A review of buffer and window layers, including an evaluation of possible alternatives, was recently conducted by Pudov [26]. The effects of the band-alignment at the CdS/CIGS interface on solar cell performance is also a related issue in this case. Broad reviews of the state-of-the-art thin-film solar cells were given in a recent special edition [27, 28], several articles in photovoltaic related magazine and journals discussed the previous work [29]. Several chapters in Ref. [30] are devoted to the discussion of a-Si, CdTe, and CIGS thin-film solar cells.

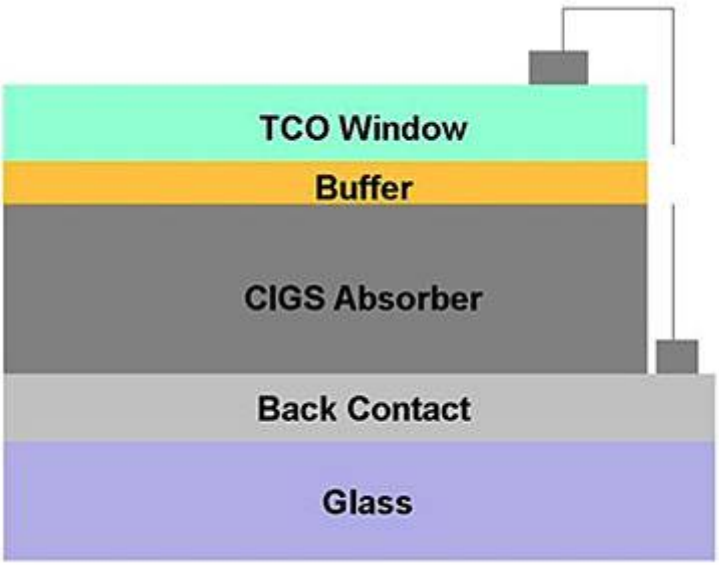

Figure 4. 1 Schematic of a ZnO/n-CdS/p-CIGS/Mo/glass solar cell

Baseline case parameters for CIGS solar cell are listed in Table 4.1.

The band alignment at the interface of CdS and 1.15 eV-CIGS is chosen to be Type I, (|ΔEC| and |ΔEV | are both smaller than the band-gap difference) with ΔEC = +0.3 eV, which was guided by experimental [31, 32] and theoretical studies [33]. The ZnO-CdS interface is assumed as Type II with ΔEC = -0.2 eV, which is in the mid-range of experimental results [34] and close to the predictions from first-principles calculations [35]. A single deep acceptor trap is used for the CdS layer and single deep donor trap is used for the CIGS layer. The high defect density in the CdS layer, similar to the density of shallow donors, is necessary to generate the often observed photoconductivity. The mobilities assigned are approximately a factor of 2–3 below crystalline material values [36, 37], the hole mobility is at the high end of what has been recently measured in thin-film CIGS at low temperature T, μ_h = 3–22 cm^2/Vs [38].

Default values of $0.2m_0$ and $0.8m_0$ are used for the electron and hole effective masses in all layers, which is similar to what is generally reported in the literature for CIS [39]. Dielectric constants are assigned mid-range values of what has been reported. Absorption is defined based on measurements on polycrystalline CdS and CIGS material. Except for the band alignments, device performance is essentially independent of ZnO and only weakly dependent on CdS parameters. Changes in the CIGS parameters are observed to correlate well with a basic diode model. These dependences have been investigated in Ref. [40].

Table 4. 1 Base-line parameters for CIGS based solar cell

A. General device properties	*Front*	*Back*
Φ_b *(eV)*	$\Phi_{bn} = 0$	$\Phi_{bp} = 0.2$
S_e *(cm/s)*	10^7	10^7
S_h*(cm/s)*	10^7	10^7
Reflectivity	*0.05*	*0.8*

B. Layer properties	*ZnO*	*CdS*	*CIGS*
W (nm)	*150*	*60*	*2500*
ϵ/ϵ_0	*9*	*10*	*13.6*
μ_e *(cm²/vs)*	*100*	*100*	*100*
μ_h *(cm²/vs)*	*25*	*25*	*25*
$N_{D/A}$ *(cm⁻³)*	N_D: 10^{19}	N_D: 2.1×10^{17}	N_A: 1×10^{17}
E_g *(eV)*	*3.3*	*2.4*	*1.20*
N_C *(cm⁻³)*	1.2×10^{18}	1.2×10^{18}	1.2×10^{18}
N_v *(cm⁻³)*	2.8×10^{19}	2.8×10^{19}	2.8×10^{19}
ΔE_C *(eV)*	*-0.2*		*+0.3*

C. Gaussian-distributed defect states	*ZnO*	*CdS*	*CIGS*
N_{DG}, N_{AG} *(cm⁻³)*	*D:* 10^{18}	*A:* 10^{17}	*D:* 10^{15}
E_A, E_D *(eV)*	*mid-gap*	*mid-gap*	*mid-gap*
W_G *(eV)*	*0.1*	*0.1*	*0.1*
σ_e *(cm²)*	10^{-12}	10^{-17}	5×10^{-13}
σ_h*(cm²)*	10^{-15}	10^{-12}	10^{-15}

4.2.2 CdTe-based solar cell

The optimum energy bandgap for photovoltaic solar energy conversion is proposed to be 1.5eV, investigated and supposed by Loferski in 1956 [41], hence he suggested that CdTe having a direct energy bandgap near to the optimum value, and a high optical absorption

coefficient for photons with energies greater than the energy bandgap ($\boldsymbol{\alpha} > 10^5$ cm^{-1}) is a promising PV material [42, 43]. It was realised that thin layers of only a few microns, would be needed to absorb most of the incident light, and will result in minimising material costs. The earliest cell developed were CdTe/Cu_2Te devices [44]. These devices were, however, found to be unstable. As the instability was identified with the use of Cu_2Te a novel device structure was developed that avoided its use, the CdS/CdTe heterojunction solar cell [45]. CdS has an energy bandgap of 2.42 eV, which is sufficiently wide to transmit most of the solar spectrum to the device junction. It is also one of the few wide energy bandgap materials that can be strongly doped (n-type) minimising series resistance problems. In 1972 Bonnet demonstrated the excellent potential of the CdS/CdTe cell by producing devices with efficiencies of 5-6% [46]. A record efficiency of 20.4% for CdTe cell is attained until date, fabricated by the First Solar and measured at Newport Technology and Applications Centre [47].

As a base-line here the case of SnO_2/CdS/CdTe solar cells is discussed. The three layer sequence is as: n-SnO_2 transparent conducting oxide (TCO), n-CdS window, and p-CdTe absorber. Baseline case parameters are listed in Table 4.2.

The conduction bands at the SnO_2/CdS interface are aligned in agreement with experiments [48]. The offset at the CdS/CdTe interface is assumed to be Type II with $\Delta EC = -0.1$ eV, which was calculated from first-principles [49] and confirmed by photo-electron spectroscopy results [50].

The back-contact is chosen as a moderate Schottky barrier, which is the standard interpretation of the frequently observed “roll-over” effect in CdTe solar cells [51, 52]. For SnO_2 and CdS, default values of effective masses, $0.2m_0$ and $0.8m_0$, are used. The model shows only weak dependences on CdS parameters, except for layer thickness. The absorption curves used were measured on polycrystalline CdS and CdTe material. CdTe mobilities are assumed approximately half of the crystalline values and the effective masses are estimated as an average from several published sources [53–55].

A single deep acceptor trap is used for the CdS layer and a single deep donor trap is used for the CdTe layer. Due to the low carrier concentration in the CdTe, the device is relatively depleted at zero bias and this causes a noticeable change in the band diagram by photo-generated carriers. This type of band deformation can lead to non-superposition of light and dark J-V curves [56].

Another possible contribution to non-superposition is the field-aided collection of photo-generated carriers [57]. Hence, in CdTe non-superposition is likely caused within the absorber layer, whereas in CIGS devices it is dominantly created in the CdS layer.

Table 4. 2 Base-line parameters for CdTe based solar cell

A. General device properties	*Front*	*Back*
Φ_b *(eV)*	$\Phi_{bn} = 0.1$	$\Phi_{bp} = 0.4$
S_e *(cm/s)*	10^7	10^7
S_h *(cm/s)*	10^7	10^7
Reflectivity	*0.1*	*0.8*

B. Layer properties	*SnO2*	*CdS*	*CdTe*
W (nm)	*400*	*50*	*3000*
ϵ/ϵ_0	*9*	*10*	*9.4*
μ_e *(cm²/vs)*	*100*	*100*	*320*
μ_h *(cm²/vs)*	*25*	*25*	*40*
$N_{D/A}$ *(cm⁻³)*	N_D: 10^{18}	N_D: 2.1×10^{17}	N_A: 2×10^{15}
E_g *(ev)*	*3.6*	*2.4*	*1.5*
N_C *(cm⁻³)*	2.2×10^{18}	2.2×10^{18}	8×10^{17}
N_V *(cm⁻³)*	1.8×10^{19}	1.8×10^{19}	1.8×10^{19}
ΔE_C *(eV)*	*0*		*-0.1*

C. Gaussian-distributed defect states	SnO_2	*CdS*	*CdTe*
N_{DG},N_{AG} *(cm−3)*	*D:* 10^{15}	*A:* 10^{18}	*D:* 2×10^{14}
E_A, E_D *(eV)*	*mid-gap*	*mid-gap*	*mid-gap*
W_G *(eV)*	*0.1*	*0.1*	*0.1*
σ_e *(cm²)*	10^{-12}	10^{-17}	10^{-12}
σ_e *(cm2)*	10^{-15}	10^{-12}	10^{-15}

4.2.3 Results of the baseline cases

The models that described for baseline case were established in several different simulation environments, and although there are minor differences in the way parameters are defined in different software packages, the solutions to the baseline problems agree very well with previous results. Other researchers have had similar experiences [58]. The J-V and QE results for the CIGS and CdTe baselines are shown in Figure 4.2 (a) and (b).

The higher band-gap in CdTe solar cells allows for higher open-circuit voltage, but also results in lower current. Both quantum efficiency curves show some losses due to CdS absorption in the low wavelength region, $\lambda < 520$ nm. CdTe solar cells with their low doping and, hence, wide space-charge region achieve generally better collection than CIGS devices. In CIGS, the longer wavelength generation occurs far from the SCR edge, and the QE is lowered for these wavelengths. The baseline cases are very similar in their layer structure and performance to record solar-cell devices; this is shown in Table 4.1, which lists J-V parameters for these cases. The baselines were intentionally "aligned" in performance to record levels. This allows to establish a well-behaved baseline case in comparison to a well-studied record device and then add other detrimental effects, such as additional recombination or grain boundaries. The experimental CIGS efficiency exceeds the simulated baseline case and some of the difference can be attributed to a "graded" band-gap absorber. The one-sun illumination introduces a splitting of the quasi-Fermi levels in the bulk of the CIGS absorber of approximately 0.56 eV, slightly less in magnitude than the observed open-circuit voltage. The density of light-generated excess minority electrons is of the order of 10^{11} cm^{-3} maximizes recombination in this area [59].

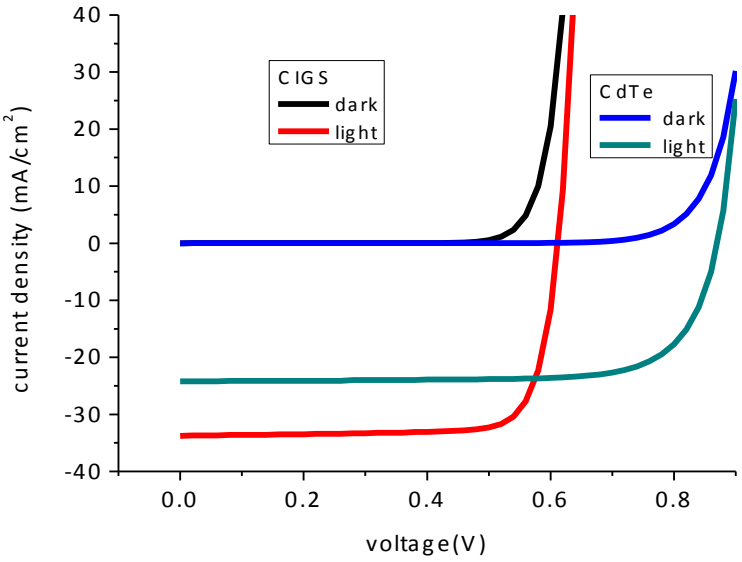

Figure 4. 2 (a) Simulation results for CdTe and CIGS baseline case, J-V in the dark and under one-sun illumination.

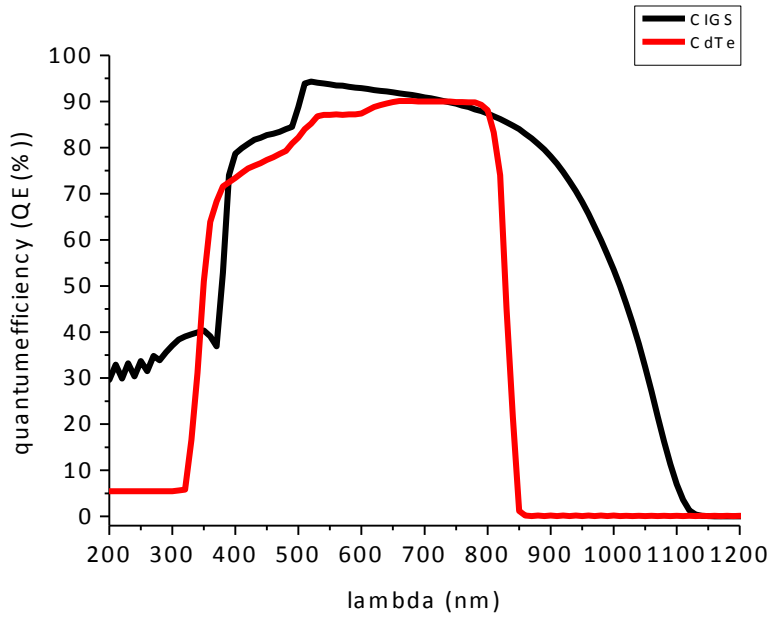

Figure 4.2 (b) QE under standard illumination (1-SUN) for CIGS and CdTe solar cells

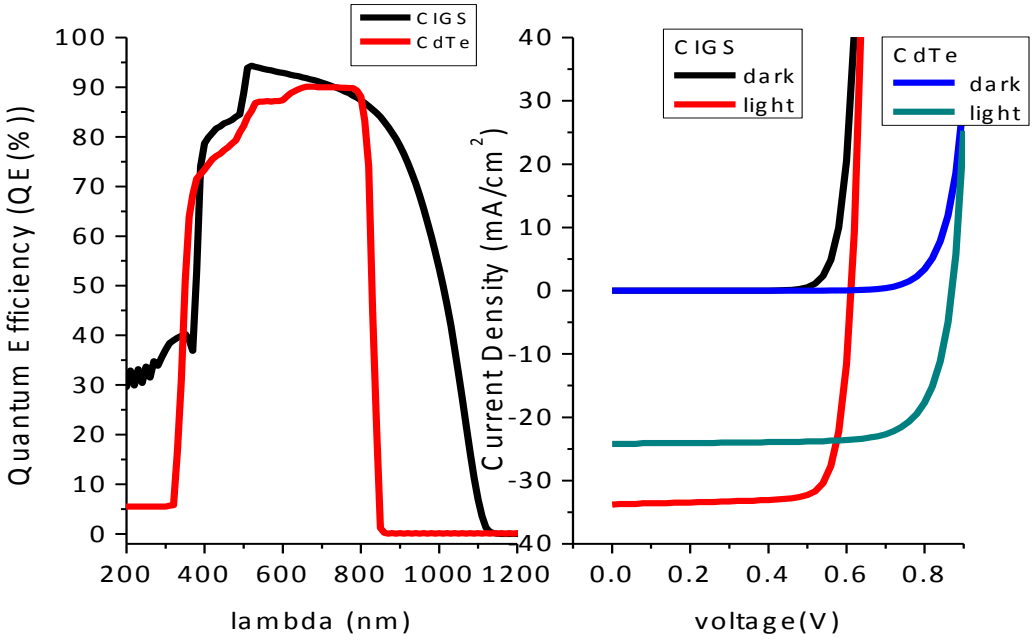

Figure 4. 2 (c) Simulation results for CdTe and CIGS baseline case. Simulation results for CdTe and CIGS, J-V in the dark and under one sun illumination

4.3 CIGS solar cells: effect of Gallium composition on the parameters

Thin-film Copper–Indium–Gallium–Diselenide (CIGS) solar cells have an adjustable band gap that varies with Ga content over a range of 1.0 – 1.76 eV. The non-uniform distribution of Ga in the layer thickness cause "grading" in the p-type CIGS absorber that causes additional fields. This section dedicated to the analysis of thin-film Copper–Indium–Gallium–Diselenide (CIGS) solar cells by using Solar Cell Capacitance Simulator software (SCAPS), the module of the PV device, consists in a CIGS absorber, a CdS buffer and a ZnO window layer. The work is related to the study of the behavior of CIGS absorber as a function of Gallium content by simulating the behavior of CIGS solar cells versus the Ga content in the absorber layer. The variation were taken from pure CIS ([Ga=0]) to pure CGS ([Ga=1]), which cause the variation of the band-gap of the absorber layer from 1.0eV for pure CIS to 1.76eV for pure CGS. The parameters of the simulated PV devices were obtained for different amount of Ga. The obtained results have revealed that the increase of Ga concentration in the absorber layer results in higher efficiency up-to an extent, reaching the maximum efficiency for Ga content about 66%. After optimization of device parameters a maximum efficiency of 30.95% was reached for 66% gallium content.

4.3.1 Review

Thin-film CIS has a band gap of 1.0 eV and the one made from pure Ga CGS has 1.76 eV, anyhow substituting Gallium (Ga) for Indium (In) in Cu(In, Ga)Se_2, changes the band gap from 1.0 to 1.76eV. The place of change is primarily the conduction band [60]. The grading due to this substitution have four possibilities, (1) front grading where the band gap increase towards the front of the absorber, (2) back grading, here the band gap increase towards the back and (3) double grading the band gap increase towards the front as well as the back (both) of the absorber [61]. The effect of various grading on the cell performance is explained in different work [62], the summary of the grading function include: (a) front grading alone or is a part of double grading leads to increased open-circuit voltage as the band gap in the space-charge region (SCR) expands; (b) back grading alone or as a part of double grading, increases minority carriers collection from the bulk due to additional drift fields for electrons are established in the quasi-neutral region, while the same current densities can maintained.

CIGS thin film has several qualities to acquire high efficiency. The band gap for CIS is 1.0eV (low band-gap) and that for CGS it is 1.67eV (high band-gap) [63]. The band gap of CIGS can be varied from 1.0eV to 1.67eV depending on the amount of doped gallium (Ga) in the composition. To absorb most of the photon an appropriate band-gap can be obtained and its thickness is chosen with the aim of achieving a maximum absorption of energy photons. The thickness of absorber layer for the purpose to absorb maximum photons will vary in between 1.5μm and 2.5μm. Moreover, increasing the thickness will cause increase in the efficiency but it will affect the cost factor [64]. In literature, it has been stated that the optimum value for band-gap is movable between 1.16eV and 1.38eV [65]. In thin-film combination the CdS layer is used as buffer layer and works as n-type with a band gap of 2.8eV. It gives the best efficiency with combination of p-type absorber layers such as CIGS, CdTe, InP and Cu_2S in the thin-film solar cells. The experimental result obtained in [66] set up a new record total-area of 19.9% efficiency with 81.2% FF, here the improvement was due to higher fill factor (FF). A new advancement was done claiming a certified word record with efficiency of 20.3% and 20.1% for CIGS cell [65]. The introduction of this high efficient thin-film in the market will boost cost reduction and market share. Exceeding 20% effectiveness barricade for CIGS solar cells is a great achievement for the PV-researchers.

4.3.2 Quantum Efficiency Analysis

The Quantum efficiency, QE (%) graph is given in Figure 4.3. It explains the details about

quantum efficiency QE (%). The QE is the ratio of the number of charge (electron-holes) carriers collected by the solar cell to the number of photons of a given energy incident on the solar cell. It is a function of energy (eV) and can also be represented as a function of wavelength (nm). The quantum efficiency is 1 or 100% when all the photons absorbed by the absorber layer and all the resulting carriers are collected. The mathematical description is given in the introduction. The conversion efficiency of a photovoltaic (PV) cell is the percentage of the solar energy shining on a PV device that is converted into electrical energy. Improving this conversion efficiency is a key goal of research and helps to make PV technologies cost-competitive with more traditional sources of energy. The spectrum for variation in Gallium contents is given in Figure 1. The absorber layer absorbs those photons whose wavelength is either equal or greater than the band-gape (Eg) of the absorber material [67].

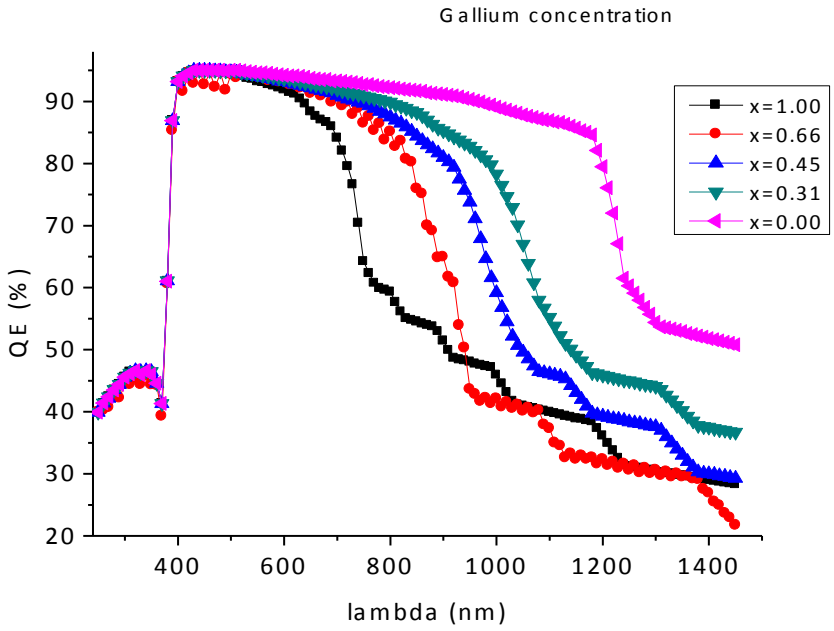

Figure 4. 2 Quantum Efficiency (QE) outputs for $CuIn_{(1-x)}Ga_xSe_2$ absorbers with different Ga content

The low energy photons cannot be absorbed and the high energy photon will contribute in thermalization process. Due to different losses like spectral mismatch, shading losses, incomplete absorption and collection losses, there will be a decrease in efficiency.

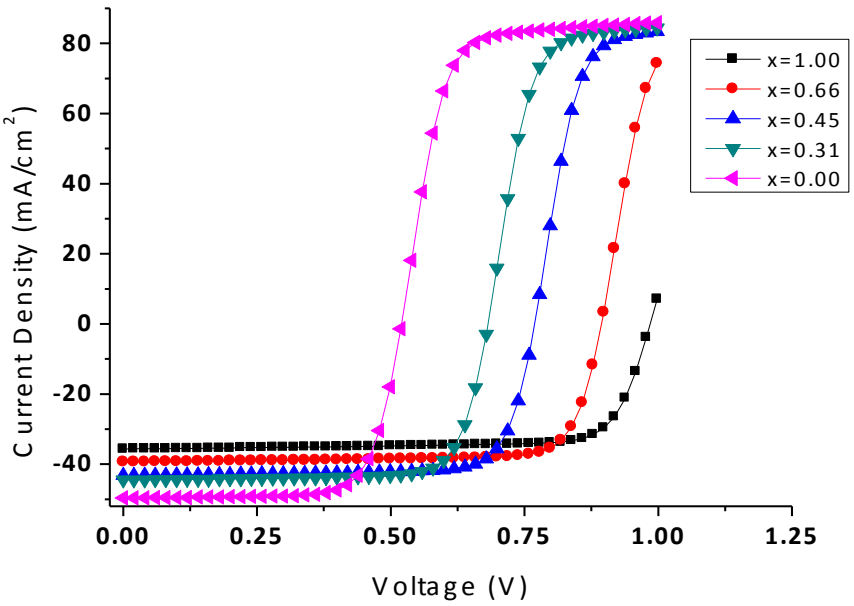

Figure 4. 3 J-V Characteristic curves for $CuIn_{(1-x)}Ga_xSe_2$ with different Ga content

4.3.3 J-V Characteristics Analysis of CIGS Solar Cells

The graph for J-V characteristics is given for thin film solar cell in figure 4.4, the content of Gallium (Ga) was changed in the film, or from pure CIS to CGS the graph was plotted. It is clear from the graph that when band gap increases, the open circuit voltage Voc also increases.

4.3.4 Optimization of different layers thickness

Different simulations have been done to optimize the thickness of CIGS absorber layer in previous work. The simulation results support the idea that efficiency is increased by increasing the thickness of absorber layer as more photon may be absorbed. The resulting graphs for open circuit voltage (Voc), short circuit current density (Jsc), fill-factor (FF) and η are shown in Figure 4.5.

4.3.5 Effect of Gallium (Ga) in the absorber-layer

Effect of other parameters while changing Ga contents in the CIGS thin film solar cell, is given in Figure 4.5.

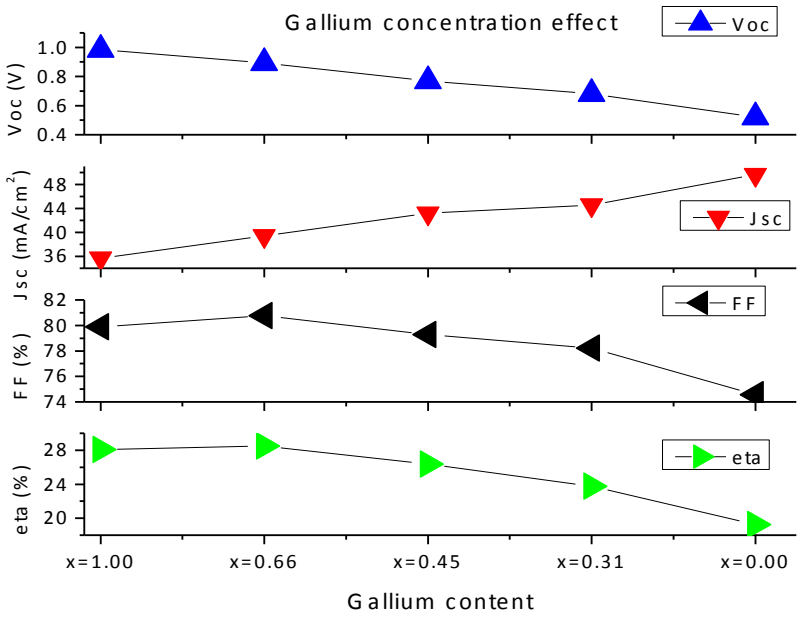

Figure 4. 4 Cell performances with variable Gallium composition in CIGS absorber layer

The open circuit voltage (Voc) increases as the gallium (Ga) content increases and the bandgap of the CIGS layer also increase. The short circuit current represented by (Jtot) decreases as bandgap increases, it has the reverse effect than that of Voc. Similarly the Fill-Factor (FF) increases with the increase of Ga up to 50% after more increase in Ga contents causes decrease in FF, the same phenomenon also observed in the case of external quantum efficiency η (%). In the beginning, the energy conversion efficiency (eta) increases up to 60% of Ga contents but further increase of Ga causes decrease in eta.

4.3.6 Effect of other layers

ZnO window layer is either intrinsic or n-type depending on the deposition methods. ZnO layer has to be an important window layer and a conducting layer to achieve high efficiency in CIGS thin-film. ZnO is wide band-gap 3.2eV and its excitation energy is 60m.eV. ZnO has got good optoelectronic properties with high transparency (> 80%) and electrical conductivity ($> 10^3 \Omega.cm^{-1}$).

The maximum carrier concentration is reported to be 10^{21} cm^{-3} with mobility of 50 cm^2/Vs [68]. The effect of ZnO thickness is shown in Figure 4.5. The value of **Voc** and **Jsc** decreases slightly when the ZnO buffer layer increases. The optimum thickness happens to be around 300-400 nm. The final result is that the conversion efficiency, **η**, can still be boosted for suns in the range 10-30 sun.

4.3.7 Conclusion

In this work we have analyzed the effect of changing Gallium concentration in the CIGS absorber layer. To understand the physical operation features of a thin-film solar cell structure, we have performed a numerical simulation by using SCAPS. There are several parameters that influence the efficiency and performance of PV cell structure. The reason is due to a complicated physical mechanism taken place inside. In order to get confidence into a solar cell model, we have to take different characteristics as well as different possible conditions to be simulated and compared. The variation were taken from pure CIS ([Ga=0]) to pure CGS ([Ga=1]), which cause the variation of the band-gap of the absorber layer from 1.0eV for pure CIS to 1.76eV for pure CGS. The parameters of the simulated PV devices were obtained for different amount of Ga. The result revealed that the increase of Ga concentration in the absorber layer results in higher efficiency up-to an extent, reaching the maximum efficiency for Ga content about 66%. After optimization of device parameters, a maximum efficiency of 30.95% was reached for 66% gallium content. Taking this into account we have considered the variation of absorber layer band-gape due to change in Ga contents in CIGS layer, the effect of electron affinity of the CdS buffer layer and the different variation of band-gap of CIGS absorber layer. It is concluded that as in many simulation processes numerical modelling alone does not guarantee for obtaining better solar cells.

4.4 Analysis of ZnTe-based solar cells

Solar cells based on II-VI semiconductors are among the leading candidates for low-cost photovoltaic conversion of solar energy due to their high absorption coefficients and therefore the low material consumption for their production. This work reports on the analysis of Zinc Telluride (ZnTe) thin films solar cells by using Solar Cell Capacitance Simulator software (SCAPS). Dark and illuminated I-V characteristic are analyzed. The variation result taken from simulation and the results for different output parameters. It has been revealed that increasing the ZnTe thickness (0.5 – 2.0 μm) results in higher efficiency of PV devices. These results are useful for understanding the fundamentals of PV devices as well as a feedback for designers and producers of high efficiency ZnTe cells. The state-of-the-art combination of the cell consists of ZnTe absorber layer, CdS as buffer and ZnO as optical window following the sequence ZnTe/CdS/ZnO. After optimization of different parameters and layer thicknesses the results are obtained. Simulation studies by varying several solar cell parameters such as thickness of various layers reveal that increasing the thickness of absorber layer results in higher efficiency.

4.4.1 Review

Numerical models have become indispensable tools for the design of any kind of efficient solar cells. They have contributed greatly to our understanding of cell operation and are necessary for future cell improvements [69]. CdTe-based solar cells have long been of interest for terrestrial usage because of their high potential conversion efficiency (in the range of 18–24%) with low-cost manufacturability and concern over environmental effects. In order to conserve material and address environmental pollution concerns as well as to reduce carrier recombination loss throughout the absorber layer, efforts have been carried out to decrease the thickness of the CdTe absorption layer to 1 μm [70].

Solar cells based on II-VI semiconductors (with II = Zn, Cd, Hg and VI = S, Se, Te) are among the leading candidates for low-cost photovoltaic conversion of solar energy due to their high absorption coefficients and therefore the low material consumption for their production. Owing to its wide direct band gap of 2.23 - 2.28 eV at room temperature [71] and low electron affinity 3.73eV [72], Zinc Telluride (a II-VI semiconductor) is a suitable material for several applications, such as solar cells where it is used as a p-type doped window materials [73] or a top layer over p-CdTe for achieving low contact resistance in CdS/CdTe photovoltaic heterojunctions [74, 75], switching devices and infrared and X-ray detectors [76, 77].

ZnTe has a direct bandgap of 2.23 - 2.29 eV at room temperature with a Zinc-blend crystal structure. ZnTe has demonstrated controllable p-type doping by Nitrogen [78, 79], with hole concentrations of up to 10^{20} cm^{-3}, with mobilities up to 30 cm^2/V-s at room temperature. The source of the unique p-type nature for this wide-band gap material is believed to be the native defect structure, such as Zinc vacancy [80,81], where defects lie within the valence band rather than within the band gap [82]. The unique p-type behaviour of ZnTe is in stark contrast to other wide-band gap compound semiconductors such as ZnO, where materials are typically n-type and difficult to convert to p-type conduction.

ZnTe films (deposited by MBE without intentional doping) were determined to be p-type with hole concentration in the range of 10^{14}-10^{15} cm^{-3}. Capacitance-voltage (C-V) measurements on n+-ZnO/p-ZnTe structures were used to determine these values due to the difficulty in achieving ohmic contacts for samples with low carrier concentration. The electron concentration of the ZnO layer is approximately 5×10^{18} cm^{-3}, providing an asymmetric doping profile to aid in analysis. Equation (4.1) is used to determine carrier concentration in ZnTe, where q is the charge of an electron, € is the static dielectric constant of ZnTe, and A is device area. Based on the background p-type doping concentration, the

Femi-level is approximately 0.3eV above the edge of the valence band at room temperature under thermal equilibrium.

$$N_A = \left(\frac{q}{q\epsilon A^2 d(1/C^2)/dV}\right) \quad (4.\ 1)$$

Nitrogen doped ZnTe thin films on GaAs substrates grown by MBE show high p-type conductivity with hole concentration of 10^{19} cm^{-3} and mobility 40 $cm^2/V.s$. The formation of n-type ZnTe remains a major challenge, where reports have only experimentally demonstrated n-type behavior for ZnTe epitaxial growth on ZnTe substrates [54]. ZnO and ZnSe thin films demonstrate n-type conduction suitable for heterojunctions with ZnTe.

The potential of achieving a p-type semiconductor with an Intermediate Band (IB) generated by doping with O has been proposed theoretically [84]. So ZnTe:O alloy is an attractive material for photovoltaic devices. In this paper we have performed a numerical study of a solar cell based on ZnTe absorbers.

4.4.2 Results and discussion

4.4.2.1 Model of a thin film ZnTe-based solar cell

Figure 4.6 shows the scheme for a photovoltaic solar cell based on ZnTe absorber.

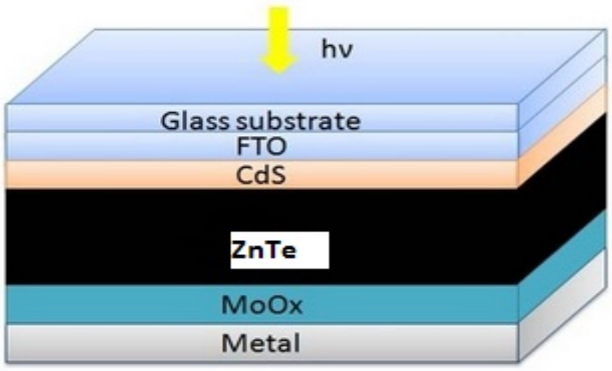

Figure 4. 5 Schema of a ZnTe-based solar cell

In order to make the calculations of the behaviour of the ZnTe-based device, several parameters concerning the absorber layer have to be defined. The basic parameters for ZnTe layers have been taken from the literature and appear in Table 4.3.

4.4.2.2 Energy band diagram for a ZnTe-based solar cell

Figure 4.7 displays the energy band diagram for a p-ZnTe/n-CdS/ZnO solar cell obtained from the output of SCAPS analysis. This model will help in explaining the properties of

ZnTe film. ZnTe has a direct optical band gap (Eg) of 2.23 - 2.28 eV at room temperature; this value is far-close to the optimum value required for efficient light absorption for those photons whose energy is either equal or greater than 1.4 eV. Proper doping can control its optical properties.

Table 4. 3 Basic parameters for ZnTe absorber layers

Parameter	Value	Reference
Thickness (µm)	0.1 - 2.7	
Bandgap (eV)	2.23 - 2.29	[3]
Electron affinity (eV)	3.73 eV	[4]
Absorption coefficient α(cm^{-1})	10^5	[6, 7]
Carrier concentration, h (cm^{-3})	10^{14} - 10^{17}	[6, 7]
Acceptor density, NA (cm^{-3})	10^{14} - 10^{15}	[8]
CB effective density of states, NC (cm^{-3})	2.2×10^{18}	SCAPS
VB effective density of state, NV (cm^{-3})	1.8×10^{19}	SCAPS
Crystal structure	Zinc-blend	
Lattice constant	6.089Å	

The results mentioned here were obtained using an acceptor concentration $N_A=10^{14}$ cm^{-3} [74, 75] except for those where N_A were changed deliberately in order to analyze its effect on the performance of PV devices. Therefore the energy band, I-V curves and studies of the efficiency dependence of ZnTe and CdS thicknesses and Temperature were obtained for $N_A=10^{14}$ cm^{-3}.

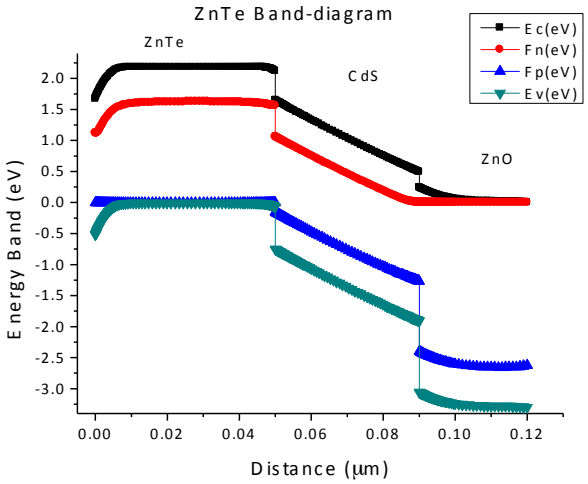

Figure 4. 6 Energy band diagram of ZnTe solar cell

4.4.2.3 J-V characteristics of a ZnTe-based PV device

The function of a solar cell is to convert light to electricity, and it might seem unusual to measure the photovoltaic cell in the dark, but for diode properties, dark measurements are precious. A solar cell in the dark is a large flat diode. A simple dark IV measurement produces the exponential curve so characteristic of diode. The current-voltage curve of a ZnTe/CdS/ZnO solar cell is shown Figure 4.8. In the dark it will give an extreme minimum value of current (I_D) that is due to the minority carriers. After illuminating the cell with 1 Sun (Air Mass 1.5) the PV process starts and due to the charge carriers produced by incident photons will cause current.

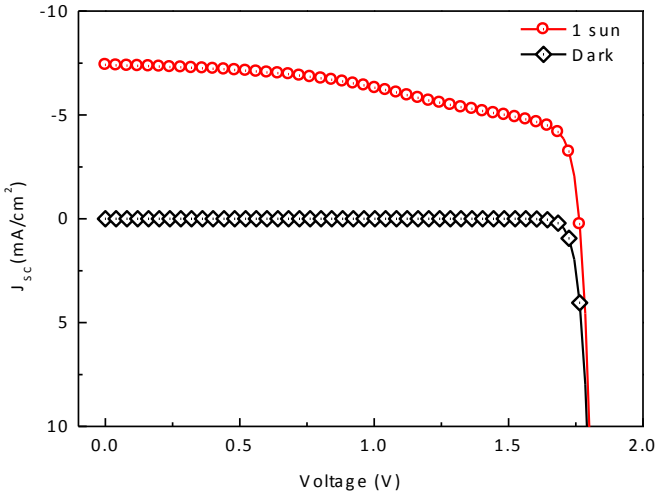

Figure 4. 7 J-V characteristic curve for a ZnTe-based solar cell under dark and 1-SUN illumination

4.4.2.4 Optimization of ZnTe absorber layer thickness

In Zinc Telluride (ZnTe) based solar cell for simulation purposes that used in this analysis is ZnO/n-CdS/p-ZnTe. Simulation is possible for different parameters. First, the thickness of ZnTe absorber layer calculated for different thickness value, from 0.1 µm up to 2.7 µm.

To justify the simulation, the conventional ZnTe structure with CdS buffer layer has been verified in terms of ZnTe absorber and CdS buffer layer. At first, the ZnTe absorber thickness has been varied to find out the prime thickness for the conventional ZnTe structure with CdS as the window layer.

Figure 4.9 shows the variation of the main parameters of PV solar cell as a function of the ZnTe absorber thickness. It was observed that the conversion efficiency of the solar cell increased with the thickness of the ZnTe absorber layer, but with a much slower rate over 1.5 µm. The optimum thickness for ZnTe absorber layer would be around 1.5 ± 0.5 µm. From

Figure 4.9, at the thickness of 0.5 µm and 1.5 µm, the calculated efficiency is 7.07% and 7.5%, respectively, further increase of thickness has an inverse effect on the efficiency, the reason is due to high band gap, the generated charge carriers (electron and holes) re-combine and hence the efficiency decreases slowly. Comparing the results with the 7.5% efficiency electrons will be captured easily by the back contact for the recombination process at optimum thickness. Therefore, fewer electrons will contribute to the quantum efficiency of the solar cell and the value for V_{OC} and J_{SC} will be either low or unchanged.

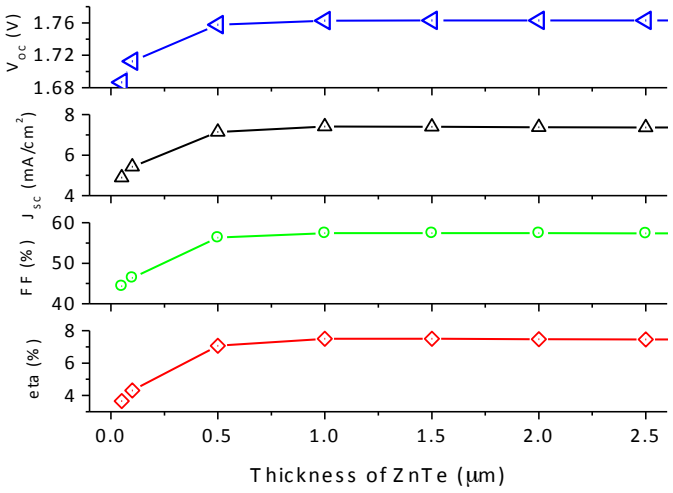

Figure 4. 8 Photovoltaic parameters for a ZnTe-based solar cell as a function of the ZnTe absorber thickness

Figure 4.10 shows the J-V characteristic curve for the different thicknesses of ZnTe layer. In the simulation it give the high efficiency at 1.5 µm.

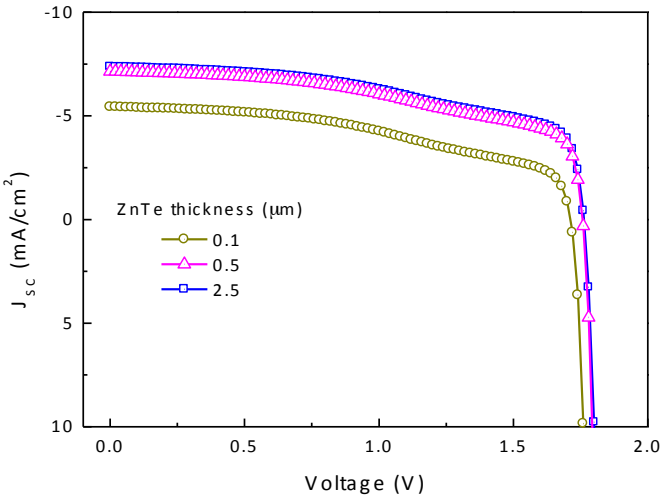

Figure 4. 9 J-V curves for ZnTe-based solar cells with different ZnTe thicknesses under 1 SUN illumination

Oxygen doping in ZnTe is applied to a junction diode with the aim of utilizing the associated electron states 0.5 eV below the band edge as an intermediate band for photovoltaic solar cells. The ZnTe:O diodes confirm extended spectral response below the band edge relative to un-doped ZnTe diodes, and demonstrate a 100% increase in short circuit current, 15% decrease in open circuit voltage, and overall 50% increase in power conversion efficiency [84].

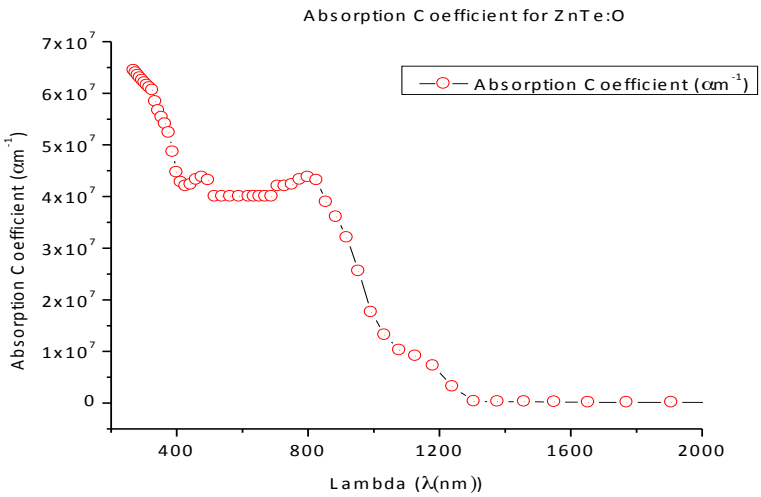

Figure 4. 10 Absorption coefficient for ZnTe:O

4.4.3 Conclusion

Numerical models have been used to examine the potentially attainable efficiency of ZnTe solar cells under several assumptions. There have been many issues that added complexity to the modeling of the cell. However, even though efforts at numerical modeling of thin film cells of ZnTe are relatively recent, progress has been good. The basic issue here was to determine the effects of CdTe thickness reduction. In case of CdS/CdTe solar cells, the conversion efficiency shows a decreasing trend with a decrease of CdTe thickness. The photo-generated carrier concentration decreases by a factor of 0.01 at just 1 mm of CdTe thickness, as found in the generation rate.

4.5 Numerical Analysis of SnS based Polycrystalline Solar Cells

SnS is a promising nontoxic and earth-abundant material suitable for photovoltaic applications. Photovoltaic solar cells based on Tin Sulphide absorbers have been analysed by using Solar Cell Capacitance Simulator software. The photovoltaic cell consists of SnS absorber layer, CdS as buffer and ZnO as optical window following the sequence p-SnS/ CdS/ZnO. After optimization of different parameters and layer thicknesses, a maximum efficiency of 10.6%, V_{OC} of 0.92 Volts, J_{SC} of 13.4 mA/cm^2 and Fill Factor of 86.3% were

reached. Simulation studies by varying several solar cell parameters such as thickness of various layers reveal that increasing the thickness of absorber layer results in higher efficiency. The concentration of shallow acceptors in the SnS has a crucial effect in the conversion efficiency, which rises up to about 15% for acceptor concentrations of 10^{19} cm^{-3}. The effect of the compensation ratio between donors and acceptors was also analysed but its effect on conversion efficiency is insignificant.

4.5.1 Review

The performance of thin films solar cells has been improving continuously in the last decade. In particular, photovoltaic (PV) devices based on CdTe and $CuInGaSe_2$ absorber materials have reached maximum efficiencies of 19.6% and 20.4% respectively [85]. These results indicate that by using thin film polycrystalline materials, high efficiency PV solar cells can be developed. By using these materials, genuine concerns arise that are Te, In and Ga are rare and very expensive for large scale use, and Cd based cells are toxic [86], which have motivated a search for alternative earth-abundant, non-toxic and inexpensive materials. In this concerns Tin Sulphide (SnS), a binary IV-group chalcogenide semiconductor, perceived to be a promising candidate for light absorption in the development of next generation of environmental friendly solar cells. SnS possesses a direct band-gap of 1.1 – 1.4 eV, which makes it a promising material for PV applications [87, 88]. Further, Sn and S are cheap and abundant in the earth crust, non-toxic, safe to handle and do not pollute the environment. PV solar cells based on SnS as absorber and the well know CdS as buffer layer has been reported for the first time with conversion efficiencies of 1.3% and quantum efficiencies of 70% [88].

Different alternate possibilities for SnS solar cell with different buffer and windows layers record increased efficiency of 2.46% is reported [89]. SnS has a high optical absorption coefficient of 10^5 cm^{-1} and a proper carrier concentration of $10^{14} – 10^{17}$ cm^{-3} [90, 91]. In some literature, it is revealed that p-SnS is obtained and have a conductivity of 10^{18} cm^{-3} in Ag-doped SnS crystal, while Sb-doped SnS crystal have a n-type (n-SnS) behaviour with carrier concentration of 10^{19} cm^{-1} [92]. A resistivity of 6.98Ω cm has also been reported [93]. Different values for parameters reported in the literature which are almost close in values but not exactly the same. In a report of SnS: Ag for annealing temperature of 260º C these values are reported as resistivity 3.1Ω cm, carriers concentration 1.3 x 10^{17} cm^{-3} and a direct band gap of 1.32eV [94].

The aim of this work is to analyse numerically the expected performance of PV devices based on SnS absorbers by means of dedicated software such as SCAPS. The effect of absorber layer thickness, the temperature variation and the sun power illumination has been investigated in this paper and a power conversion efficiency higher than 10% has been numerically simulated.

4.5.2 Experimental results

Different types of numerical simulators are used for analysis purposes. One of those simulator is SCAPS which is a one dimensional computer software to simulate the AC and DC electrical characteristics of thin film heterojunction solar cells. It is developed especially for CdTe and CIGS solar cells but can also be extended for the use of other types of solar cells. From the solution provided by SCAPS simulation, outputs such as current voltage characteristics in the dark and under illumination can be obtained. In addition, important information such as electric field distributions, free and trapped carrier populations, recombination profiles, and individual carrier current densities as a function of position can be extracted from the SCAPS program [95].

The three layers that are emphasized in this simulation are ZnO, n-CdS and p-SnS layer. By incorporating the various material parameters into SCAPS for all of the analysis aspects, changes in the values for efficiency, Voc, Jsc and FF as well as the effect of operating temperature are observed.

Table 4. 4 Basic parameters for SnS absorber layers

Parameter	**Value**	**Reference**
Thickness (μm)	1-4	
Bandgap (eV)	1.1 - 1.4	[3,4]
Electron affinity (eV)	4.0	[11]
Absorption coefficient α(cm^{-1})	10^5	[6, 7]
Carrier concentration, h (cm^{-3})	10^{14} - 10^{17}	[6, 7]
Acceptor density, N_A (cm^{-3})	10^{14} - 10^{19}	[8]
CB effective density of states, N_C (cm^{-3})	$2.2 \cdot 10^{18}$	SCAPS
VB effective density of state, N_V (cm^{-3})	$1.8 \cdot 10^{19}$	SCAPS

Obviously SCAPS output is highly dependent on the value of the parameters used to define the optical and electrical characteristics of all materials involved in the photovoltaic device to be simulated. ZnO and CdS are well known materials and their properties can be easily found in the literature [96]. However, regarding SnS material, few related literature has been produced up to now. The required parameters for SCAPS simulations in PV devices involving SnS absorbers are displayed in Table 4.4. Most of these values were obtained from available literature and some of them, N_C and N_V, were taken from the SCAPS files.

4.5.3 Results and discussions

4.5.3.1 Energy band diagram

Figure 4.12 displays the energy band diagram for a p-SnS/n-CdS/ZnO solar cell obtained from the output of SCAPS analysis. This model will help in explaining the properties of SnS film. SnS has a direct optical band gap (Eg) of 1.4eV; this value is close to the optimum value required for efficient light absorption for those photons whose energy is either equal or greater than 1.4 eV. Proper doping can control its optical properties.

The results mention here were obtained using an acceptor concentration $N_A=10^{14}$ cm^{-3} [90] except for those where N_A were changed deliberately in order to analyse its effect on the performance of PV devices. Therefore the energy band, I-V curves and studies of the efficiency dependence of SnS and CdS thicknesses and Temperature were obtained for $N_A=10^{14}$ cm^{-3}.

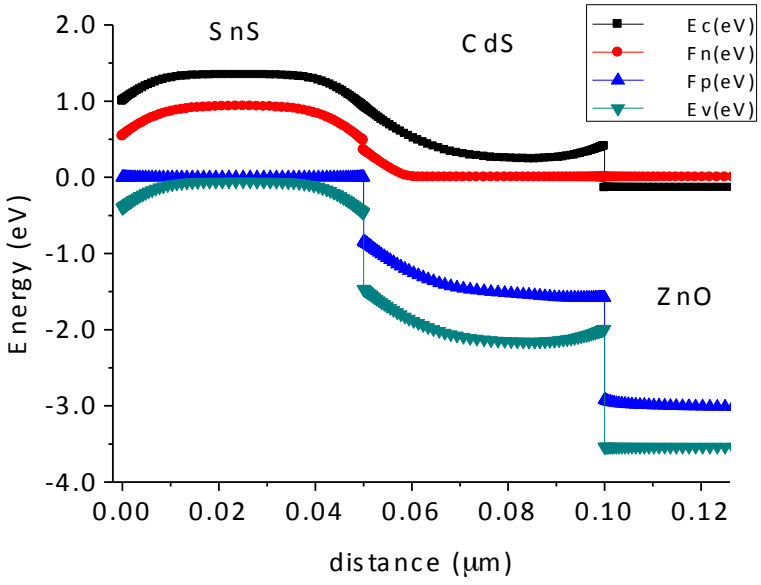

Figure 4. 11 Energy band diagram of SnS thin film

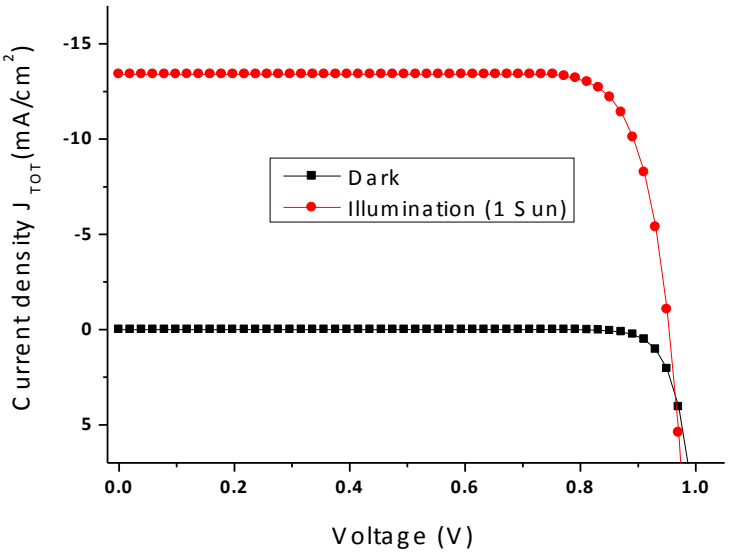

Figure 4. 12 Dark and illuminated curves for SnS/CdS/ZnO solar cell

4.5.3.2 J-V characteristics of a SnS-based PV device

The function of a solar cell is to convert light to electricity, and it might seem unusual to measure the photovoltaic cell in the dark, but for diode properties, dark measurements are precious. A solar cell in the dark is a large flat diode. A simple dark I-V measurement produces the exponential curve, a characteristic curve of diode. The current-voltage curve of a SnS/CdS/ZnO solar cell is shown Figure 4.13. In the dark it will give an extreme minimum value of current (I_D) that is due to the minority carriers. After illuminating the cell with 1 Sun (Air Mass 1.5) the PV process starts and due to the charge carriers produced by incident photons will cause current.

4.5.3.3 Effect of CdS buffer layer

In this simulation the analysis has taken out by varying the thickness of CdS buffer layer, while keeping the other thickness constant (SnS and ZnO). We have varied CdS thickness from 100nm to 1µm. Figure 4.14 shows the variation of the main parameters of PV solar cell as a function of the CdS thickness. The thinner the CdS layer the higher the Voc, Jsc and eta and the lower the FF. Increasing the thickness only increases the FF value and the other three parameters undergoes the opposite effect. Therefore, to achieve higher efficiencies the CdS thickness must be the thinnest allowed by the deposition method.

4.5.3.4 Optimization of SnS absorber layer thickness

In Tin Sulphide (SnS) based solar cell for simulation purposes used in this analysis is ZnO/n-CdS/p-SnS. Simulation are possible for different parameters. First, the thickness of SnS absorber layer is calculated for different thickness value, from 1µm up to 4µm.

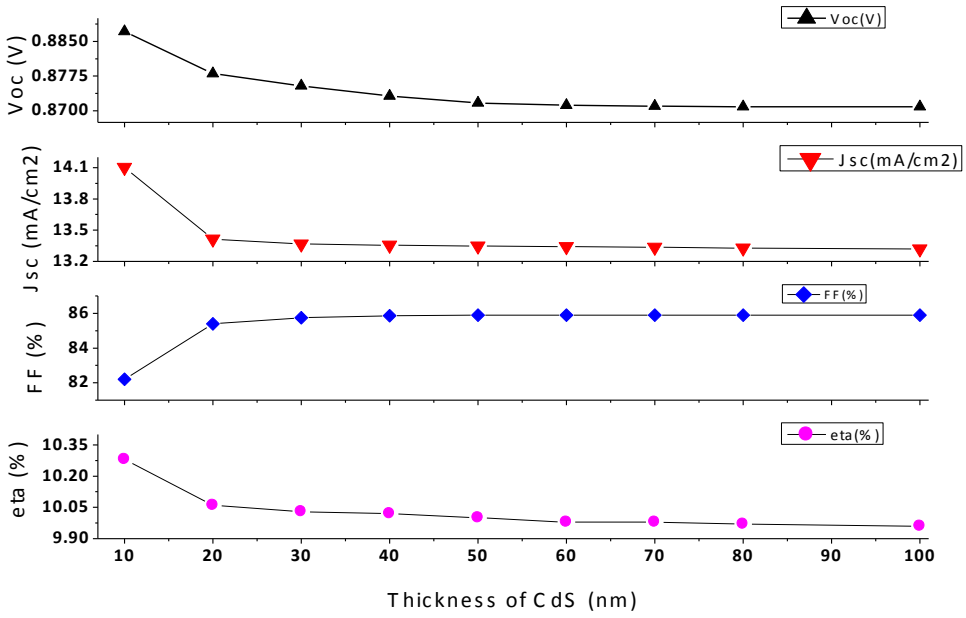

Figure 4. 13 Cell performance for different CdS thicknesses

To justify the simulation, the conventional SnS structure with CdS buffer layer has been verified in terms of SnS absorber and CdS buffer layer. At first, the SnS absorber thickness has been varied to find out the prime thickness for the conventional SnS structure with CdS as the window layer.

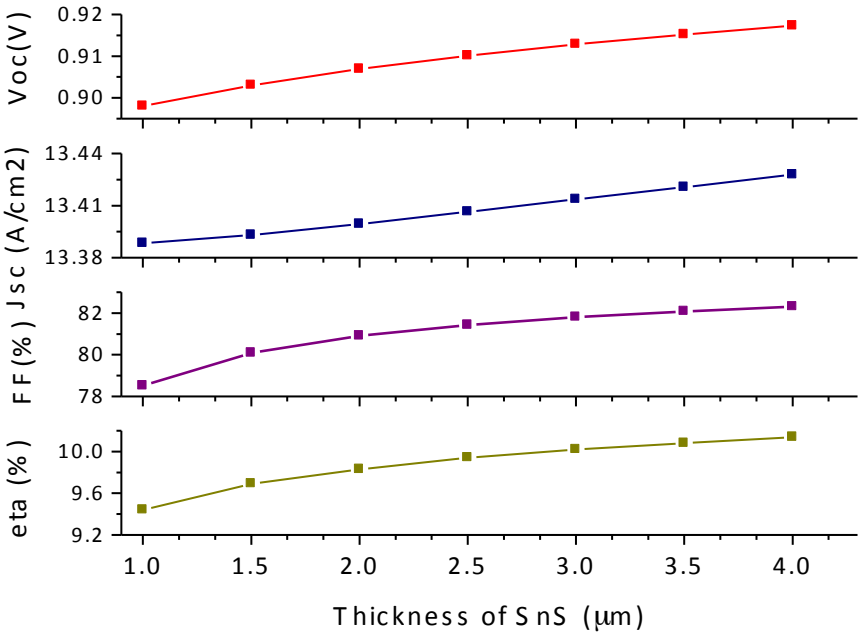

Figure 4. 14 Effect of SnS absorber thickness

Figure 4.15 shows the variation of the main parameters of PV solar cell as a function of the SnS absorber thickness. It was observed that the conversion efficiency of the solar cell increases with the thickness of the SnS absorber layer, but with a much slower rate over 3µm. The optimum thickness for SnS absorber layer would be around 3-4µm. From Figure 4.15, at the thickness of 1µm and 4µm, the calculated efficiency is 9.44% and 10.14%, respectively. Comparing the results with the 10.14% efficiency, electrons will be captured easily by the back contact for the recombination process. Therefore, fewer electrons will contribute to the quantum efficiency of the solar cell and the value for Voc and Jsc will be low. The increasing trend in Voc and Jsc can be seen when the absorber layers are increased.

4.5.3.5 Effect of Temperature

Operating temperature plays a dynamic role in the overall performance of solar cell. Normally for various calculations and analysis 27 ºC or 300 ºK is used as the room temperature. Here we have varied the temperature from 200 ºK to 400 ºK.

Figure 4.16 shows the variation of the main parameters of PV solar cell as a function of the operating temperature. It is observed that at room temperature the SnS-based PV device would operate near its maximum. But whenever the temperature is increased all basic parameters are severely affected. At higher temperature the electron and hole mobility,

carrier concentrations and band gaps of the materials would be effected which would alter the efficiency and other cell parameters.

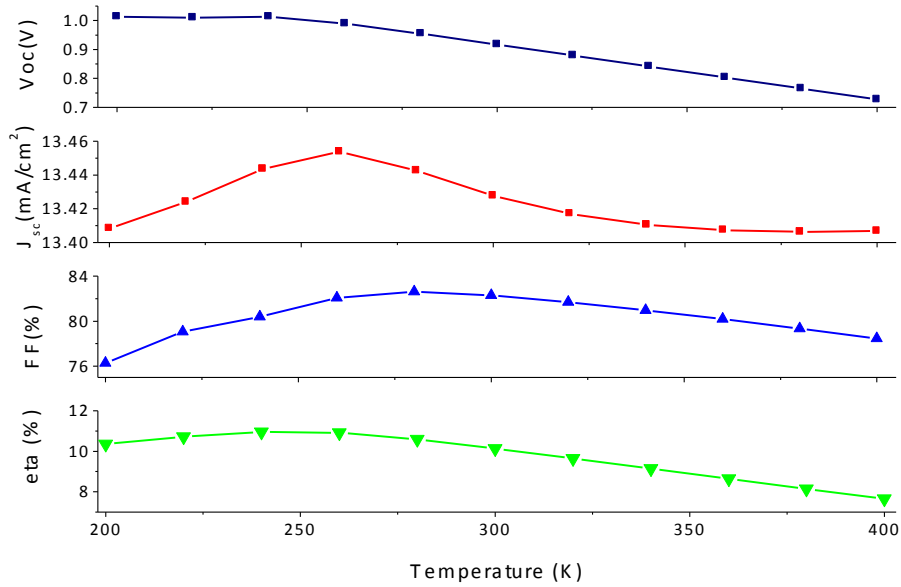

Figure 4. 15 Cell performance parameters as a function of temperature

As expected, the conversion efficiency decreases when the PV device operates at higher temperatures than the room temperature.

4.5.3.6 Effect of dopant concentration on the solar cell parameters

Dopant concentration highly affects the efficiency and other parameters of the solar cell. In the literature different values are reported for the acceptor concentration of SnS layers [90-92].

4.5.3.7 Effect of shallow acceptors density (N_A)

The results summarised in Figure 4.17 reveal that the acceptor concentration, N_A strongly affects the efficiency. A higher efficiency solar cell will be obtained by increasing the acceptor concentration. The results in Figures 4.12 - 4.16 are based on the value of $N_A=10^{14}$ cm^{-3}. Elsewhere Figure 4.17 shows the solar cell parameters as a function of the acceptor density, N_A.

In the analysis we have varied N_A value between 10^{14} cm^{-3} and 10^{19} cm^{-3} in the p-SnS absorber layer, here eta increased from 10.0% to 14.5%, which reveals that proper doping of the absorber layer would produce higher efficiency. Similarly, V_{OC} and J_{SC} also increase with the increase of N_A values.

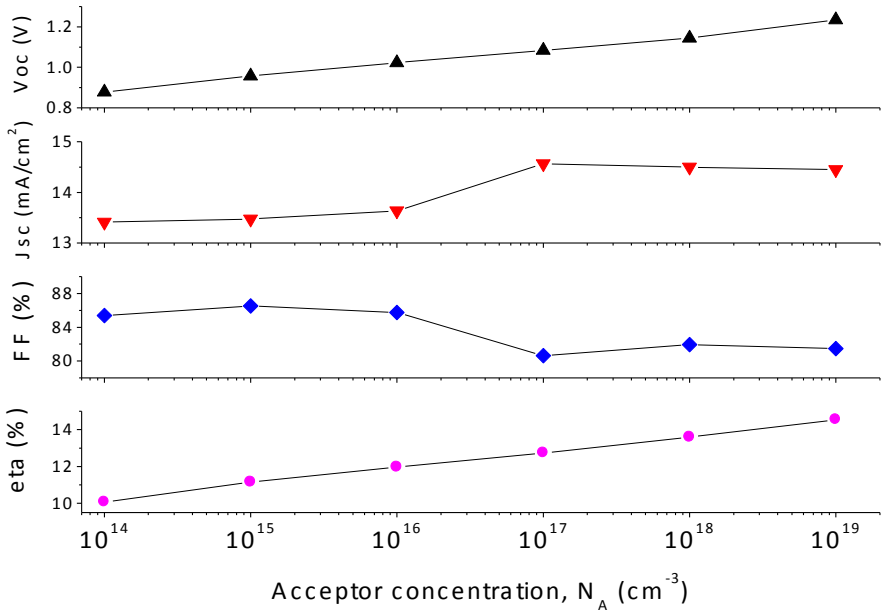

Figure 4. 16 Cell performance parameters for variable acceptor density (N_A)

The effect of N_A on FF is different as in Figure 4.17. The concentration of shallow donor considered uniform along the SnS layer for all the analysis except for Figure 4.18, where N_D has been varied.

4.5.3.8 Effect of shallow donors density (N_D)

Even if SnS is a p-type semiconductor it would contain some donors as the majority of the semiconductors. In order to check the effect of the presence of donors in the absorber SnS material, we have calculated the performance parameters as a function of the compensation ratio, ß=N_D/N_A, which is the ratio between the concentration of donors and the concentration of acceptors. Figure 4.18 summarizes the effect of the presence of an increasing amount of donors on the photovoltaic parameters of a SnS-based PV device. Calculations were made for an acceptor concentration of $N_A=10^{18}$ cm^{-3} and the compensation ratio was varied from 0.2 to 20%, which means a concentration of shallow donors ranging from $2*10^{15}$ to $2*10^{17}$ cm^{-3}. Increasing the amount of donors results in a slight decrease in V_{OC}, FF and eta while a slight increase in J_{SC}. This effect is much smaller than that obtained for the variation of the majority carriers (holes), which is proportional to the shallow acceptor concentration.

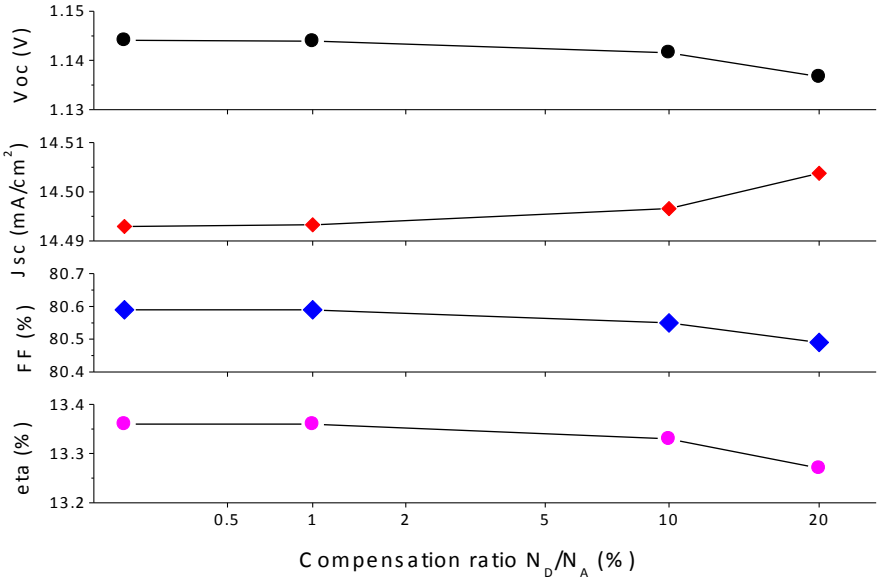

Figure 4. 17 Cell performance parameters as a function of the compensation ratio ß=N_D/N_A

The analysis and simulation performed here reveal that the acceptor concentration has a high influence on the performance of SnS-based solar cell. Therefore further development in the performance of SnS-based PV devices should focus on the achievement of higher p-type doping which will result in higher holes concentration.

4.5.4 Conclusion

Numerical simulation and analysis can lead to improved in-depth details of the physical operation of thin film cell structure. In order to develop thin film solar cells that are free from material constraints, an inexpensive thin film solar cell has been analysed with a good efficiency of 10.62%, which is a very promising result and further enhancement is possible. Electrical performance for the SnS based solar cell has been investigated in term of absorber and buffer layer thickness. Operating temperature also effect the performance of the solar cell. The optimum temperature that is used for most of the simulation and for this analysis is near to 300 ^{o}K. The overall efficiency decreases by increasing the temperature.

We have found that the acceptor concentration has a high influence on the performance of SnS-based solar cell. Increasing the shallow acceptor concentration from 10^{14} to 10^{19} cm^{-3} the conversion efficiency of SnS-based PV devices boosts from 10 to near 15%. Therefore further development in the performance of SnS-based PV devices should focus in the achievement of higher p-type doping.

References

[1] Movla, H., Abdi, E., & Salami, D. (2013). Simulation analysis of the CIGS based thin film solar cells. *Optik-International Journal for Light and Electron Optics*, *124*(22), 5871-5873.

[2] Gloeckler, M., Fahrenbruch, A. L., & Sites, J. R. (2003, May). Numerical modeling of CIGS and CdTe solar cells: setting the baseline. In *Photovoltaic Energy Conversion, 2003. Proceedings of 3rd World Conference on* (Vol. 1, pp. 491-494). IEEE.

[3] Burgelman, M., Verschraegen, J., Degrave, S., & Nollet, P. (2005). Analysis of CdTe solar cells in relation to materials issues. *Thin solid films*, *480*, 392-398.

[4] Burgelman, M., Verschraegen, J., Degrave, S., & Nollet, P. (2004). Modeling thin-film PV devices. *Progress in Photovoltaics: Research and Applications*, *12*(2-3), 143-153.

[5] Romeo, A., Terheggen, M., Abou-Ras, D., Bätzner, D. L., Haug, F. J., Kälin, M., & Tiwari, A. N. (2004). Development of thin-film Cu (In, Ga) Se2 and CdTe solar cells. *Progress in Photovoltaics: Research and Applications*, *12*(2-3), 93-111.

[6] Tiwari AN, Krejci M, Haug F-J, Zogg H. 12.8% Efficiency Cu(In, Ga)Se2 solar cell on a flexible polymer sheet. Progress in Photovoltaics: Research and Applications 1999; 7: 393–397.

[7] Tuttle J.R, Szalaj A, Keane J. A 15.2% AMO/1433 W/kg thin-film Cu(In,Ga)Se2 solar cell for space applications. Proceedings of the 28th IEEE Photovoltaic Specialists Conference, Anchorage, 2000; 1042–1045.

[8] S. M. Sze, Physics of Semiconductor Devices (John Wiley & Sons, 1981), 2nd Ed.

[9] A manual for AMPS-1D for Windows ’95/NT, Pennsylvania State University 1997

[10] Pala, R. A., White, J., Barnard, E., Liu, J., & Brongersma, M. L. (2009). Design of Plasmonic Thin-Film Solar Cells with Broadband Absorption Enhancements.Advanced Materials, 21(34), 3504-3509.

[11] J. T. Heath, J. D. Cohen, and W. N. Shafarman,” Bulk and metastable defects in CuIn1−xGaxSe2 thin films using drive-level capacitance profiling” J. Appl. Phys. 95, 1000 (2004).

[12] Breitenstein, O., Rakotoniaina, J. P., Al Rifai, M. H., & Werner, M. (2004). Shunt types in crystalline silicon solar cells. Progress in Photovoltaics: Research and Applications, 12(7), 529-538.

[13] Kendig, D., Alers, G. B., & Shakouri, A. (2010, May). Thermoreflectance imaging of defects in thin-film solar cells. In Reliability Physics Symposium (IRPS), 2010 IEEE International (pp. 499-502). IEEE.

[14] A. L. Fahrenbruch and R. H. Bube, Fundamentals of Solar Cells (Academic Press, Inc., New York, 1983).

[15] S. Wagner, J. Shay, P. Migliorato, H.M. Kasper, Applied Physics Letters 25 (1974) 434.

[16] L.L. Kazmerski, et al., Applied Physics Letters 46 (1976) 268.

[17] K. Ramanathan, et al., Progress in Photovoltaics: Research and Applications 11 (2003) 225-230.

[18] K. Siemer, et al., Proceedings of 16th European Photovoltaic Solar Energy Conference, Glasgow, pp. 895-898.

[19] Jackson, P., Hariskos, D., Lotter, E., Paetel, S., Wuerz, R., Menner, R., & Powalla, M. (2011). New world record efficiency for Cu (In, Ga) Se2 thin-film solar cells beyond 20%. Progress in Photovoltaics: Research and Applications, 19(7), 894-897.

[20] Ward, J. S., Ramanathan, K., Hasoon, F. S., Coutts, T. J., Keane, J., Contreras, M. A., and Noufi, R. (2002). A 21.5% efficient Cu (In, Ga) Se2 thin-film concentrator solar cell. Progress in Photovoltaics: Research and Applications, 10(1), 41-46.

[21] W. N. Shafarman and L. Stolt, Handbook of Photovoltaic Science and Engineering" Wiley Chichester, 2003, chap. Cu(In,Ga)Se_2 Solar Cells, pp. 567–616.

[22] U. Rau and H. W. Schock, Appl. Phys. A 69, 131 (1999).

[23] Miles, R. W., Hynes, K. M., & Forbes, I. (2005). Photovoltaic solar cells: An overview of state-of-the-art cell development and environmental issues. *Progress in Crystal Growth and Characterization of Materials*, *51*(1), 1-42.

[24] M. A. Contreras, K. Ramanathan, J. AbuShama, F. Hasoon, D. L. Young, B. Egaas, and R. Noufi, Prog. Photovoltaics 13, 209 (2005).

[25] K. Ramanathan, M. A. Contreras, C. L. Perkins, S. Asher, F. S. Hasoon, J. Keane, D. Young, M. Romero, W. Metzger, R. Noufi, et al., Prog. Photovoltaics 11, 225 (2003).

[26] A. Pudov, Ph.D. thesis, Colorado State University (2005).

[27] [33] A. Romeo, M. Terheggen, D. Abou-Ras, D. L. B¨atzner, F.-J. Haug, M. K¨alin, D. Rudmann, and A. N. Tiwari, Prog. Photovoltaics 12, 93 (2004).

[28] K. L. Chopra, P. D. Paulson, and V. Dutta, Prog. Photovoltaics 12, 69 (2004).

[29] U. Rau and H. W. Schock, Appl. Phys. A 69, 131 (1999)

[30] A. Luque and S. Hegedus, eds., Handbook of Photovoltaic Energy Conversion and Engineering (John Wiley & Sons Ltd, Chichester, West Sussex, England, 2003).

[31] Schmid, D., Ruckh, M., & Schock, H. W. (1994, December). A comprehensive characterization of the interfaces in Mo/CIS/CdS/ZnO solar cell structures. InPhotovoltaic Energy Conversion, 1994., Conference Record of the Twenty Fourth. IEEE Photovoltaic Specialists Conference-1994, 1994 IEEE First World Conference on (Vol. 1, pp. 198-201). IEEE.

[32] Schulmeyer, T., Hunger, R., Klein, A., Jaegermann, W., & Niki, S. (2004). Photoemission study and band alignment of the CuInSe 2 (001)/CdS heterojunction. Applied physics letters, 84(16), 3067-3069. S.-H. Wei and A. Zunger, Appl. Phys. Lett. 63, 2549 (1993).

[33] F. S¨auberlich and A. Klein, Mat. Res. Soc. Symp. Proc. 763, 471 (2003).

[34] S. H. Wei and A. Zunger, Appl. Phys. Lett. 72, 2011 (1998).

[35] D. K. Schroder, Semiconductor Material and Device Characterization (John Wiley & Sons, Inc., New York, 1998).

[36] S. J. Fonash, Solar Cell Device Physics (Academic Press, New York, 1981).

[37] J. Lee, J. D. Cohen, and W. N. Shafarman, Thin Solid Films 480-481, 336 (2005).

[38] W. N. Shafarman and L. Stolt, Handbook of Photovoltaic Science and Engineering (Wiley Chichester, 2003), chap. Cu(In,Ga)Se2 Solar Cells, pp. 567–616.

[39] M. Gloeckler, Ph.D. thesis, Colorado State University (2002).

[40] J.J. Loferski, Journal of Applied Physics 27 (1956) 777.

[41] J.J. Loferski, Proceedings of the 12th IEEE Photovoltaics Specialists Conference, 1976, p. 853.

[42] N.A. Gokcen, J.J. Loferski, Solar Energy Materials 1 (24) (1979) 271.

[43] D.A. Cusano, Solid State Electronics 6 (1963) 217.

[44] E.I. Adriorvich, Y.M. Yuanov, G.R. Yadudaev, Soviet Physics e Semiconductors 3 (1969) 61.

[45] D. Bonnet, H. Rabenhorst, Proceedings of the 9th IEEE Photovoltaics Specialists Conference, 1972, pp. 129-131.

[46] First Solar press release. 25 February, 2014. First solar sets world record for CdTe solar cell efficiency (http:// investor.firstsolar.com/releases.cfm?sect=all; accessed 24 April 2014).

[47] D. W. Niles, D. Rioux, and H. H¨ochst, J. Appl. Phys. 4586-4590 (1993).

[48] S.-H. Wei, S. B. Zhang, and A. Zunger, J. Appl. Phys. 87, 1304 (2000).

[49] J. Fritsche, T. Schulmeyer, D. Kraft, A. Thißen, A. Klein, and W. Jaegermann, Appl. Phys. Lett. 81, 2297 (2002).

[50] G. Stollwerck and J. R. Sites, in Proc. 13th European Photovoltaic Sol. Energy Conf. (1995), pp. 2020–2022.

[51] A. Niemegeers and M. Burgelman, J. Appl. Phys. 81, 2881 (1997).

[52] C. Neumann, A. N¨othe, and N. O. Lipari, Phys. Rev. B 37, 922 (1988).

[53] L. S. Dang, G. Neu, and R. Romestain, Solid State Comm. 44, 1187 (1982).

[54] O. Madelung, ed., Semiconductors: Others Than Group IV Elements and III-V Compounds (Data in Science and Technology) (Springer Verlag, 1992).

[55] M. Gloeckler, A. L. Fahrenbruch, and J. R. Sites, in Proc. 3rd World Conf. Photovoltaic Energy Conversion (2003), pp. 491–494.

[56] S. S. Hegedus and W. N. Shafarman, Prog. Photovoltaics 12, 155 (2004).

[57] M. Burgelman, J. Verschraegen, S. Degrave, and P. Nollet, Prog. Photovoltaics 12, 143 (2004).

[58] Gloeckler, M., A. L. Fahrenbruch, and J. R. Sites. "Numerical modeling of CIGS and CdTe solar cells: setting the baseline." *Photovoltaic Energy Conversion, 2003. Proceedings of 3rd World Conference on*. Vol. 1. IEEE, 2003.

[59] Lundberg, O., Edoff, M., & Stolt, L. (2005). The effect of Ga-grading in CIGS thin film solar cells. Thin Solid Films, 480, 520-525.

[60] R.W. Birkmire, L. Kazmerski. Harnessing the Sun with Thin-Film Photovoltaics, Electrochemical Society International Symposium. Seattle (Washington): NREL 1999, 1-6.

[61] A. Fahrenbruch, R.H. Bube. Fundamentals of Solar Cells. Academic Press, New York 1983.

[62] A.O. Pudov, A. Kanevce, H. Al-Thani, J.R. Sites, F.S. Hasoon,"Secondary barriers in CdS–$CuIn_{(1-x)}Ga_xSe_2$ solar cells," Journal of applied physics, (2005), 97(6), 064901-064901

[63] Marc Burgelman. Simulation programme SCAPS-1D for thin film solar cells. Jan 23, 2013. http://users.elis.ugent.be/ELISgroups/solar/projects/scaps.html.

[64] J.N. Duenow, T.A. Gessert, D.M. Wood, T.M. Barnes, M. Young, B. To, T.J. Coutts. (2007). Transparent conducting zinc oxide thin films doped with aluminum and

molybdenum. Journal of Vacuum Science & Technology A: Vacuum, Surfaces, and Films, 25(4), 955-960.

[65] P. Jackson, D. Hariskos, E. Lotter, S. Paetel, R. Wuerz, R. Menner, W. Wischmann, M. Powalla. New world record efficiency for Cu(In,Ga)Se2 thin-film solar cellsbeyond 20%. Progress in Photovoltaics: Research and Applications 2011. DOI: 10.1002/pip.1078 (Presented at 25th EU PVSEC WCPEC-5, Valencia, Spain, 2010).

[66] N. Amin, K. Sopian, M. Konagai, "Numerical modeling of CdS/CdTe and CdS/CdTe/ZnTe solar cells as a function of CdTe thickness", Solar Energy Materials and Solar Cells, 91 (2007), 1202-1208.

[67] L. A. Kosyachenko, "Possibilities to decrease the absorber thickness reducing optical and recombination losses in CdS/CdTe solar cells", Materials for Renewable and Sustainable Energy, 3 (2013) 1-20.

[68] A. Kaneta, S. Adachi, Photoreflectance study in the E-1 and E-1+Delta(1) transition regions of ZnTe, J. Phys. D: Appl. Phys. 33 (2000) 901-905.

[69] A. Pistone, A. S. Arico, P. L. Antonucci, D. Silvestro, V. Antonucci, "Preparation and characterization of thin film ZnCuTe semiconductors", Sol. Energy Mater. Sol. Cell. 53 (1998) 255-267.

[70] D. H. Han, J. S. Choi, S. M. Park, Electrochemical preparation of zinc telluride films on gold electrodes, J. Electrochem. Soc. 150 (2003) C342-C346.

[71] T. Mahalingam, V. S. John, S. Rajendran and P. J. Sebastian, Electrochemical deposition of ZnTe thin films, Semicond. Sci. Technol. 17 (2002) 465-470.

[72] K. Ernt, I. Seiber, M. Neumann-Spalart, M. C. Lux-Steiner, R. Könenkamp, "Characterization of II-VI compounds on porous substrates", Thin Solid Films 361 (2000) 213-217.

[73] A. Mondal, R. W. Birkmire, B. E. McCandless, Proc. 22nd Photov. Special. Conf. (IEEE, New York 1997) 1126.

[74] C. Winnewiser. P. U. Jepsen, M. Schall, V. Schiyja, H. Helm, Electro-optic detection of THz radiation in LiTaO3, LiNbO3, and ZnTe,Appl. Phys. Lett. 70 (1997) 3069-3071.

[75] O. Skhouni, A. El Manouni, M. Mollar, R. Schrebler, B. Marí, "ZnTe thin films grown by electrodeposition technique on Fluorine Tin Oxide substrates " Thin Soild Films (2014), DOI : 10.1016/j.tsf.2014.06.002

[76] S.O. Ferreira, H. Sitter, W. Faschinger, G. Brunthaler, “Growth of highly doped p-type ZnTe layers on GaAs using a nitrogen DC plasma cell”, Journal of crystal growth, 140 (1997) 282-286.

[77] I. W. Tao, M. Jurkovic, W.I.Wang, “Doping of ZnTe by molecular beam epitaxy”, Appl. Phys. Lett., 64 (1994) 1848-1849.

[78] Robert F. Brebrick, "Deviations from stoichiometry in binary ionic crystals", Journal of Physics and Chemistry of Solids 43 (1958) 190-195.

[79] G. Mandel, "Self-compensation limited conductivity in binary semiconductors”. Phys. Rev. 134 (1964) A1073.

[80] J. D. Dow, R.-D. Hong, S. Klemm, S. Y. Ren, M.-H. Tsai, O. F. Sankey and R. V. Kasowski, Phys. Rev. B (Condensed Matter) 43 (1991) 5396.

[81] W. Wang, A.S. Lin, J.D. Phillips, “Intermediate-band photovoltaic solar cell based on ZnTe:O”, Appl. Phys. Lett., 95 ((2009) 011103.

[82] M. A. Green, K. Emery, Y. Hishikawa, W. Warta and E. D. Dunlop, Prog. Photovoltaics. 21 (2013) 827–837.

[83] C. Wadia, A. P. Alivisatos, and D. M. Kammen, Environ, Sci. Technol. 43 (2009) 2072–2077.

[84] A. R. H. F. Ettema, R. A. Groot, C. Haas, and T. S. Turner, Phys. Rev. B 46 (1992) 7363-7373.

[85] K. T. R. Reddy, N. K. Reddy, and R. W. Miles, Sol. Energy Mater. Sol. Cells. 90 (2006) 3041–3046.

[86] P. Sinsermsuksakul, K. Hartman, S. B. Kim, J. Heo, L. Sun, H. H. Park, R. Chakraborty, T. Buonassisi and R. G. Gordon, Applied Physics Letters. 102 (2013) 053901-053905.

[87] N. K. Reddy, Y. B. Hahn, M. Devika, H. R. Sumana, and K. R. Gunasekhar, J. Appl. Phys. 101(9) (2007) 093522-093527.

[88] J. Vidal, S. Lany, M. d’Avezac, A. Zunger, A. Zakutayev, J. Francis, and J. Tate, Appl. Phys. Lett. 100 (2012) 032104-4.

[89] W. Albers, C. Hass, H.J. Vink , Applied Physics. 32 (1961) 2220-2225.

[90] M. Devika, R.N. Koteeswara, K. Ramesh, Journal of the Electrochemical Society. 153 (2006) 727-733.

[91] H. J. Jia, S.Y. Cheng, S.K. Wu, Y.L Yang, Natural Science 2 (2010) 197-200.

[92] M. Sugiyama, K.T.R. Reddy, N. Revathi ,Y. Shimamoto and Y. Murata, Thin Solid Films, 519 (2011) 7429-7431.

[93] Burgelman, M., Nollet, P., & Degrave, S. Modelling polycrystalline semiconductor solar cells. Thin Solid Films, 361, 527-532, 2000.

[94] Burgelman, M., Verschraegen, J., Degrave, S., and Nollet, P. Modeling thin-film PV devices. Progress in Photovoltaics: Research and Applications, 12(2-3), 143-153, 2004.

[95] Rau, U., and Schmidt, M, "Electronic properties of ZnO/CdS/Cu(In,Ga)Se_2 solar cells - aspects of heterojunction formation," Thin Solid Films, 387(1), 141-146, 2001.

CHAPTER 5

Multi-layer and intermediate band concept for thin-film solar cells

5 Multi-Layer solar cells: in comparison with CIGS thin films

Different materials have different band gaps and can absorb the appropriate portion of solar spectra that can give the corresponding conversion efficiency. To harness maximum number of photons and to enhance the conversion efficiency of solar cell, the use of tandem-solar cell is the ultimate option. Different materials with different band-gap respond to the appropriate wavelength, and hence the efficiency will be reached up to 46% or even high. The analysis here is for the CIS/CGS based multi-layer with two absorber and their conversion efficiency. In PV cell structure there are many parameters influencing the efficiency and performance. To get confidence in a solar cell model, one has to take different characteristics as well as different possible conditions to be simulated and compared. Various layer thickness and parameter variations have been investigated. The variation of absorber layer band-gap CIGS, the effect of electron affinity of the CdS buffer layer, and the different variation of band-gap of CIGS absorber layer have been investigated. At least it is clear that numerical modelling alone is not adequate to obtain better solar-cell.

5.1 CIGS based multi-layer solar cells

The recent boom in the demand of photovoltaic solar cells might create a material shortage in the future. For space as well as terrestrial use, thin-film solar cells are promising alternate in terms of the device design, fabrication and cost effectiveness. As thin film have the potential to revolutionize the present cost structure it will replace the expensive silicon wafers modules which dominate above 50% of the market share. This work deals with comparing thin-film CIGS solar cell with multilayer CIS/CGS solar cells. Replacing the existing CIGS by multilayer will increase the efficiency by 40-50% and will decrease the use of material by 30-40%. Simplicity of manufacturing and the cost per reliable watt will encourage the researcher and academia. ZnO/CdS/$CuInSe_2$/$CuGaSe_2$ multilayer solar cell with two absorbers and different bandgap values, with Solar Cell Capacitance Simulator (SCAPS) calculations increases conversion efficiencies up to 50% and with multi sun, it can boost up to 60%. But for single absorber layer $CuInGaSe_2$ (CIGS) solar cells, the simulated efficiency is increased by 30% while its thickness is increased by 50% or more. Cheap, efficient and moderate solar cells are expected to dominate the market and fulfil the energy requirements.

5.1.1 Introduction

This work is related to the realization of higher conversion efficiencies in thin-film solar cells as well as modules that is an important goal for the photovoltaic industry. Record-efficiency

devices provide a proof of concept for developing products. Dedicated simulation software offer a suitable tool for exploring new concepts. The use of several absorber layers (tandem-concept) in solar cells allow harnessing a higher amount of photons and hence the conversion efficiency increases. To describe and demonstrate the physical behaviour of photovoltaic devices theoretically, different type of numerical modelling software are used [1]. Numerous simulation and experimental work is performed in the photovoltaic field to obtain high conversion efficiency and to increase the stability and durability of the technology. The evolution from 6% efficient crystalline silicon (c-Si) cell is reached to 25.0% [2]. The emergence of new materials, and the new concept that boost the efficiency up to 44.7% for multi-junction (tandem four junction) solar cell [3]. For chalcopyrite thin-film solar cell, in CIGS the experimental and simulation results for different combination compared in a recent work [4]. The efficiency for CIGS obtained is 20.8% for 1-SUN but it is 22.8% for concentrated solar cells application [5].

In this work we have analyzed the performance of CIGS thin-film (ZnO/CdS/CIGS) solar cell and a multilayer ZnO/CdS/CIS/CGS solar cell. The results obtained from multilayer combination was higher than that of the earlier one.

5.1.2 $CuInGaSe_2$ (CIGS) Solar cells

I-III-VI chalcopyrite materials have some very desirable properties for PV application. The bandgap for $CuInSe_2$ is 1.53eV, an Ideal material for PV purposes. Further, the bandgap can be controlled by alloying with Ga, Al or S [6]. Moreover $Cu(In, Ga)Se_2$ has gained worthy reputation with high efficiency.

Table 5. 1 Photovoltaic parameters for CIGS solar cells with different Ga content

Ga content	V_{OC} (V)	J_{SC} (mA/cm^2)	FF (%)	eta (%)
0.00	0.5282	48.3933	79.75	20.38
0.31	0.6747	46.2690	82.37	25.71
0.45	0.7733	45.7018	83.43	29.48
0.66	0.8768	42.0037	84.04	30.0
1.00	0.8807	38.5823	83.59	28.40

The experimental results reported already give the efficiency above 20% [4, 5]. A higher value of 20.1% and 20.3% efficient CIGS solar cell for 1-sun is reported [7]. The efficiency for concentrated (multi sun) is 22.8% as reported in the latest literature [5]. The CIGS film consists of a p-CIGS absorber layer with a combination of n-CdS layer and ZnO window layer. The bandgap here is a function of Gallium and can be varied from 1.0 – 1.72eV that would cause the effect in the variation of other solar cell parameters [8]. Simulation results giving efficiencies above 25% are also published.

Though its efficiency is high but still it is difficult to commercialize this due to the availability of resources and particularly the rare metals Indium (In) and gallium (Ga) that adds to the cost of CIGS based technology [9]. The Gallium concentration was changed and the effect of different parameters has been observed in the CIGS thin film solar cell, the summary of results is demonstrated in Table 5.1. The open circuit voltage (V_{OC}) increases as the Gallium (Ga) content increases and the bandgap of the CIGS layer also increases.

The short circuit current represented by (J_{SC}) decreases as bandgap increases due to the recombination of carriers. It has the reverse effect then Voc. Similarly the Fill-Factor (FF) increases up to an increase of 50%, moreover after increase in Ga contents beyond 50% causes decrease in FF. The same phenomenon is also observed in the case of external quantum efficiency QE (%). In the beginning, eta (η) increases up to 66% of Ga contents but further increase of Ga causes decrease in eta [10]. The results obtained by using SCAPS are given in Table 5.1.

5.1.3 Multi-layer CIS/CGS Solar cells

The aim of multi-junction solar cells is to exploit and convert all the incident photon from the sun into electricity. Because the major factor of energy loss is due to the gap between the photon energy and the bandgap energy (Eg) of the absorber material. A tandem (multi-junction) solar cell is the combination of two or more solar cells and an intervening buffer layer between the two cells. Each cell absorbs the corresponding wavelength and the resultant efficiency increases. The highest efficiency with 44.7% is reported recently for a triple-junction III-V based solar cell under concentration of 297 suns [3].

The same concept can be applied to CIGS based devices. Such a multi-layer CIS/CGS solar cell is based on the combination of two different absorbent layers with different band gaps. The CIS/CGS multi-layer cell used for simulation has two absorber layers, $CuGaSe_2$ of 0.5 µm and $CuInSe_2$ of 0.5µm (optimum thickness), for obtaining best output values, the

thickness of $CuInSe_2$ is varied from 0.080µm up to 0.50µm. The thickness of n-CdS and i-ZnO layers are 0.050µm each. The total thickness is 1.0µm for both layers, 100% less than that of CIGS layer (1.5µm -3µm). A general schematic is given in Figure 5.1.

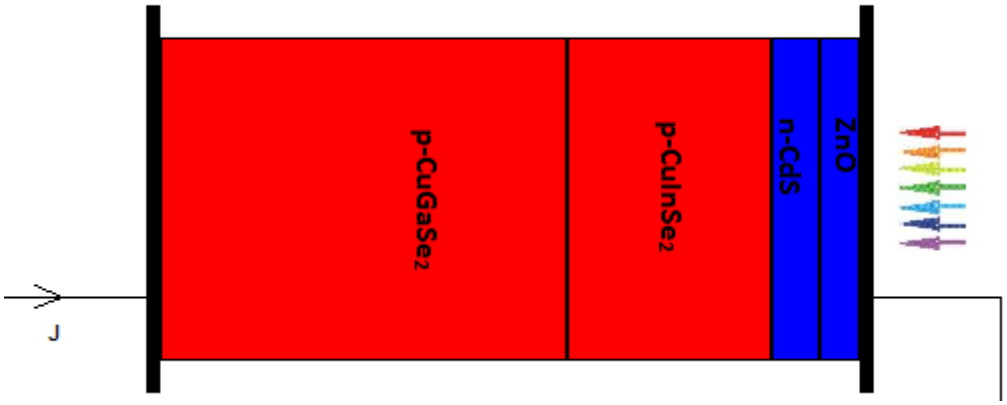

Figure 5. 1 Schematic of CIS/CGS multi-layer solar cell

Figure 5.2 displays the energy band diagram of a $CuInSe_2/CuGaSe_2$ multilayer solar cell. The Valence band of both absorbents are aligned and the higher $CuGaSe_2$ gap results in a step of about 0.8 eV in the Conduction bands.

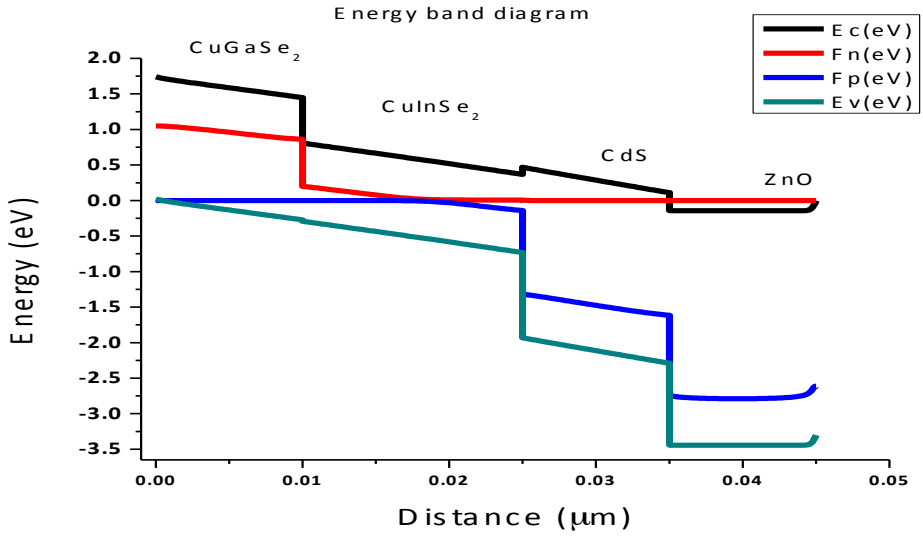

Figure 5. 2 Band diagram of a CIS/CGS multi-layer solar cell

The simulation results for both cells (CIGS single layer, and CIS/CGS multi-layer) is given. In Table 5.1, the simulated results are for the first case, giving maximum efficiency of 30.0% for Ga contents of 0.66, and a layer thickness of 2.5µm. The experimental result giving maximum efficiency of above 20% and similar results were obtained from simulations in a recent work [4]. Our simulation gives better results.

The PV parameters of a CIS/CGS multi-layer solar cell are specified in detail in Figure 5.3. The values obtained here are eta 52.0%, FF 81.83%, J_{SC} 0.04896 (A/cm^2) and open circuit voltage V_{OC} 1.298 (V). The high conversion efficiency of such a device is mainly due to the higher open circuit voltage (Voc) of such a PV device and the higher photon absorption related to the lower bandgap absorber ($CuInSe_2$). Moreover, the material used in the multilayer combination is less (40%) than that of single layer CIGS thin-film, and the conversion efficiency obtained is more than 50% from that of experimental results and 30% more than the simulated results.

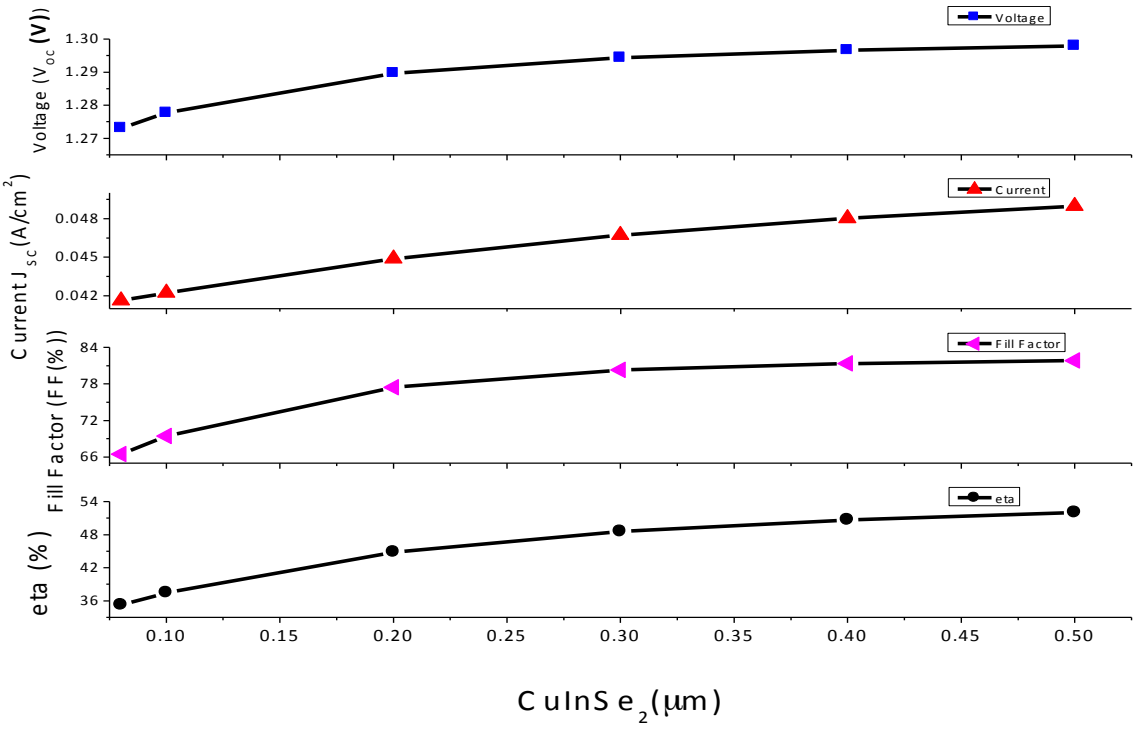

Figure 5. 3 Photovoltaic parameters of CIS/CGS multi-layer solar cell

5.2 Multi Sun Analysis: A case study for CIGS-based solar cell

Sun power concentration (multi-sun) has a prominent effect on the overall performance of the solar cell. In the case of CIGS- based solar cell, the effect is prominent up to 20-30 suns, further concentration will have adverse effect. The spectra of multi-sun is elaborated in figure 5.5. We have also used SCAPS to analyse the behaviour of CIGS solar cells under concentrated illumination conditions (multi-sun analysis). Figure 5.4, shows the behaviour of

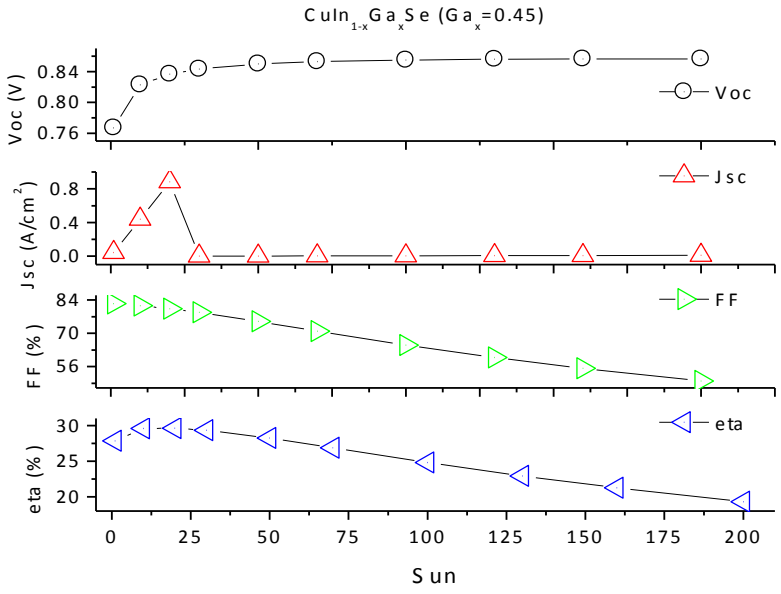

Figure 5. 4 Multi sun Analysis for CIGS based solar cell

the most important parameters of a solar cell as a function of the illumination density(multi-sun, 1-200 SUNs). The maximum values of the output are reported for 20-suns, after that the values decrease.

Table 5. 2 Photovoltaic parameters for CIGS solar cells with different suns

Sun	V_{OC}	J_{SC}	FF	eta
Unit	Volt	A/cm^2	%	%
1	0.7669	0.04397	82.55	27.84
10	0.8229	0.4404	81.65	29.59
20	0.8366	0.88221	80.32	29.64
30	0.8433	0.00133	78.78	29.35
50	0.8498	0.00222	75.03	28.25
70	0.8529	0.00311	70.88	26.86
100	0.8551	0.00446	64.99	24.79
130	0.856	0.00582	59.83	22.93
160	0.8563	0.00719	55.27	21.27
200	0.8562	0.00903	49.91	19.3

An experimental value of 21.5% efficiency was reported under a mildly concentrated sun-power (15-SUNs) [9].

Table 5.2 gives the corresponding values for the important solar cell parameters. V_{OC} increases smoothly with increase in sun-power, J_{SC} first increasing abruptly and then decreases after 30-sun, giving a maximum value for 20-SUNs. FF decreases while increasing the sun-power, and conversion efficiency first increases and then decreases.

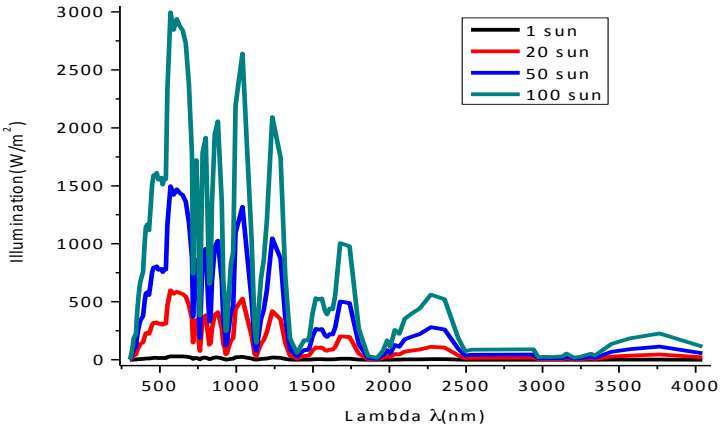

Figure 5. 5 Multi-sun spectra 1-100 sun

The graph for multi-sun in figure 5.5 is for up-to 100-SUNs, maximum concentrating values are also possible, but for CIGS solar cell, 15-25 suns values are optimum, beyond this the effect will be reversed. The reason is the capacity of charge carriers and temperature that may affect the behaviour of the solar cells and conversion efficiency.

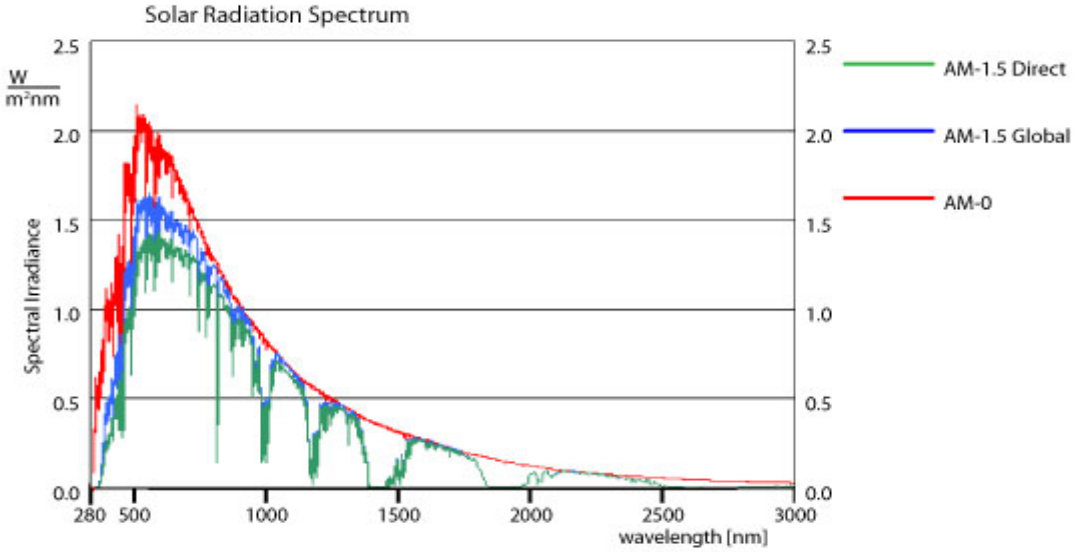

Figure 5. 6 A general solar radiation Spectrum

A general solar spectrum is shown in figure 5.6. As we know, the atmosphere does not just change the overall intensity, but the whole spectral distribution. For instance, most of the high-energy wavelengths that are present in the sun light are filtered out by the Ozone layer. Generally, with longer paths through the atmosphere (at higher latitudes or around sunset), the larger the part of infrared light, the lower the energy spectrum. In order to be able to compare solar modules, standard test conditions have been designed. These conditions include spectrum, intensity and temperature. The standard spectra refer to generic locations. They are prefixed "AM", which stands for "Air Mass" followed by a number, which refers to the length of the path through the atmosphere in relation to the shortest length if the sun was in the apex. It is "The Committee Internationale d'Eclaraige (CIE)" and the "American Society for Testing and Materials (ASTM)" that have published a number of spectra. Their origins are from actual measurements, which are subsequently declared standard. They are also designed such that the spectrum can be reproduced artificially [10].

5.3 Intermediate band (IB) concept for thin film solar cells

To increase the efficiency of single gap solar cells by introducing an impurity level in the semiconductor band gap, the intermediate band solar cell (IBSC) concept was developed. Theoretically, it has been proved that its efficiency can exceed not only the Shockley and Queisser efficiency for ideal solar cells but also that for ideal two-terminal tandem cells which use two semiconductors, as well as that predicted for ideal cells with quantum efficiency above one but less than two [11].

Intermediate band solar cells aim to exploit the energy of below bandgap energy photons. They are based on materials that are characterised by the existence of an additional electronic band (intermediate band) located in-between the conduction and valence bands. An optimised IBSC has near the same limiting efficiency potential (63.2%) than a triple junction solar cells but without requiring tunnel junctions to connect the single gap solar cells. Different possible approaches that review its fundamental theory and introduce different technologies that are being followed towards its implementation: quantum dots, the insertion of suitable impurities into a semiconductor host at sufficiently high densities (bulk approach) and the molecular approach [12].

Different research groups are dedicated to this work, a project (IBPOWER: Intermediate Band Materials and Solar Cells for Photovoltaics with High Efficiency and Reduced Cost) that is solely devoted to the development of the intermediate band solar cell (IBSC) concept.

The IBSC is implemented on the basis of intermediate band materials. Typically these materials are characterised by the existence of the so-called "intermediate band" (IB) within a semiconductor bandgap.

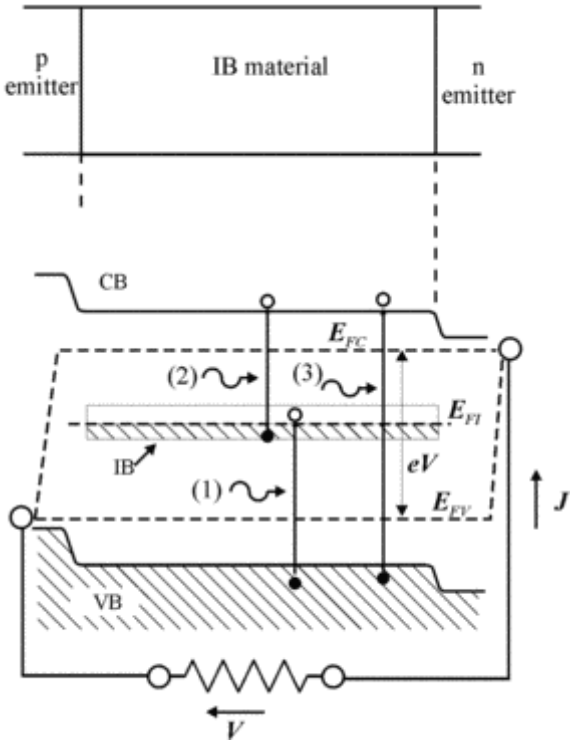

Figure 5. 7 Description of the structure and operation of an intermediate band solar cell [13]

Figure 5.7 sketches the basic structure of an intermediate band solar cell (IBSC). It consists of the so-called intermediate band material sandwiched between conventional p- and n-type semiconductors (emitters). This IB splits the bandgap into two, two-sub-band-gaps, EL and E_H (Fig.5.7) and allows the absorption of below-bandgap energy photons. Thanks to the IB, the absorption of two below bandgap energy photons (photons "1" and "2") creates one electron-hole pair that adds to the ones conventionally generated by the absorption of photons with energy higher than the bandgap E_G (photon "3"). This increases the solar cell photocurrent. In order to be able to absorb the two below bandgap energy photons, the IB must be partially filled with electrons so it can provide both empty states to accommodate electrons from the valence band (VB) as to provide electrons to be pumped to the conduction band (CB).

However, increasing the cell photocurrent is not enough (it could be easily done by choosing a low band-gap semiconductor for manufacturing the cell) if the potential for achieving a high output voltage is not preserved. To this end, according to the fundamental IBSC theory, the

IB material must be sandwiched between two conventional semiconductors (emitters) to isolate the IB from the electrical contacts. The output voltage is determined then by the electron and hole quasi-Fermi level split ($eV=E_{FE}-E_{FH}$) and is still limited by the total bandgap E_G [13]. The intermediate band material is characterised by the existence of a set of energy levels located inside the semiconductor bandgap and separated from the conduction band (CB) and valence band (VB) by a null density of states. We designate this collection of energy levels as a band to emphasise that we want them to behave differently from conventional deep centres.

5.3.1 Intermediate band (IB) concept for ZnTe: O

Solar cells based on II-VI semiconductors are among the leading candidates for low-cost photovoltaic conversion of solar energy due to their high absorption coefficients and therefore the low material consumption for their production. To understand the basics of photovoltaic (PV) cells, several types of simulation software are available. This work reports on the analysis of Zinc Telluride (ZnTe) thin films solar cells by using Solar Cell Capacitance Simulator software (SCAPS). The state-of-the-art combination of the cell is consists of ZnTe:O absorber layer, CdS as buffer and ZnO as optical window following the sequence ZnTe:O/CdS/ZnO. Simulation studies by varying several solar cell parameters such as thickness of various layers, and replacing ZnTe by ZnTe:O layer results in higher efficiency. Figure 5.9 explains that by introducing IB layer, cause to expand the gap for more photons and hence the graph. Solar cells based on standard ZnTe absorbers give conversion efficiencies about 8% due to the high bandgap value of the absorber. However, if the absorption coefficient is modified to take into account the presence of an Intermediate Band, like in ZnTe:O absorbers, the overall performance of PV devices increases dramatically and the conversion efficiency provided by SCAPS is close to 60%. Dark and illuminated J-V characteristic analysed for both ZnTe and ZnTe:O are graphically demonstrated in Figure 5.8. These results are useful for understanding the fundamentals of PV devices based on ZnTe, as well as a feedback for designers and producers of high efficiency ZnTe cells.

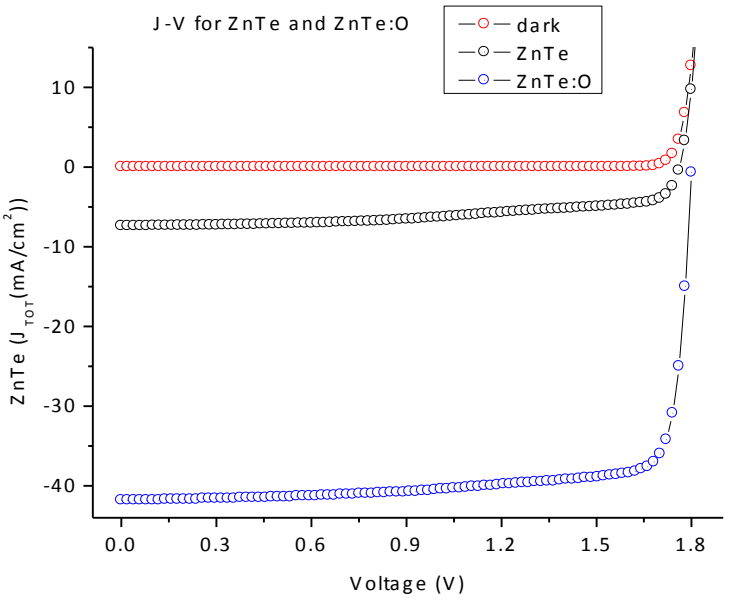

Figure 5. 8 J-V characteristic curve for ZnTe/ZnTe:O based solar cell

The dark-current (in red circle), illuminated current for ZnTe (in green circles) and illuminated current for ZnTe:O (in blue circles) in Figure 5.8 illustrates the effect of intermediate band gap (IB) as in the case of ZnTe:O, on the J-V curve. A huge boost occur here, thanks to the effect of IB in this case. The quantum efficiency (QE) for both ZnTe and ZnTe:O are illustrated in Figure 5.9. The insertion of intermediate band (IB) in ZnTe boosts the efficiency that is above 60% and showed with blue triangles in Figure 5.9. Conversely, for pure ZnTe, as in Figure 4.9 (in chapter 4) is related to ZnTe-based solar cell, shows the variation of the main characteristic parameters of PV solar cell as a function of the ZnTe absorber thickness. It was observed that the conversion efficiency of the solar cell increased with the thickness of the ZnTe absorber layer, but over 1.5µm it decrease slightly. The optimum thickness for ZnTe absorber layer would be around 1.5 ± 0.5µm. From Figure 4.9, at the thickness of 0.5µm and 1.5µm, the calculated efficiency is 7.07% and 7.5%, respectively. Further an increase of thickness has an inverse effect on the efficiency, the reason is due to the high band gap, the generated charge carriers (electron and holes) re-combine and hence the efficiency decreases slowly.

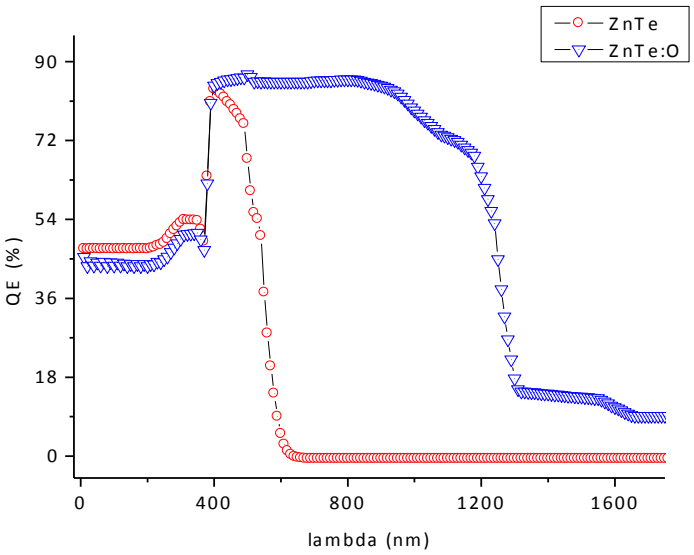

Figure 5. 9 Quantum Efficiency (QE) for ZnTe and ZnTe:O

Comparing the results with the 7.5% efficiency electrons will be captured easily by the back contact for the recombination process at optimum thickness. Therefore, fewer electrons will contribute to the quantum efficiency of the solar cell and the value for Voc and Jsc will be either low or unchanged.

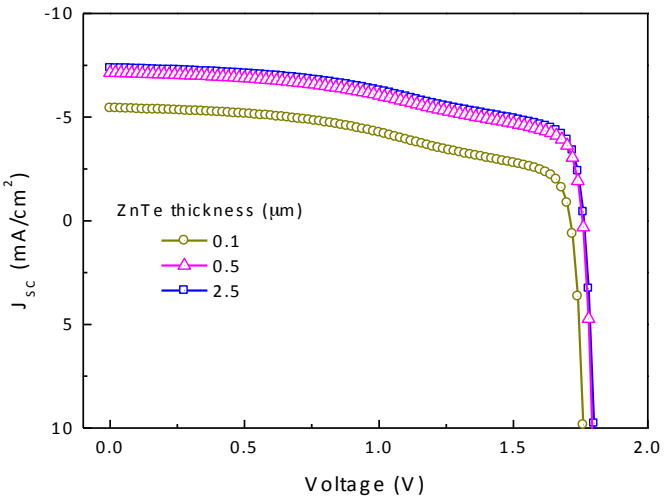

Figure 5. 10 J-V curves for ZnTe-based solar cells with different ZnTe thicknesses under 1-SUN illumination

Figure 5.10 shows the J-V characteristic curve for the different thicknesses of ZnTe layer. In the simulation it gives a high efficiency at 1.5µm.

The efficiency of solar cells can be highly improved by using materials with intermediate bands (IB) as absorbers ZnTe. In the case of ZnTe, an Intermediate Band can be achieved by doping with Oxygen, usually referred as ZnTe:O. Doping with Oxygen, at suitable concentrations, produces a partially fill band located at about 1.2eV from the Valence Band of ZnTe [16]. The presence of an Intermediate Band is very convenient for photovoltaic solar cells because it allows converting low energy photons (sub-bandgap photons) into electrons through a process involving two photons without lowering the open circuit voltage of the PV device. Then higher conversion efficiency is achieved. Figure 5.11 shows the absorption coefficient for PV solar cells based on standard ZnTe absorbers (Blue circles) and ZnTe:O with approved absorption coefficient as a result of introducing intermediate band gap (IB) (Black triangles).

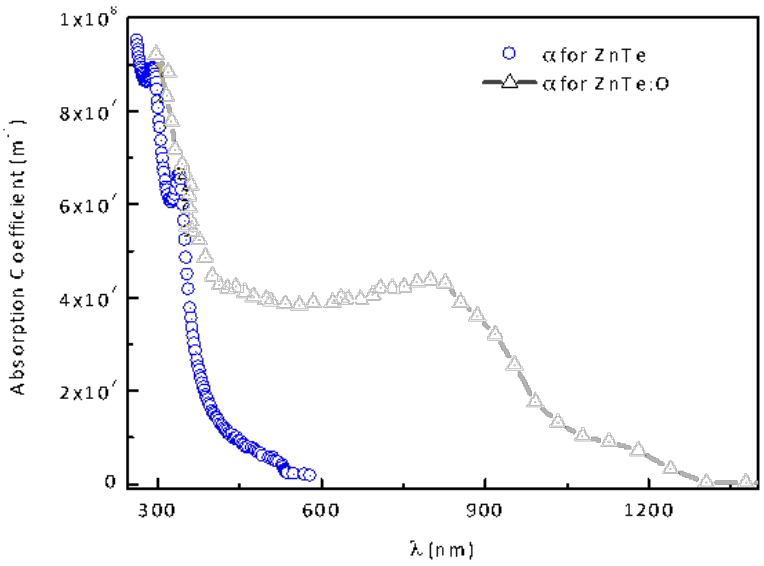

Figure 5. 11 Absorption coefficient for ZnTe and ZnTe:O

This absorption coefficient has been used in earlier calculations for obtaining the photovoltaic parameters of ZnTe-based solar cells.

Figure 5.11 also displays the simulated absorption coefficient for a ZnTe:O absorber with an Intermediate Band located at about 1.2eV from the Valence Band (Black triangles). In this case photons between 1.2 and 2.eV are able to promote electrons from the Valence Band to the Conduction Band through the Intermediate Band. In that case the photovoltaic parameters for ZnTe: O-based devices as provided by SCAPS are as follows: V_{OC}=1.8 V, J_{SC} =41.8

mA/cm^2 (four times the J_{SC} for PV devices based on standard ZnTe absorbers) and FF=82.9%. The conversion efficiency for such a device is close to 60%.

5.3.2 Intermediate band (IB) concept for $CuGaS_2$:V

The potential of the intermediate band solar cell (IBSC) concept to improve the efficiency of thin-film chalcopyrite solar cells has been discussed, the theoretical results show that solar cells based on $CuGaS_2$ with a radiative limiting efficiency of 46.7%, exhibits the highest potential. A simple method for the identification of transition elements that when incorporated in $CuGaS_2$ could possibly introduce an intermediate band is also described [14].

This work informed that electronic structure calculations are carried out for $CuGaS_2$ partially substituted with Ti, V, Cr or Mn to ascertain if some of these systems could provide an intermediate band material that is able to give a high efficiency photovoltaic cell [15]. Absorption coefficient for $CuGaS_2$ with an Intermediate Band centred at 1.6eV is given in figure 5.12.

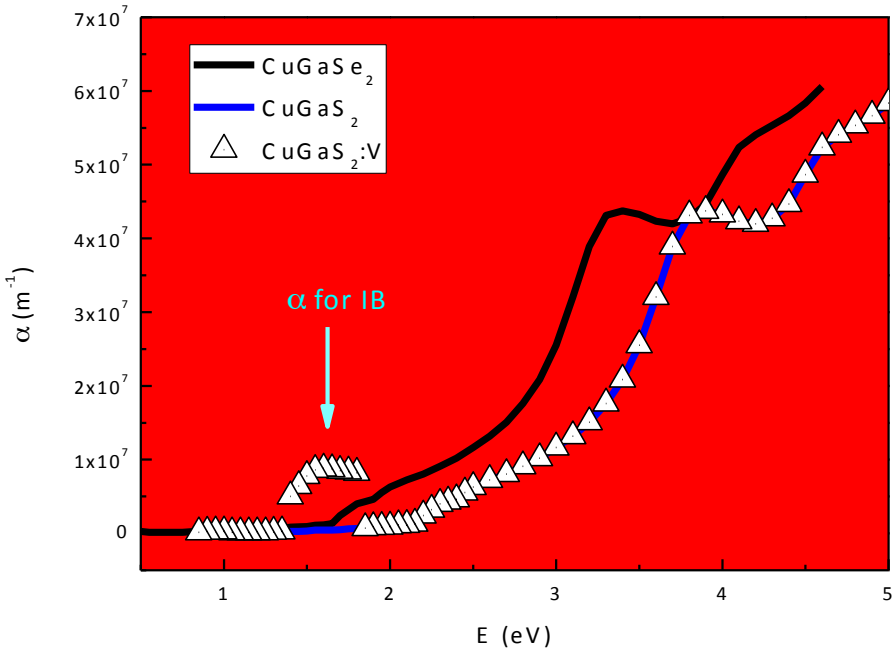

Figure 5. 12 Absorption coefficient for $CuGaSe_2$, $CuGaS_2$ and $CuGaS_2$:V

Such an IB allows harvesting of photons with energy below the band gap via transitions from the host semiconductor valence band (VB) to the IB and from the IB to the conduction band (CB) in addition to the conventional VB to CB transitions. The absorption of the additional

IB assisted photons increases the photocurrent, while preserving the open circuit voltage, thus improving the external efficiency of the cell. Figure 5.7 describes the process.

5.4 Conclusion

The role of CIS/CGS and CIGS replacement for photovoltaic solar cell are discussed. To make the technology cheap and consumer friendly, bulk production and simple module of solar technology is now softening, and the technology is capturing a high market share. Alternate cheap technological growth will make it possible for common use. This work is the comparison of thin-film CIGS solar cell and multilayer CIGS solar cells. Replacing the existing CIGS by multilayer will increase the efficiency by 40-50% and will decrease the use of material by 30-40%. Simplicity of manufacturing and the cost per reliable watt will encourage the academia and industry.

ZnO/CdS/$CuInSe_2$/$CuGaSe_2$ multilayer solar cell with two absorbers and with different bandgap values, with Solar Cell Capacitance Simulator (SCAPS) calculations gives conversion efficiencies up to 50% and with multi sun it even can be boost up to 60%. However, for single absorber layer $CuInGaSe_2$ (CIGS) solar cells the simulated efficiency is increased by 30% while it is 50% thicker. Cheap, efficient and moderate solar cells are expected to dominate the market and fulfil the energy requirement. The evolution in photovoltaic technologies will soon make the economical green revolution.

Numerical models have also been used to examine the potentially attainable efficiency of ZnTe solar cells under several assumptions. There have been many issues that added complexity to the modelling of the cell. Nevertheless, even though efforts at numerical modelling of thin film cells of ZnTe are relatively recent, progress has been good.

Due to high band gap, a number of unmatched photons will not contribute to the PV action. The intermediate band (IB) formation will make the low energy photon to contribute in the PV action, hence the performance of ZnTe:O will dramatically enhance.

References

[1] Burgelman, M., Verschraegen, J., Degrave, S., & Nollet, P., "Modeling thin film PV devices", *Progress in Photovoltaics: Research and Applications,* vol. 12, no. 23, pp. 143-153, 2004.

[2] M. A. Green, “The path to 25% silicon solar cell efficiency: history of silicon cell evolution”, *Progress in Photovoltaics: Research and Applications,* vol. 17, no. 3, pp. 183-189, 2009.

[3] Dimroth, F., Grave, M., Beutel, P., Fiedeler, U., Karcher, C., Tibbits, T. N., ... & Schwarzburg, K., “Wafer bonded four junction GaInP/GaAs//GaInAsP/GaInAs concentrator solar cells with 44.7% efficiency”, *Progress in Photovoltaics: Research and Applications,* March 2014*,* vol. 22, no. 3, pp. 277-282, 2014.

[4] S. Keshmiri, and H.S. Sharbati,, “Model for increased efficiency of CIGS solar cells by a stepped distribution of carrier density and Ga in the absorber layer”, *Science China Physics, Mechanics and Astronomy,* vol. 56, no. 8, pp. 1533-1541, 2013.

[5] P. Jackson, D. Hariskos, R. Wuerz, W. Wischmann, and M. Powalla, “Compositional investigation of potassium doped Cu (In, Ga) Se_2 solar cells with efficiencies up to 20.8%”, *Physica Status Solidi (RRL)-Rapid Research Letters,* DOI: 10.1002/pssr.201409040, 2014.

[6] K. L. Chopra, P. D. Paulson, and V. Dutta, “Thin film solar cells: an overview”, *Progress in Photovoltaics: Research and Applications,* vol. 12, no. 23, pp. 69-92, 2004.

[7] P. Jackson, D. Hariskos,E. Lotter, S. Paetel, R. Wuerz,R. Menner, and M. Powalla, “New world record efficiency for Cu (In, Ga) Se_2 thin film solar cells beyond 20%”, *Progress in Photovoltaics: Research and Applications,* vol. 19, no. 7, pp. 894-897, 2011.

[8] H. Ullah, B. Marí, and H. N. Cui, “Investigation on the Effect of Gallium on the Efficiency of CIGS Solar Cells through Dedicated Software”, Applied Mechanics and Materials, vol. 448, pp. 1497-1501, 2014.

[9] Ward, J. S., Ramanathan, K., Hasoon, F. S., Coutts, T. J., Keane, J., Contreras, M. A. and Noufi, R., “A 21.5% efficient Cu (In, Ga) Se_2 thin-film concentrator solar cell,” Progress in Photovoltaics: Research and Applications, 10(1), 41-46, 2002.

[10] Defining solar spectra for solar modules July 22, 2014. http://www.greenrhinoenergy.com/solar/radiation/spectra.php

[11] Luque, A., & Martí, A., “Increasing the efficiency of ideal solar cells by photon induced transitions at intermediate levels,” Physical Review Letters,78(26), 5014, 1997.

[12] A. López, A. M. Vega, and A. L. López, “Next Generation of Photovoltaics,” Springer Series in Optical Sciences, 2012.

[13] IBPOWER July 19, 2014 http://www.ies.upm.es/index.php?id=459

[14] A. Martí, David Fuertes Marrón, and Antonio Luque, "Evaluation of the efficiency potential of intermediate band solar cells based on thin-film chalcopyrite materials," Journal of Applied Physics 103(7), 073706, 2008.

[15] Palacios, P., K. Sánchez, J. C. Conesa, J. J. Fernández, and P. Wahnón., "Theoretical modelling of intermediate band solar cell materials based on metal-doped chalcopyrite compounds," Thin Solid Films 515, no. 15, 6280-6284, 2007.

CHAPTER 6

Conclusions

6.1 Conclusions

This work has been presented the use of computer-assisted numerical modelling for the simulation and analysis of novel solar cell design concepts. Such an approach is beneficial for two primary reasons. First, it is important to know the theoretical limits towards which one is working towards. This helps to support motivation for the experimental work to be undertaken and gives an accurate gauge of how the work is progressing. Second, realistic, physical device simulations enable for the analysis and possible optimization of experimental devices without the need for physically making said devices. This allows for the crucial saving of resources by performing only the experiments and fabrications that are truly necessary. It is hopeful that this work may serve as a guide to the next series of modelling and simulation efforts that will aid in the development of novel photovoltaic devices and that the analysis performed herein will aid in their experimental realization. The chapter wise summary of the work is presented below:

Chapter 1: History, developments, types and state-of-the art of solar cell revolution has been described in this chapter. The basics of semiconductor physics and thin-film technologies are reviewed in the introduction of this work.

Chapter 2: In this chapter the brief introduction on the important principles and properties of semiconductors and solar cells have been discussed. This unit includes a brief description of state-of-the-art CIGS thin film solar cells. As the dissertation is mainly focused on numerical simulations of solar cells; therefore, of review basic measurements, theory principle and governing mathematical and physical processes is presented. There are many processes inside the solar cells, but our discussion is limited to the basic current density vs. voltage (J-V) characteristic curve, quantum efficiency (QE, eta), and fill factor (FF) measurements.

Chapter 3: This chapter introduces the concept of numerical simulation and explain the relevant physical models for the inside physical phenomenon like generation, recombination and transport of charge carriers (holes and electrons) in photovoltaic materials. This will be done with essential input parameters, to have consistent and acceptable results. It is extremely useful to have a common baseline or starting point. This numerical analysis will produce results for, fitting of modelling out-put to experimental results, predicting the effect of changes in material properties and geometry of cell performance and testing the viability of proposed physical explanation. Subsequently baseline parameter sets are presented that describe various (CdTe, CIGS, SnS, ZnTe, etc.) thin-film solar cells. These models can be

used as a baseline for more complicated models. Different type of software that used for PV analysis, here a brief discussion on each selected software is done.

Chapter 4: This is the main chapter of the thesis. Here we have analysed CIGS, SnS, ZnTe and CdTe based solar cells. All the analysis is based on: theoretical investigation of a photovoltaic (PV) device based on simulation, used to obtain an optimum solution of the parameters for a proposed model. Hence, numerical modelling of polycrystalline thin-film solar cells is an important strategy to test the viability of proposed physical explanations and to predict the effects of physical changes on cell performance. For this work, a sound knowledge of the related field is very important to module new problems as well as to optimise and improve the existing models. Strategies that should be considered when assigning input parameters for numerical models are briefly discussed here, and subsequently, specific baseline parameters for PV devices (CIGS, ZnTe, SnS and CdTe) are proposed. The absence of a precise model implies further attempts to explain the complicated structure of polycrystalline materials. Efforts have been made to find an exact analytic expression for the J-V characteristic. The simulations can, if correctly used and accurately interpreted, be a high-quality compliment to experiments and give a better knowledge of the behaviours in thin-film devices.

Chapter 5: Multi-sun analysis (concentrated solar cells CSC is a big and dominated area in the SC technology), is described for the CIGS based solar cell as a case study here in this chapter. The effect of concentrated illumination on the parameters of solar cells were simulated and discussed. The concept of multi-layer CIGS solar cell was introduced and analysed for the first time, the cell structure that discussed and analysed is ZnO/CdS/CIS/CGS. It give good output results as compare to single layer CIGS solar cell. For high band gap absorber materials/layers, the concept of intermediate band (IB) is very appropriate and convenient for additional photon harnessing and enhancing the cell performance. This IB concept was also discussed here for ZnTe:O and $CuGaS_2$:V materials used as absorber for solar cells. And the last discussion of the thesis is the conclusion and future work.

This final discussion is used to link these results to state-of-the-art of experimental devices and highlight where this work has substantially contributed to their understanding. The idea of thin-film solar cells goes almost as far back as the invention of solar cells. From the early days of solar-energy conversion, it was obvious that to substantially contribute to the energy requirement of our society, solar cells will be needed in large or huge scale applications. Many different material systems and combinations have been tested over the last five

decades, but no other system has shown performance as high as ZnO/CdS/CIGS solar cells. This study establishes a connection between theoretically predicted properties, material studies, and observed device performance.

For a practical approach, the use of a free available device simulator was evaluated for the possible analyses of novel solar cell schemes. Optimum design of these devices has therefore been confirmed or recommended. Discussion of the device simulations began with an introduction and overview of the specific models that were invoked and the physics that they aim to describe. A discussion and tables of the parameters of relevant semiconductors was also presented. For exemplary and pedagogical purposes the device model was presented before and after the inclusion of performance enhancing layers; namely, CIGS, CdTe, SnS and ZnTe. These layers have been shown to provide a significant enhancement to the performance of the device. The current solar cell design (simulated) has also been shown to be currently optimized.

6.2 Future work

A number of extension to the modelling work is possible, which could improve the predictive qualities of the numerical models developed in this work and enable further investigation of efficiency enhancement and alternatives.

Further the one-dimensional presented in this work could be extended to two-dimension. Why? Though one-dimensional problems effectively average the effect of grain boundary states over the bulk, they have been surprisingly successful. Also, transition to two or three dimensions programs will increase substantially the number of input parameters. Polycrystalline thin-film solar cells appropriately require the use of two- or even three-dimensional programs because of grain boundaries and non-planar interfaces.

Experimentally and in industry the technology is facing several challenges, of cost and technology aspects. New materials are necessary for several reasons: (a) to replace the rare earth (In, etc.) and toxic (Cd, Te, etc.) materials, (b) use as transparent front and back contacts in tandem devices, (c) minimization of current losses by window and buffer absorption, by replacing a suitable alternate materials,

Multi-layer concept (thin-film tandem cells): This will require a stable and efficient top and bottom cell, both integrated mechanically or monolithically into one package. This very challenging topic has become a major field of research within the recently established

Calculations with very thin absorber layers will further decrease the manufacturing cost.

Defects are always involved in semiconductor materials and indeed defects have a high influence on the performance of devices. So, to better approach the reality of devices the simulation of defects, both in the layers as well as in the interlayers has to be taken into account.

LIST OF PUBLICATIONS

1. **Hanif Ullah**, and Bernabé Marí. "Numerical analysis of SnS based polycrystalline solar cells," *Superlattices and Microstructures* 72 (2014): 148-155.
2. **Hanif Ullah**, Bernabé Marí, and Hai Ning Cui. "Investigation on the Effect of Gallium on the Efficiency of CIGS Solar Cells through Dedicated Software," *Applied Mechanics and Materials* 448 (2014): 1497-1501.
3. **Hanif Ullah**, and Bernabé Marí, "Numerical Analysis of $CuInS_2$ Based Solar cell by SCAPS," 2nd ENEFM 2014, Lykia, Oludeniz Turkey.
4. **Hanif Ullah**, Bernabé Marí, O. Skhouni, and A. El Manouni,"A numerical simulation study of ZnTe-based solar cells. In Renewable and Sustainable Energy Conference (IRSEC), International (pp. 686-690) IEEE. Ouarzazate, Morocco – October 17-19, 2014.
5. Thierno Sall, Bernabé Marí Soucase, Miguel Mollar, Mounir Fahoume, and **Hanif Ullah** "Influence of Alcohol Percentage on the β-In2S3 Thin Films Properties Deposited by Chemical Spray Pyrolysis Technique for Photovoltaic Applications," 3rd International Conference on Environment and Sustainable Development (EESD) Oct 22-24, 2014.
6. **Hanif Ullah**, and Bernabé Marí, "Baseline of numerical simulations for ZnTe based thin-film solar cells," International Conference on Energy Systems and Policies (ICESP 14), Nov 24 – 26, Islamabad Pakistan 2014.
7. Inmaculada Guaita-Pradas, **Hanif Ullah**, Shafi Ullah and Bernabé Marí "Engineering Education in Third Countries through International EU Cooperation Programmes," 4TH VALENCIA GLOBAL 2014, 19-20 June 2014, Valencia, Spain.
8. Rahat Ullah, Fisal, N., Safdar, H., Khalid, Z., Maqbool, W., & **Hanif Ullah**. "Stochastic Geometry Based Dynamic Fractional Frequency Reuse for OFDMA Systems," *Jurnal Teknologi*, *67*(1), (2014).
9. **Hanif Ullah**, Shafi Ullah and Bernabé Marí "Photovoltaic Solar cells a technological review," The 2nd Abasyn International Conference on the Technology and Business Management (AiCTM-2014), Peshawar, Pakistan 2014 (Oral)
10. **Hanif Ullah**, Inmaculada Guaita-Pradas and Bernabé Marí "Emerging of photovoltiac technology in Energy deficient market of Pakistan," 2nd International Conference on

11.

12. Business Innovation and Management (ICBIM-2014), Islamabad Pakistan 26-27 April 2014.
13. **Hanif Ullah** and Bernabé Marí "Comparative analysis of CIGS thin film and Multilayer Solar cells," ICEE/ICIT 2014, Riga, Latviya 2-6 June 2014.
14. **Hanif Ullah**, Shafi Ullah and Bernabé Marí "Numerical Analysis of Photovoltaic Solar Cells based on low cost thin film sulfides," E-MRS SPRING MEETING, Congress Center - Lille, France 26-30 May, 2014 (Poster).
15. **Hanif Ullah** and Bernabé Marí "Modelling and Analysing CIGS Thin-film Solar Cell by SCAPS" 2013 international conference on engineering education and research iceer-2013 Marrakesh, Morocco July 1 -5, 2013 (Poster).
16. **Hanif Ullah**, Bernabé Marí "Boosting the efficiency of CIGS-based solar cells using dedicated software," **Journal** of Beijing Institute of Technology, Vol. 22, Suppl. 1. 2013.
17. **Hanif Ullah** and Bernabé Marí "Understanding the behaviour of thin film solar cells by using dedicated software," 21st University Conference on Educational Innovation in Technical Education (xx1cuieet 2013) Valencia, Spain July 10 - 12, 2013.
18. **Hanif Ullah**, Bernabé Marí "Effect of Gallium (Ga) on the Parameters of CIGS Solar Cell through dedicated Software SCAPS," FEIIC 5th World Engineering Congress 2013 NUST Islamabad Pakistan 23-25 September 2013.
19. **Hanif Ullah**, Bernabé Marí "Modelling and Analysing CdTe Thin-film Solar Cell by SCAPS," International Congress on Energy Efficiency and Energy Related Materials (ENEFM 2013) Antalya, Turkey, 9 -12 October 2013.
20. **Hanif Ullah**, Bernabé Marí "Numerical Analysis of SnS based (SnS/**ZnS**/ZnO) Polycrystalline Solar Cell," 12th International Conference on Condensed Matter and Statistical Physics (ICCMSP) Errachidia-Morocco October 30 - November 01, 2013.
21. **Hanif Ullah**, Bernabe Mari Soucase "Numerical Analysis of SnS based (SnS/**CdS**/ZnO) Polycrystalline Solar Cell," EMRS 2013 Fall Meeting Warsaw University of Technology Poland 16 -20 September 2013.
22. O. Skhouni, A. El Manouni , Bernabé Marí, and **Hanif Ullah,** "Preparation of ZnTe thin films and numerical simulation of znte based solar cell," ICOME'15, Tetouan, Morocco, May 19-22, 2015.
23. **Hanif Ullah**, Bernabe Mari Soucase**,** "$CuInSe_2$, $CuGaSe_2$ and $CuInGaSe_2$ based thin film solar cells: Theoretical vs experimental analysis," International Conference

24. Power Generation Systems and Renewable Energy Technologies (PGSRET 2015), Islamabad, Pakistan, 10-11 June, 2015.
25. **Hanif Ullah**, Bernabe Mari Soucase "Effect of defects on the performance of some photovoltaic solar cells: an introduction to research methods to engineering students," International Conference on Engineering Education (ICEE 2015), Zagreb Zadar (Croatia), 20-24 July 2015.

Member of Organising Committee, "7th International Image Processing and wavelet on Real-world Applications Conference" IWW 2013, Valencia

"Bismillah al Rahman al Rahim"

"In the name of Allah, most Gracious, most Compassionate"

Escuela Técnica Superior de Ingeniería del Diseño